JRC Scientific and Technical Reports

Biofuels: a New Methodology to Estimate GHG Emissions from Global Land Use Change

A methodology involving spatial allocation of agricultural land demand and estimation of CO_2 and N_2O emissions

Roland Hiederer, Fabien Ramos, Claudia Capitani, Renate Koeble, Viorel Blujdea, Oscar Gomez, Declan Mulligan and Luisa Marelli

EUR 24483 EN - 2010

JRC EUROPEAN COMMISSION

Institute for Environment and Sustainability

Institute for Energy

The mission of the JRC is to provide customer-driven scientific and technical support for the conception, development, implementation and monitoring of EU policies. As a service of the European Commission, the JRC functions as a reference centre of science and technology for the Union. Close to the policy-making process, it serves the common interest of the Member States, while being independent of special interests, whether private or national.

European Commission
Joint Research Centre

Contact information
Address: Via E. Fermi, 2749 I-21027 Ispra (VA), Italy
E-mail: luisa.marelli@jrc.ec.europa.eu
Tel.: +39 0332 786332
Fax: +39 0332 78 5869

http://re.jrc.ec.europa.eu/bf-tp/
http://www.jrc.ec.europa.eu/

Legal Notice
Neither the European Commission nor any person acting on behalf of the Commission is responsible for the use which might be made of this publication.

Europe Direct is a service to help you find answers
to your questions about the European Union

Freephone number (*):
00 800 6 7 8 9 10 11

(*) Certain mobile telephone operators do not allow access to 00 800 numbers or these calls may be billed.

A great deal of additional information on the European Union is available on the Internet.
It can be accessed through the Europa server http://europa.eu/

JRC59764

EUR 24483 EN
ISBN 978-92-79-16389-0
ISSN 1018-5593
DOI 10.2788/48910

Luxembourg: Publications Office of the European Union

© European Union, 2010

Reproduction is authorised provided the source is acknowledged
Printed in Italy

This document may be cited as follows:

Hiederer, R., F. Ramos, C. Capitani, R. Koeble, V. Blujdea, O. Gomez, D. Mulligan and L. Marelli. (2010) Biofuels: a New Methodology to Estimate GHG Emissions from Global Land Use Change. EUR 24483 EN. Luxembourg: Office for Official Publications of the European Communities. 150pp.

European Commission Joint Research Centre
TA 3 (IES, IE)
TP 261
21027 Ispra (VA)
Italy

ACKNOWLEDGMENTS

The authors would like to thank the IFPRI team and the colleagues of the *Support to Agricultural Trade and Market Policies* (AGRITRADE) Action at the JRC-IPTS, for providing us with their data and for the continuous exchange of information.

In particular the authors would like to acknowledge the contributions of:

David Laborde (IFPRI)

Hugo Valin (CEPII)

Robert M'Barek (JRC-IPTS)

Olexandr Nekhay (JRC-IPTS)

María Blanco Fonseca (JRC-IPTS)

Hubertus Gay (JRC-IPTS)

Aikaterini Kavallari (JRC-IPTS)

Without their valuable support, this report would not have been possible.

The authors also wish to thank our colleague Robert Edwards (JRC-IE) for his important inputs into devising the concept of the study and Grainne Mulhern (JRC-IES) for her patience in making this report more accessible to a wider audience

Table of Contents

Page

1. Study Background 3

1.1. GHG Emissions from Indirect Land Use Change 3

1.2. Purpose of Study 4

1.3. JRC Method for Calculating GHG Emissions from ILUC 5

2. Data Sources and Processing 9

2.1. Spatial Data Sets 10

2.1.1. Land Use and Cover Layers 10

2.1.2. Cropland and Individual Crop Data 12

2.1.3. Soil Properties 13

2.1.4. MODIS Land Cover 13

2.1.5. Global Agro-Ecological Zones (GAEZ) 14

2.2. Agro-Economic Data 17

2.2.1. IFPRI-MIRAGE 17

2.2.2. JRC-IPTS AGLINK-COSIMO 19

2.2.3. Baseline and Scenario Assumptions 22

2.3. Data Preparation 22

2.3.1. Standard Spatial Layer Properties 23

2.3.2. GlobCover and GLC2000 Legend Adaptation 26

2.3.3. McGill M3-Cropland and Crop Data 34

2.3.4. Merging LC Layers with M3-Cropland and M3-Crops Data 37

2.3.5. Soil Types for IPCC Reference Values 41

2.3.6. Climate Regions 58

2.3.7. Land Management System Factors 68

3. Calculating GHG Emissions from ILUC Using Spatial Allocation Procedure 73

3.1. Database Creation 73

3.2. Spatial Allocation Process 75

3.3. Filtering and Sorting Areas with Potential for Cropland Expansion 76

3.4. Filtering Data with MODIS Land Cover Typology 77

3.5. Cropland Distribution 78

3.6. General Comments on Spatial Allocation Procedure 79
3.7. Methodology for Estimating GHG Emissions 81
3.7.1. Carbon Emissions from Soil 81
3.7.2. N_2O Emissions from Loss of Carbon in Mineral Soils 83
3.7.3. CO_2 Emissions from Changes in Above- and Belowground Biomass Carbon Stocks 88

4. Results of Applying Methodology 93
4.1. IFPRI-MIRAGE data 93
4.1.1. Spatial Allocation and Soil Carbon Emissions 93
4.1.2. N_2O Soil Emissions 98
4.1.3. CO_2 Emissions from Changes in Above- and Belowground Biomass Carbon Stock 100
4.2. JRC-IPTS AGLINK-COSIMO Data 107
4.2.1. Spatial allocation and Soil Carbon Emissions 109
4.2.2. N_2O Emissions 113
4.2.3. CO_2 Emissions from Changes in Above and Below Ground Biomass 114
4.3. Overall Emissions Estimated from Agro-Economic Models 117
4.4. Annual GHG Emissions per Amount of Energy 118
4.5. Total Emissions from Biofuel Production 120
4.5.1. Total Emissions from Biofuel Production Under IFPRI Scenarios 121
4.5.2. Total Emissions from Biofuel Production Under JRC-IPTS Scenario 122
4.5.3. Comparison of total Annual GHG Emissions from Models 123
4.5.4. Uncertainty Ranges for Input Data 126

5. Summary and Conclusions 129
5.1. Base Data and Preparation 129
5.2. Spatial Allocation of Extra Land Demand 130
5.3. GHG Emissions from ILUC 130
5.4. Outlook 133

List of Figures

Page

Figure 1: Scheme of the Spatial Allocation and GHG Emissions Calculations 7

Figure 2: Land Evaluation Concept for Suitability Maps 15

Figure 3: Suitability for Rain-fed Wheat, Intermediate Input (Plate 29, GAEZ, 2002) 16

Figure 4: Regions as Defined for IFPRI-MIRAGE 19

Figure 5: Regions as Defined for AGLINK-COSIMO JRC-IPTS Data 21

Figure 6: Location of Major Cross-Classification Differences between Forest and Other LC Types in GlobCover and GLC2000 after Reclassification to Common Legend 30

Figure 7: Difference in Proportion by Grid Cell for McGill M3-Cropland and Re-Classified GlobCover Data 35

Figure 8: Difference in Proportion by Grid Cell for McGill M3-Pasture and Re-Classified GlobCover Data 36

Figure 9: LC Types and Crop Classes of IPCC Tier 1, GlobCover, McGill M3-Crops Data and Economic Model 40

Figure 10: Main Tables of Harmonized World Soil Database v.1.1 42

Figure 11: Spatial and Typological Units in Harmonized World Soil Database 43

Figure 12: IPCC Soil Classification applied to Soil Type of Principal Mapping Unit of HWSD 50

Figure 13: Areas without IPCC Default Values for SOC Stock in Combination of HWSD and Climate Zones 52

Figure 14: Mapped IPCC Default Reference Values of Soil Organic Carbon under Native Vegetation and Applied to Dominant STU 55

Figure 15: Mapped IPCC Default Reference Values of Soil Organic Carbon under Native Vegetation and Applied to all STUs after Spatial Weighting 56

Figure 16: Difference in Mapped IPCC Default Reference Values of Soil Organic Carbon under Native Vegetation between dominant STU and integrating all STUs 57

Figure 17: IPCC Default Climate Regions, Figure 3A.5.1, (reproduced IPCC, 2006) 58

Figure 18: IPCC Default Climatic Regions from PET Modelled for Mean Daily Temperature 60

Figure 19: IPCC Default Climatic Regions from PET Modelled after Hargreaves 62

Figure 20: Classification Scheme for Ecological Zone Layer 64

Figure 21: Differences in Spatial Distribution of Warm and Cool Temperate Regions vs. Subtropical and Temperate Zones 66

Figure 22: Ecological Zones from Climatic Criteria..... 67

Figure 23: Schematic Representation of the 3 Processes Performed by the Spatial Allocation Procedure 76

Figure 24: 3,000 ha of Cropland Expansion Homogeneously Distributed between Forest and Savannah in a 10,000 ha Area 79

Figure 25: C:N Ratio Classes - Topsoil, Edition 3.6, 2007-02-08 (Source: FAO, 2007)..... 85

Figure 26: Input Data and Result of the Delineation of Areas where Water Holding Capacity is Exceeded (central map) and Leaching/Runoff Occurs (bottom map) 87

Figure 27: Climate Regions and Geographic Aggregations for ABCS 90

Figure 28: Change in Total Cropland Area by Country / Region from IFPRI BAU Scenario..... 94

Figure 29: Changes in Soil Organic Carbon Following LUC in IFPRI BAU Scenario 95

Figure 30: Change in Total Cropland Area by Country / Region from IFPRI FT Scenario 96

Figure 31: Changes in Soil Organic Carbon following LUC in IFPRI FT2020 Scenario 97

Figure 32: N2O Soil Emissions over a Period of 20 Years Related to Mineralized N Resulting from Loss of SOC for IFPRI-MIRAGE Regions (BAU and FT scenarios, in Mt of CO2eq.) 99

Figure 33: Relationship between N2O Soil Emissions Related to Mineralized N and CO2 Emissions from Loss of SOC 100

Figure 34: Land Use/Cover Converted to Cropland for IFPRI BAU Scenario According to Table S14 of IFPRI (2010) 102

Figure 35: Land Use/Cover Converted to Cropland According to Spatial Allocation Procedure Based on IFPRI LUCRED (BAU scenario) Compared to LU2000 102

Figure 36: Decrease of Non-agricultural Land Cover (total global decrease = 100%) in Different Regions and Land Cover Types Based on Spatial Allocation Procedure Applied to IFPRI LUCRED (BAU scenario) Compared to LU2000 103

Figure 37: Decrease of Non agricultural Land Cover (total global decrease = 100%) in Different Regions and Land Cover Types Based on Spatial Allocation Procedure Applied to IFPRI LUCRED (FT scenario) Compared to LU2000 104

Figure 38: Change in Above- and Belowground Biomass Carbon Stock (Mt C) in Different Regions Based on Spatial Allocation Procedure Applied to IFPRI LUCRED (BAU scenario) Compared to LU2000 104

Figure 39: Change in Above- and Belowground Biomass Carbon Stock - ABCS-(Mt C) in Different Regions. Based on spatially allocated IFPRI LUCRED (FT scenario) compared to LU2000 105

Figure 40: Change in Land Use/Cover in EU Countries Based on Spatial Allocation Procedure applied to IFPRI LUCRED (BAU scenario) Compared to LU2000 106

Figure 41: Change in Total Cropland Area by Country / Region from AGLINK Scenario (CG Run) 110

Figure 42: Changes in Soil Organic Carbon following LUC in AGLINK Scenario (CG Run) 111

Figure 43: Changes in Soil Organic Carbon following LUC in AGLINK Scenario (GM Run) 112

Figure 44: N2O Soil Emissions Related to Mineralized N Resulting from Loss of Soil Organic Carbon for IPTS AGLINK-COSIMO Results (CG and GM runs, in Mt CO2eq. over 20 years) 114

Figure 45: Land Use/Cover Converted to Cropland Based on Spatial Allocation Procedure Applied to IPTS LUCRED (CG Run) Compared to LU2000 115

Figure 46: Change in Non-agricultural Land Cover (total global decrease = 100%) by Region Based on Spatial Allocation Procedure Applied to IPTS LUCRED (CG Run) Compared to LU2000 116

Figure 47: Change in Above- and Belowground Biomass Carbon Stock by Land Cover and Region Based on Spatial Allocation Procedure Applied to IPTS LUCRED (CG Run) Compared to LU2000 116

Figure 48: Distribution of Cropland in 2000 [Ramankutty et al. 2008] 143

Figure 49: Spots of Marginal Increase in Cropland According to Biofuel Scenario Compare to Baseline 144

List of Tables

Page

Table 1: Summary of the Datasets Used in the Study 9
Table 2: GlobCover Level 1 Classification 11
Table 3: Global Land Cover 2000 Global Data Classification 12
Table 4: IGBP Land Cover Legend 14
Table 5: IFPRI-MIRAGE Economic Regions 18
Table 6: AGLINK-COSIMO Economic Regions 20
Table 7: Specifications of Spatial Data Layers 23
Table 8: GlobCover and GLC2000 Related to Simplified Common Legend 28
Table 9: Results of Cross-Classification of GlobCover and GLC2000 Common Legend Layers 29
Table 10: Weighting Factors for GlobCover Level 1 Legend to Biofuel LC Categories 32
Table 11: Weighting Factors for GLC2000 Legend to Biofuel LC Categories 33
Table 12: Proportion of Harvested Area for Selected Crops and Crop Groups in M3-Crops Data 38
Table 13: Classification of Soil and Surface Types of [HWSD_SMU.SYMBOL] to Field [HWSD_DATA.ISSOIL] 44
Table 14: Soil and Non-Soil Combinations for FAO Soil Classes 45
Table 15: Relating HWSD.SYMBOL Entries to IPCC Tier 1 Soil Type 47
Table 16: Distribution of IPCC Soil Classes Across Main Land Mass 51
Table 17: Comparison of SOC Stock in Topsoil from HWSD / Climate Zone Data to IPCC Default Values (GLC2000, 95% Coverage) 54
Table 18: Land Management System Components and Factors 69
Table 19: Proxies for Land Management System Components and Factors 70
Table 20: Cultivated Land in the World According to Different Datasets 81
Table 21: Reclassification Scheme of FAO (2007) C:N Ratio Classes into Single Value C:N classes 85
Table 22: Soil C Emissions from IFPRI Economic Model BAU and FT Scenarios 98
Table 23: Global N2O Soil Emissions over a Period of 20 Years Related to Mineralized N Resulting from Loss of Soil Organic Carbon due to Land Use Change in 2020 99
Table 24: Land Use/Cover Classes Available for Cropland Extension 102

Table 25: Emissions from change in Above- and Belowground Biomass Carbon Stock Related to Biofuel Cultivation in 2020 by IFPRI Region 107

Table 26: Crop Types and Aggregations in AGLINK-COSIMO Model Data 108

Table 27: Soil Carbon Emissions from AGLINK-COSIMO Economic Model Scenario 113

Table 28: Global N2O Soil Emissions Related to Mineralized N Resulting from Loss of Soil Organic Carbon due to LUC in 2020 over 20 Years 114

Table 29: Emissions from Change in ABCS Related to Biofuel Cultivation in 2020 by Region 117

Table 30: Total Greenhouse Gas Emissions from Changes in Soil and Biomass Carbon Stocks Induced by ILUC 118

Table 31: Annual GHG Emissions from Changes in Soil and Biomass Carbon Stocks per Amount of Energy Produced 119

Table 32: Total Emissions from Cultivation, Processing, Transport and Distribution of Production from IFPRI Scenarios 121

Table 33: Sum of "Weighted Emissions" from Cultivation, Processing, Transport and Distribution and ILUC Emissions 122

Table 34: Total Emissions from Biofuel Production from IFPRI Scenarios 123

Table 35: Annual GHG Emissions from LUC, Cultivation, Processing, Transport and Distribution of the Biofuels and Default Annual Fossil Fuel Emissions 124

Table 36: Annual Greenhouse Gas Emissions from Biofuels Compared to Emissions of Fossil Fuel – values calculated using the methodology and default values in the RED 125

Table 37: Annual Greenhouse Gas Emissions from Biofuels Compared to Emissions of Fossil Fuel – values calculated using the methodology and default values in the WTW analysis 126

Table 38: Uncertainty Ranges for the Input Data to Calculate Emissions from LUC 127

Table 39: Crop Demands for Baseline, Business As Usual and Free Trade Scenario in 2020 142

Table 40: World Regions Used for ABCS 145

Table 41: Shares of Shrub and Tree Crops in Land Use Classes Fruits and Vegetables, Oilseeds and Sugar Crops 146

Table 42: Above- and Below-Ground Biomass Carbon Stocks (ABCS) in t C ha-1 Used in this Study 149

List of Acronyms and Abbreviations

Acronym	Label
ABCS	Above and below-ground biomass carbon stock
AGLINK-COSIMO	OECD/FAO international agricultural markets model
BAU	Business As Usual scenario
CAP	Common Agricultural Policy
CAPRI	Common Agricultural Policy Regionalised Impact model
CEPII	Centre d'Etudes Prospectives et d'Informations Internationales
CGE	Computable general equilibrium
CIS	Commonwealth of Independent States
CGIAR	Consultative Group on International Agricultural Research
COSIMO	Commodity Simulation Model
DEWA	UNEP Division of Early Warning and Assessment
EEA	European Environment Agency
ESA	European Space Agency
ESIM	European Simulation Model
ESRI	Environmental Systems Research Institute, Inc., Redlands, California
ETRS89	European Terrestrial Reference System 1989
FAO	Food and Agriculture Organization of the United Nations
FGGD	Food Insecurity, Poverty and Environment Global GIS Database
FRA2000	Global Forests Resources Assessment 2000
FT	Free Trade scenario
GAEZ	Global Agro-Ecological Zones
GHG	Greenhouse gas
GIS	Geographic Information System
GOFC	Global Observation of Forest Cover
GLC2000	Global Land Cover 2000
GISCO	Geographic Information System for the Commission (Eurostat)
GRID	UNEP Global Resource Information Database
HAC	High-activity soils (IPCC)
HWSD	Harmonized World Soil Database
ICONE	Institute for International Trade Negotiations (Brazil)
IFPRI	International Food Policy Research Institute
IGBP	International Geosphere-Biosphere Programme
IIASA	International Institute for Applied Systems Analysis
ILUC	Indirect land use change
ISRIC	International Soil Reference and Information Centre
ISSCAS	Chinese Academy of Sciences
JRC	European Commission Joint Research Centre
JRC IE	JRC Institute of Energy
JRC IES	JRC Institute for the Environment and Sustainability
JRC IPTS	JRC Institute for Prospective Technological Studies
LAC	Low-activity soils (IPCC)
LADA	Land Degradation Assessment in Drylands
LC	Land Use and Cover

Acronym	Label
LCCS	UN Land Cover Classification System
LMS	Land Management System
LUC	Land Use Change
MERIS	Medium Resolution Imaging Spectrometer Instrument
MIRAGE	Modelling International Relationships in Applied General Equilibrium
MODIS	Moderate Resolution Imaging Spectroradiometer
MU	Mapping Unit
OECD	Organisation for Economic Co-operation and Development
ORNL DAAC	Oak Ridge National Laboratory Distributed Active Archive Center
RED	Renewable Energy Directive (Directive 2009/28/EC)
REF	Reference scenario
SAM	Spatial Allocation Model
SOC	Soil organic carbon
SOM	Soil organic matter
TIFF	Tagged Image File Format
UNEP	United Nations Environment Programme
USDA	United States Department of Agriculture
WRB	World Reference Base for Soil Resources

Executive Summary

This study implements a new methodology developed by the JRC IES and IE for estimating changes in greenhouse gas (GHG) emissions from soil and above- and belowground biomass resulting from global land use changes caused by the production of biofuels. The methodology is based on the Tier 1 approach as developed under the IPCC 2006 Guidelines for National Greenhouse Gas Inventories. Under this approach, GHG emissions are estimated by comparing the carbon stocks before the land use change with the carbon stocks after the conversion.

To calculate the related GHG emissions, the study incorporates the output from global economic models on land use change as input data, namely cropland demands from the general equilibrium model MIRAGE (processed by IFPRI) and from the partial equilibrium model AGLINK-COSIMO (processed by JRC-IPTS).

A new approach of the study is the development of a harmonised spatial dataset and advanced analysis methods for all aspects of estimating GHG emissions. In the spatial allocation process, cropland demands provided by economic models are processed using global raster layer with approx. 10 km grid spacing. The outcome of the spatial allocation process allows for the computation of changes in land use, which result in changes in soil carbon stock, N_2O emissions and levels of carbon in the affected biomass.

The output of the IFPRI-MIRAGE analysis was available to the study for two scenarios, assuming "Business as Usual" (BAU) and "Free Trade" conditions (FT) respectively. The attribution of total cropland area subject to indirect land use change (ILUC) for 2020 over the reference area is 8,209 km^2 (BAU) and 9,759 km^2 (FT). Most of the additional cropland is assigned to Brazil and the Commonwealth of Independent States, while changes in cropland attributed to ILUC in Europe are small. For the BAU scenario, total GHG emissions from ILUC are estimated at 201 Mt CO_2eq (BAU) and 248 Mt CO_2eq (FT) over a period of 20 years. The JRC-IPTS AGLINK-COSIMO simulation calculated the area change due to biofuels policy to be 52,372 km^2. Major cropland extension occurs in EU27, followed by Brazil, Argentina and some Asian countries. Estimated total GHG emissions are 1,092 Mt CO_2eq.

For all the scenarios, the major contribution (approx. 80%) to total GHG emissions results from the removal of above- and belowground biomass. Changes in soil carbon stock contribute 15 to 20%, whereas N_2O emissions related to loss in soil carbon stocks make up only a small share (2 - 3%).

The emissions from the removal of above- and belowground biomass estimated by this study are about 4 times higher than the figures published by IFPRI. The differences between the emissions calculated for the two models, and between that of this study and the IFPRI assessment, are attributed to different assumptions made on the share of crops allocated to bioethanol or biodiesel production, and on the proportion of forest and shrubland converted to cropland to cater for the additional demand.

1. STUDY BACKGROUND

The 10% target share of renewable energies in transport set by the *Directive 2009/28/EC on the Promotion of the Use of Energy from Renewable Sources* (RED) affect energy and agricultural markets and will change the extent and intensity of agricultural land use, since worldwide production of biofuels is growing rapidly (OECD-FAO, 2010, FAO-STAT[1]).

The overall environmental impact and sustainability of biofuels is the objective of intensive societal and political debate in Europe and worldwide. Analysing and modelling the effects of bioenergy policies is a very complex exercise that requires a combination of energy, agro-economic, global land use and so-called "bio-physical" modelling approaches.

1.1. GHG EMISSIONS FROM INDIRECT LAND USE CHANGE

A particularly controversial topic is how to estimate emissions from indirect land use change (ILUC), when crops for food are diverted to biofuels or bioenergy. Using more (conventional) biofuels in the EU, even if they are produced from EU crops, will increase the overall world demand for crops. If not managed properly, it could displace arable production onto land used for other purposes, both inside and outside the EU, and could lead to extra GHG emissions. In practice, if biofuels crops are grown on uncultivated land, direct land use change will be caused. If crops grown on existing arable land are used for biofuels instead of food, this will cause ILUC because of the necessity to replace the food. Models do not specify where the extra production comes from; they just calculate the total change in crop area for a given increase in biofuel or crop demand. The models thus estimate simply land use change (LUC) and emissions form LUC, and for the purpose of this study the two terms are used indistinguishable.

The RED and the *Fuel Quality Directive* (2009/30/EU) contain provisions on monitoring and limiting the possible ILUC effects, but also give the Commission the task to further explore the issue, in order to establish the most appropriate mechanism for minimising ILUC.

During 2009 and 2010, the Commission worked intensively to give a better understanding of ILUC effects from increased biofuels use. Various Commission services carried out modelling and analytical exercises to investigate the nature of ILUC and provide quantitative estimates of the effects (additional cropland areas required and related GHG emissions):

[1] http://faostat.fao.org/

1. *Global Trade and Environmental Impact Study of the EU Biofuels Mandate*

   This work was carried out by the International Food Policy Institute (IFPRI) for the Directorate General for Trade (DG TRADE), and uses a global computable general equilibrium model (and extended and modified version of the existing MIRAGE model) to estimate the impact of EU biofuels policies.[2]

2. *Impacts of the EU biofuel target on agricultural markets and land use - a comparative modelling assessment*

   This work, commissioned by the Directorate General of Agriculture (DG AGRI), was carried out by the JRC Institute for Prospective Technological Studies (JRC-IPTS). It provides an outlook of agricultural production until 2020 with and without EU Biofuels policy, using the partial equilibrium models AGLINK-COSIMO (the model is developed by the OECD and FAO secretariats), ESIM (European Simulation Model), and CAPRI (specifically designed to analyse Common Agricultural Policy (CAP) measures and trade policies for agricultural products).[3]

3. *Indirect Land Use Change from increased biofuels demand. Comparison of models and results for marginal biofuels production from different feedstocks*

   This study, carried out by the JRC Institute for Energy (JRC-IE) under request of the Directorate General for Climate (DG CLIMA), compares the ILUC results produced by different economic models for marginal increases in biofuel production from different feedstocks.

1.2. PURPOSE OF STUDY

The purpose of the present study is to implement and evaluate the methodology developed under the guide for the calculation of land carbon stocks in biofuels as specified in *Commission Decision of 10 June 2010 on guidelines for the calculation of land carbon stocks for the purpose of Annex V to Directive 2009/28/EC (2010/335/EU)*[4].

To achieve the study purpose changes in land carbon stocks are translated into estimates of GHG emissions, which results from the indirect land use changes caused by the

[2] Full report (al-Riffai *et al*, 2010) available at http://trade.ec.europa.eu/doclib/docs/2010/march/tradoc_145954.pdf

[3] Full report available at http://ipts.jrc.ec.europa.eu/publications/pub.cfm?id=3439

[4] OJ L151 17.06.2010 pp. 19-41.

production of biofuels as modelled by agro-economic models. For the distribution of the extra land a spatial allocation procedure was developed which fully integrates with other spatial data sets.

Not part of this study are matters related to biodiversity and land degradation. Specifically excluded for allocating extra land demands are wetlands and peatlands.

1.3. JRC METHOD FOR CALCULATING GHG EMISSIONS FROM ILUC

Agro-economic models provide output of how much extra crop would be produced in different countries/world regions as a result of biofuels policy. Some models also predict the area of lands converted to cropping from pasture, forest, or natural land in each region, but the crucial question to calculate the corresponding GHG emissions is where ILUC occurs and how can the area be allocated spatially.

For this purpose, the JRC Institute for the Environment and Sustainability (IES), with the support of the Institute of Energy (IE) is developing a methodology to trace on a map the extra agricultural land demand provided by agro-economic models.

This report includes an estimation of the GHG emissions calculated taking as input data the results from studies using the MIRAGE model (IFPRI) and the AGLINK-COSIMO model (JRC-IPTS). With some minor implementations, the spatial allocation procedure and the GHG calculation methodology could be also applied in future to the results of other models, for example the marginal calculations reported in the JRC-IE modelling comparison exercise.

The first task of this methodology is to locate geographically where the land use change predicted by models could occur, (also where the potential exists for avoiding land use change), on the basis of existing cropped areas, land availability and land suitability. Making use of the results and output of the agro-economic models, the study provides soil and land-use maps that identify regions where the expansion of biofuels production are most likely to occur.

The second task of the present study is to convert the land use changes positioned in the previous steps into an estimate of GHG emissions resulting from the given change in biofuel demand. In case of land use/cover change, e.g. conversion of forest into cropland, carbon stocks and carbon dynamics in biomass and soil may change. Converting land cover types with high biomass and soil carbon stocks (e.g. forests) into cropland usually results in an immediate loss in biomass (removal of trees including roots) and a more gradual decline of carbon in the soil organic matter (SOM). The carbon released from biomass is emitted to the atmosphere as CO_2. SOM contains both nitrogen and carbon and a decline of SOM releases both CO_2 and N_2O. However, land use change may also cause an increase in soil carbon stock over the existing level (e.g. through changes in crop management) or in biomass (e.g. if grassland is cultivated with

permanent crops as tree crops or sugarcane). These effects on carbon stocks in the soil and vegetation are accounted for in the carbon balance.

There are at least three aspects to consider then:

a) The first aspect of the GHG impact, for correct estimate of size and location of the indirect GHG emissions, is the characteristic of the land which would be converted to evaluate how much carbon would be released as a result. Therefore, global maps of soil organic carbon levels under different land uses need to be provided in order to estimate the effects of changes in soil carbon associated with scenarios of change in cropping systems under demand for biofuels.

b) A second aspect is the calculation N_2O emissions due to mineralization of N accompanying soil carbon stock decrease

c) The thirds aspect is the evaluation of the CO_2 emissions which results from change in above and belowground biomass carbon stock due to changes in cropland area

A schematic representation of the whole methodology is explained in Figure 1.

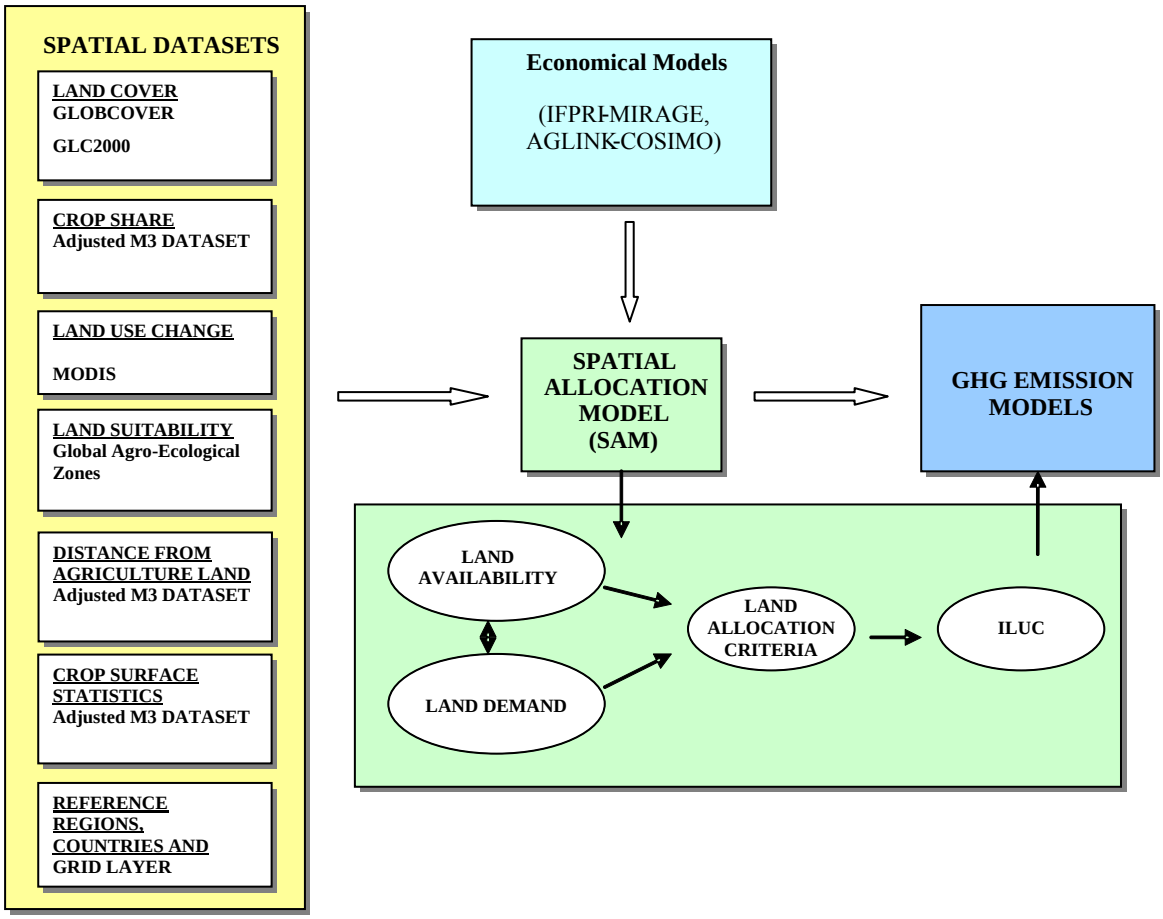

Figure 1: Scheme of the Spatial Allocation and GHG Emissions Calculations

The main focus of this work was to test and describe the methodology developed to provide quantitative estimates of changes in soil and vegetation carbon stocks and to evaluate the methodology when applied to the outputs of economic models with respect to indirect land use changes.

2. DATA SOURCES AND PROCESSING

A summary of the datasets that are used in this study is shown in Table 1. Additional datasets used to calculate land carbon stocks are described in detail in Carré *et al*., (2010).

Table 1: Summary of the Datasets Used in the Study

Name	Description	Year	Source
GlobCover	Land cover classification	2005	ESA-JRC
GLC2000	Land cover classification	2000	JRC-IES
McGill M3 Cropland and Pasture	Global agricultural lands distribution	Circa 2000 (1997-2003)	McGill and Wisconsin University
McGill M3 Crops	Crop Areas and Yields Reference	Circa 2000 (1997-2003)	McGill and Wisconsin University
MODIS Land Cover (MOD12Q1)	Historical Land Cover conversion trends	2001 and 2004	NASA and Boston University
SOIL	Harmonized World Soil Database (HWSD)	2009	IIASA, FAO, JRC and ISSCAS
GAEZ	Crop suitability maps	2002	IIASA
ESRI Data & Maps[5]	Administrative Boundaries	2008	ESRI
WorldClim	Historical climate data	1960	WorldClim
Aquastat	Irrigation		FAO and University of Frankfurt
MIRAGE model	Projection of cropland demand in 2020 for different biofuel policy scenarios	2008-2020	IFPRI-
AGLINK-COSIMO model	Projection of cropland demand in 2020 for different biofuel policy scenarios	2008-2020	JRC-IPTS

[5] ESRI Data & Maps [CD-ROM]. (2008). Redlands, CA: Environmental Systems Research Institute

2.1. SPATIAL DATA SETS

This work used several land cover datasets in combination because no single land cover map was suitable for this exercise.

2.1.1. LAND USE AND COVER LAYERS

For a reference on global land use / land cover (LC) data from the GlobCover[6] and the Global Land Cover 2000[7] projects were considered. Details on evaluating and processing the data are given in this section.

- **GlobCover**

  GlobCover is an initiative from ESA and realized in partnership with JRC, EEA, FAO, UNEP, GOFC-GOLD and IGBP. The images, on which the classification is based, were acquired from December 2004 to June 2006 by the MERIS instrument on the Envisat platform. The instrument sensors store data with a nominal resolution of 300m. The data are classified according to the categories of two schemes:

  - **Level 1** classification is applied to the global map product;
  - **Level 2** classification is used for 11 regional maps.

  The categories are largely compatible with the FAO Land Cover Classification System (LCCS; di Greggio & Jansen, 2000). Version 2.2 of the global map with the Level 1 legend has been used in this project.

  A list of the GlobCover Level 1 classes is given in Table 2.

[6] http://ionia1.esrin.esa.int/index.asp

[7] http://bioval.jrc.ec.europa.eu/products/glc2000/glc2000.php

Table 2: GlobCover Level 1 Classification

Class	Label
11	Post-flooding or irrigated croplands (or aquatic)
14	Rainfed croplands
20	Mosaic cropland (50-70%) / vegetation (grassland/shrubland/forest) (20-50%)
30	Mosaic vegetation (grassland/shrubland/forest) (50-70%) / cropland (20-50%)
40	Closed to open (>15%) broadleaved evergreen or semi-deciduous forest (>5m)
50	Closed (>40%) broadleaved deciduous forest (>5m)
60	Open (15-40%) broadleaved deciduous forest/woodland (>5m)
70	Closed (>40%) needleleaved evergreen forest (>5m)
90	Open (15-40%) needleleaved deciduous or evergreen forest (>5m)
100	Closed to open (>15%) mixed broadleaved and needleleaved forest (>5m)
110	Mosaic forest or shrubland (50-70%) / grassland (20-50%)
120	Mosaic grassland (50-70%) / forest or shrubland (20-50%)
130	Closed to open (>15%) (broadleaved or needleleaved, evergreen or deciduous) shrubland (<5m)
140	Closed to open (>15%) herbaceous vegetation (grassland, savannas or lichens/mosses)
150	Sparse (<15%) vegetation
160	Closed to open (>15%) broadleaved forest regularly flooded (semi-permanently or temporarily) - Fresh or brackish water
170	Closed (>40%) broadleaved forest or shrubland permanently flooded - Saline or brackish water
180	Closed to open (>15%) grassland or woody vegetation on regularly flooded or waterlogged soil - Fresh, brackish or saline water
190	Artificial surfaces and associated areas (Urban areas >50%)
200	Bare areas
210	Water bodies
220	Permanent snow and ice
230	No data (burnt areas, clouds, etc.)

- **Global Land Cover 2000**

The Global Land Cover 2000 product (GLC2000) of the JRC[8] is available for specific regions, but also as a single global layer. The layers for specific regions are available at advanced processing levels, but use different regional classification schemes. For the project the GLC2000 global product Version 1.1 from 26.01.2004

[8] http://bioval.jrc.ec.europa.eu/products/glc2000/glc2000.php

with the nominal spatial resolution of 1km at the Equator was used (approx. 30 arc sec.). The classification scheme of the global layer is given in Table 3.

Table 3: Global Land Cover 2000 Global Data Classification

Class	Label
1	Tree Cover, broadleaved, evergreen (closed > 40% tree cove; open 15-40% tree cover)
2	Tree Cover, broadleaved, deciduous, closed
3	Tree Cover, broadleaved, deciduous, open (open 15-40% tree cover)
4	Tree Cover, needle-leaved, evergreen
5	Tree Cover, needle-leaved, deciduous
6	Tree Cover, mixed leaf type
7	Tree Cover, regularly flooded, fresh water (& brackish)
8	Tree Cover, regularly flooded, saline water,
9	Mosaic: Tree cover / Other natural vegetation
10	Tree Cover, burnt
11	Shrub Cover, closed-open, evergreen
12	Shrub Cover, closed-open, deciduous
13	Herbaceous Cover, closed-open ((i) natural, (ii) pasture, (iii) sparse trees or shrubs)
14	Sparse Herbaceous or sparse Shrub Cover
15	Regularly flooded Shrub and/or Herbaceous Cover
16	Cultivated and managed areas
17	Mosaic: Cropland / Tree Cover / Other natural vegetation
18	Mosaic: Cropland / Shrub or Grass Cover
19	Bare Areas
20	Water Bodies (natural & artificial)
21	Snow and Ice (natural & artificial)
22	Artificial surfaces and associated areas

2.1.2. CROPLAND AND INDIVIDUAL CROP DATA

For the spatial allocation - assessing increase and decrease in area cultivated for single crops/crop groups - the crop distribution prior to the LUC is required. The McGill M3-Cropland and Crops Datasets[9] were used, because currently the McGill M3 maps are the only data set providing this information in the required spatial resolution. The data were

[9] http://www.geog.mcgill.ca/landuse/pub/Data/Agland2000/

produced by the Department of Geography, McGill University (Ramankutty *et al*., 2008). The McGill M3-Cropland layer was generated based on the land cover products of Boston University (Friedel *et al*., 2002) and the GLC2000 data set. The LC product from Boston University is based on MODIS data, from which an annual land cover type layer at 1km resolution grid (short name MOD12Q1)[10] is produced. For 159 countries the distribution of cropland and pastures were adjusted to the national statistics as available from FAOSTAT[11].

The McGill M3-Crop Data set contains the harvested areas and yields for 175 single crops. The dataset is provided at a 5 arc min. grid-cell resolution. The harvested areas and yields are also available aggregated into 11 crop groups.

2.1.3. SOIL PROPERTIES

Soil properties are derived from the Harmonized World Soil Database (HWSD)[12]. The database was developed by the Land Use Change and Agriculture Program of IIASA and the Food and Agriculture Organization of the United Nations (FAO) in collaboration with ISRIC-World Soil Information, the European Commission Joint Research Centre (JRC) and the Institute of Soil Science, Chinese Academy of Sciences (ISSCAS). The project used data as published under V.1.1 from 29.03.2009.

The database contains a spatial coverage on soil mapping units (SMUs) and tables containing the attributes in form of soil typological attributes (STUs). The spatial layer is distributed as a raster layer with a nominal resolution of 30 arc sec. The soil property information is arranged in two main tables, one related to the mapping units (HSWU_SMU) and one to the information of the properties of the typological units (HWSD_DATA). Codes and class values are stored in dictionary tables with explanatory comments.

2.1.4. MODIS LAND COVER

Historical land use change trends were derived from MODIS time series data. The MODIS Land Cover product contains multiple classification schemes, which describe land cover properties derived from observations spanning a year's input of "Terra" and "Aqua" satellite data. The primary land cover scheme identifies 17 land cover classes defined by the International Geosphere Biosphere Programme (IGBP), which includes

[10] https://lpdaac.usgs.gov/lpdaac/products/modis_products_table/land_cover/yearly_l3_global_1km2/mod12q1

[11] http://faostat.fao.org

[12] http://www.iiasa.ac.at/Research/LUC/External-World-soil-database/HTML/index.html?sb=1

11 natural vegetation classes, 3 mosaic land classes, and 3 non-vegetation land classes. The spatial resolution is 500 m and data are available for 4 years between 2001 and 2004.

Table 4: IGBP Land Cover Legend

Value	Description
0	Water Bodies
1	Evergreen Needle leaf Forest
2	Evergreen Broadleaf Forest
3	Deciduous Needle leaf Forest
4	Deciduous Broadleaf Forest
5	Mixed Forest
6	Closed Shrublands
7	Open Shrublands
8	Woody Savannas
9	Savannas
10	Grasslands
11	Permanent Wetlands
12	Croplands
13	Urban and Built-Up
14	Cropland/Natural Vegetation Mosaic
15	Permanent Snow and Ice
16	Barren or Sparsely Vegetated
17	Unclassified

The MODIS land cover dataset was not chosen as the reference for cropland acreage values, because of important discrepancies between MODIS land cover data and FAO statistics for the period 2001-2004 (differences that have been pointed out in a note provided by ENSUS (2009).

2.1.5. GLOBAL AGRO-ECOLOGICAL ZONES (GAEZ)

Land suitability for agriculture was derived from International Institute for Applied Systems Analysis (IIASA) and FAO's GAEZ (Global Agro-Ecological Zones) data for 2002. This data is used to drive the cropland expansion in the modelling framework.

The GAEZ uses a land resources inventory to assess feasible agricultural land-use options for specific management conditions and level of inputs, and to quantify the expected production of relevant cropping activities. The characterization of land

resources includes components of climate, soils, and landform, which are basic for the supply of water, energy, nutrients and physical support to plants (Fischer *et al*., 2002).

A conceptual overview of the method used to define the GAEZ is given in Figure 2.

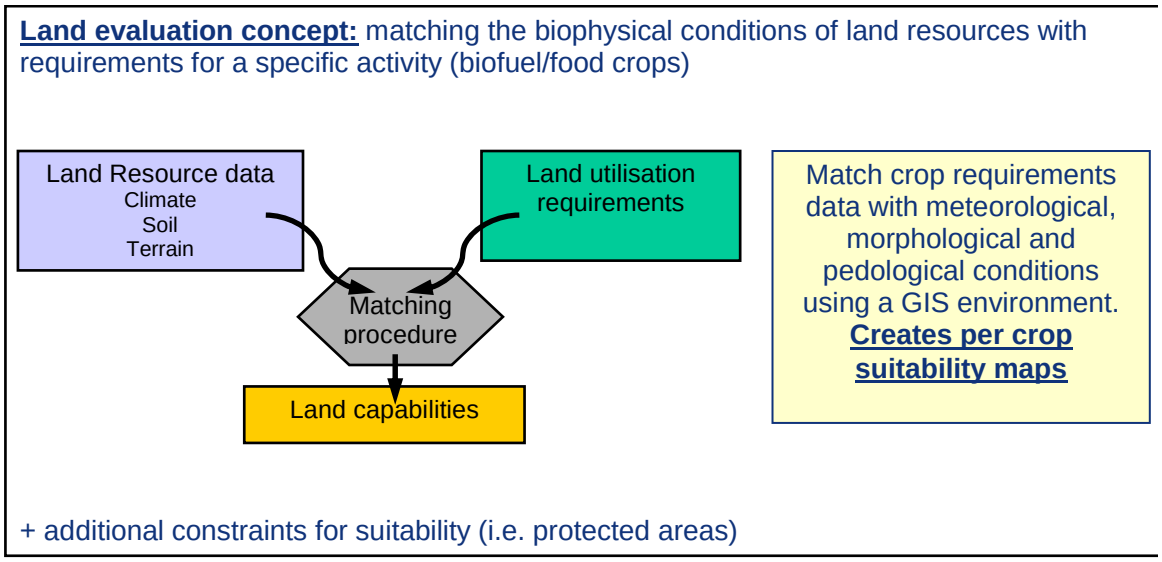

Figure 2: Land Evaluation Concept for Suitability Maps

In the spatial allocation procedure developed for this study by the JRC (Chapter 5.1), the GAEZ is used to estimate the likelihood of land for cropland expansion. Cropland will be allocated first on land with a good biophysical suitability for the concerned crop. An example of the suitability map for rain-fed rapeseed is presented in Figure 3.

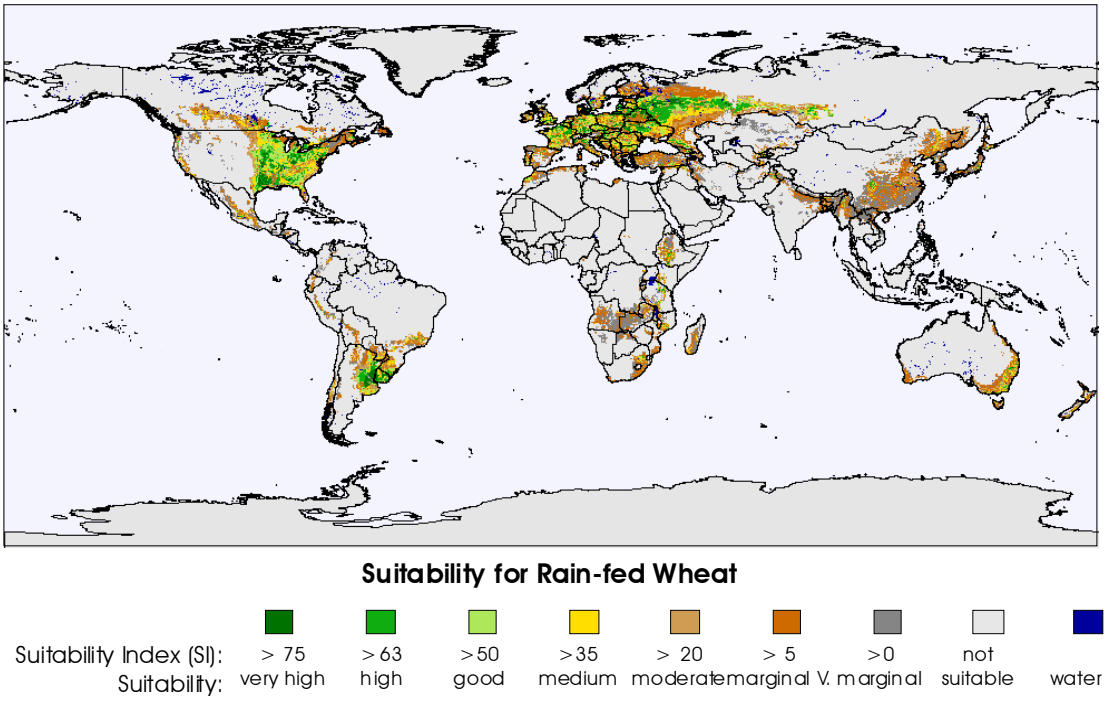

Figure 3: Suitability for Rain-fed Wheat, Intermediate Input (Plate 29, GAEZ, 2002)[13]

The suitability index (SI) reflects the suitability make-up of a particular grid-cell. In this index VS (very suitable) represents the portion of the grid-cell with attainable yields that are 80% or more of the maximum potential yield. Similarly, *S* (suitable), *MS* (moderately suitable) and *mS* (marginally suitable) represent portions of the grid-cell with attainable yields 60%-80%, 40%-60%, and 20%-40% of the maximum potential yield, respectively (IIASA).

There are differences in the data presented at the data downloaded from the GAEZ site und the data available form the SAEZ site: The GAEZ site provides access to crop suitability maps with intermediate inputs for rain-fed data, whereas the SEAZ site hosts suitability maps for high-level inputs. The data from the GEAZ site uses the older 16-bit Idrisi storage format, the SEAZ data is available in the newer 32-bit format. In the data available from the GEAZ site different class limits are given for the suitability values in the file metadata than are presented on the site. In the study the suitability index classes were used as given in the metadata for the files.

[13] http://www.iiasa.ac.at/Research/LUC/SAEZ/index.html or http://www.iiasa.ac.at/Research/LUC/GAEZ/index.htm

2.2. AGRO-ECONOMIC DATA

Data on land use change under different biofuel policy scenarios, which are used as input data for the spatial allocation procedure, come from agro-economic modelling work carried out by -IFPRI with the MIRAGE model and IPTS with the AGLINK-COSIMO model.

2.2.1. IFPRI-MIRAGE

The IFPRI-MIRAGE dataset provides the land use change as a consequence of EU biofuels policy assuming first-generation land-using ethanol and biodiesel achieving a 5.6% share of transport fuel consumption in 2020. The model assumes alternative trade policy scenarios: business as usual trade policy and full, multilateral trade liberalization in biofuels.

The trade policy scenarios are:

1. **MEU_BAU** (Business As Usual)

   Implementation of the EU biofuels mandate of achieving 5.6% consumption of ethanol and of biodiesel in 2020 under a Business as Usual trade policy assumption;

2. **MEU_FT** (Free Trade)

   Implementation of the EU biofuels mandate of achieving 5.6% consumption of ethanol and of biodiesel in 2020 with the assumption of full, multilateral, trade liberalization in biofuels. Contingent protection on US biodiesel remains.

In this study the agro-economic analysis is broken down into 7 crops or group of crops, namely:

- wheat
- maize
- rice
- sugar (sugar beet and sugar cane)
- oilseeds (including palm seed)
- fruits and vegetable
- other crops

The economic regions covered by IFPRI-MIRAGE economic analysis are presented in Table 5 and the corresponding map in Figure 4. These mapped regions were derived from the Eurostat GISCO countries dataset. More details about these economic regions are described in the IFPRI report (al-Riffai *et. al*., 2010).

Table 5: IFPRI-MIRAGE Economic Regions

Region Code	Region Description
Africa	Sub Saharan Africa
Brazil	Brazil
CAM Carib	Central America and Caribbean countries
China	China
CIS	CIS countries (inc. Ukraine)
EU27	European Union (27 members)
IndoMalay	Indonesia and Malaysia
LAC	Other Latin America countries (inc. Argentina)
RoOECD	Rest of OECD (inc. Canada & Australia)
RoW	Rest of the World
USA	United States of America

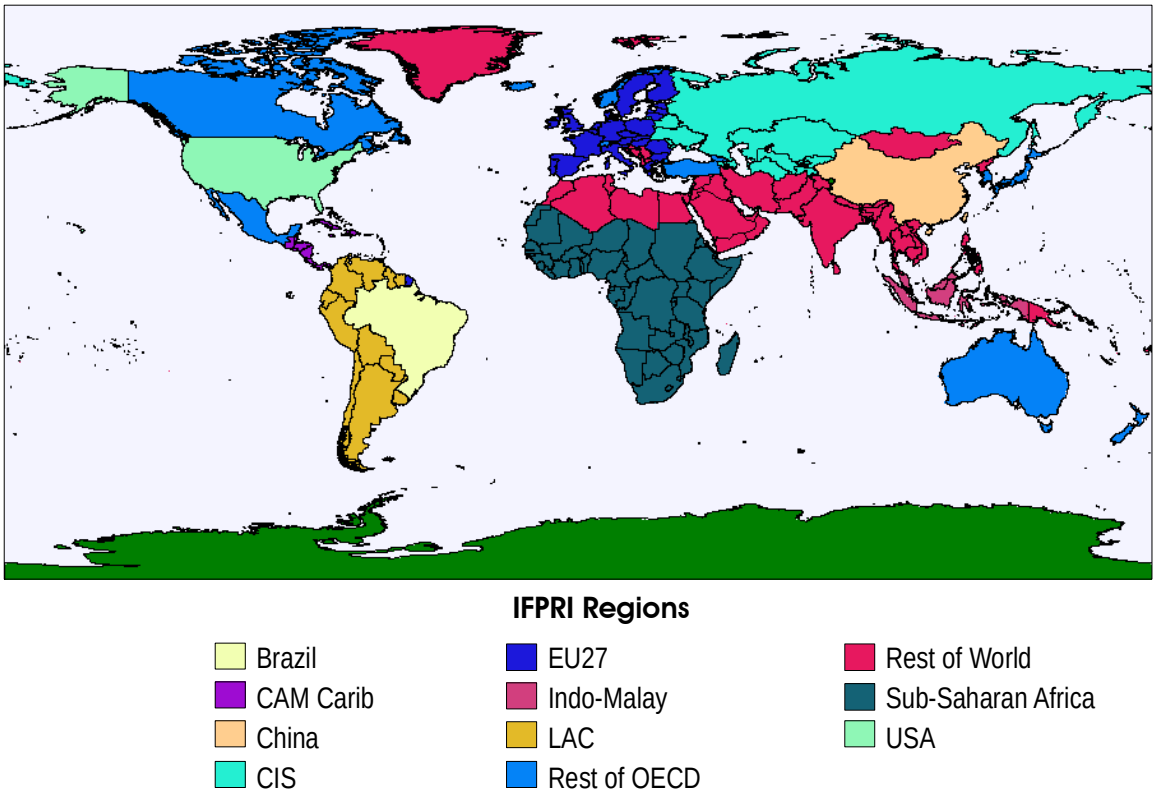

Figure 4: Regions as Defined for IFPRI-MIRAGE

2.2.2. JRC-IPTS AGLINK-COSIMO

The study carried out by the JRC-IPTS agro-economic modelling platform makes use of the AGLINK-COSIMO model (developed by OECD/FAO) to quantify the land use caused by EU biofuels policy. To compare the results with the IFPRI-MIRAGE model many of these regions were aggregated into the regions shown in Table 6.

Table 6: AGLINK-COSIMO Economic Regions

Region Code	Region Description
ARG	Argentina
AUS	Australia
BRA	Brazil
CAN	Canada
CHN	China (main)
EU27	EU27 (EU15, EU12)
JPN	Japan
KOR	South Korea
MEX	Mexico
NZL	New Zealand
RUS	Russia
USA	United States of America
IND	India
TUR	Turkey
ZAF	South Africa
IND	India
TUR	Turkey
OAF	Other African Countries: GHA, MOZ, ETH, TZA, ZMB, DZA, EGY, NGA, AWO, AWL, ASO, ASL, ANO, AEO
OAS	Other Asian Countries BGD, IDN, IRN, MYS, SAU, PAK, PHL, THA, VNM, OIS, OAP, APL
OEC	Other European Countries: OEE, OWE, UKR
OLA	Other Latin American Countries: CHL, COL, PER, CCD, OCA, OSA, PRY, URY
OTH	Others

The representation of commodities in AGLINK-COSIMO used in JRC-IPTS study is different from the one in IFPRI's analysis:

- wheat
- coarse grains (barley, maize, oats, sorghum)
- rice
- oilseeds (soy bean, rapeseed, sunflower seed)
- oilseed meals (soy bean meal, rapeseed meal, sunflower meal)
- vegetable oils (oilseed oil: soy bean oil, rapeseed oil, sunflower oil; palm oil)
- sugar beet
- sugar cane

- raw sugar
- white sugar

To allow a better comparison of the results of the two models and to apply the same methodology to both, the same crop categories provided in the IFPRI-MIRAGE dataset where applied to AGLINK-COSIMO data by aggregating some of the crops (e.g. sugar beet and sugar cane) into one category. According to the IFPRI-MIRAGE model crop categories, the groups considered are Maize, Wheat, Rice, Sugar crops, Oilseed crops, Vegetables and Fruit, and Other crops.

In the AGLINK-COSIMO dataset, Coarse Grain data (including barley, maize, oats, rye, triticale, millet, sorghum and other cereals) were available for all the modelled regions, whereas data solely for Maize were only available for a few of the regions. Therefore, two consecutive runs were executed: in one run, values for Coarse Grain instead of Maize were used, while in the second run Maize data were used where this data was available, and the remaining coarse grains were included in the group "Other".

Regional aggregation in the spatial allocation procedure was changed with respect to the one developed for IFPRI-MIRAGE, according to region definition in the AGLINK-COSIMO model as shown in Figure 5.

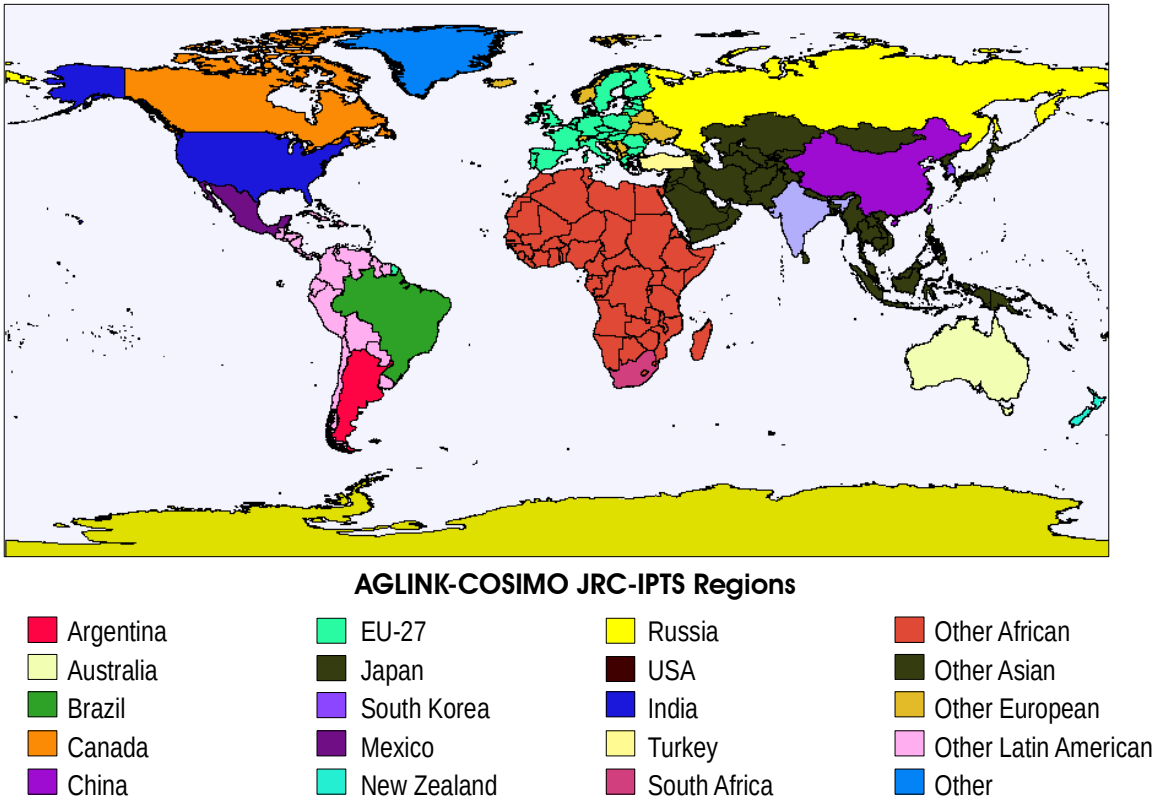

Figure 5: Regions as Defined for AGLINK-COSIMO JRC-IPTS Data

A modified version of the McGill M3 dataset was used as a baseline and reference layer was used. Then marginal area changes between the AGLINK biofuel scenario and the counterfactual scenario in 2020 were calculated and added to the McGill M3 reference.

2.2.3. BASELINE AND SCENARIO ASSUMPTIONS

This study derived the change in land demand for 2020. JRC-IPTS baseline includes EU biofuel policies and the counterfactual scenario, which assumes the absence of all internal EU biofuel policies. The impact of higher palm oil production in Indonesia and Malaysia on oil palm area is not calculated by AGLINK-COSIMO.

Regarding the EU biofuel policies, in the baseline scenario of AGLINK-COSIMO the energy share of biofuels is assumed to reach 8.5% in 2020, of which 7% consists of first generation and 1.5% second generation biofuels. Consistent with the RED, the energy provided by the latter is counted double for the purpose of meeting the 10% target. Starting from separate exogenous estimates of petrol and diesel consumption by the transport sector in 2020, the ethanol and biodiesel consumption in 2020 are each fixed at 8.5% of the total 2020 consumption of the corresponding fuel type. Second generation biofuel production is assumed to have no land use implications. Furthermore, it is assumed that tariffs are applied for EU imports of ethanol and biodiesel.

2.3. DATA PREPARATION

A considerable amount of effort went into the preparation of the spatial data layers. One task was to identify suitable thematic data to be used as reference in the computations. This was followed by investigating the data properties and identifying any deficiencies with respect to the completeness of the areas covered and thematic range of parameters included. The data retained were then harmonized for geographic and thematic properties.

Consistency of the data was found to be a crucial component in the methodology applied, which uses spatial modelling to estimate the effect of ILUC. The changes from ILUC are at times very marginal and small aberrations, such as differences in coastlines between spatial layers, may override the ILUC effect. Where a small change is distributed across a large number of grid cells even the storage format of the data can be of significant to the result. Therefore, all spatial data layers used in the study were processed to fully comply with the reference specifications.

2.3.1. STANDARD SPATIAL LAYER PROPERTIES

The spatial data layers with global coverage use a common raster format with standardized characteristics. All layers use a regular grid size of 5 arc min. The grid spacing corresponds to approx. 10 km at the equator. The data are arranged in geographic co-ordinates following the ETRS89 specifications (Annoni *et al.*, 2001). The specifications of the spatial layers are given in Table 7.

Table 7: Specifications of Spatial Data Layers

Feature	Value
Data type	16-bit integer or real*
File type	binary
No. of columns	4320
No of rows	2160
Reference system	ETRS89
Reference units	deg
Min. X co-ordinate	-180.0000
Max. X co-ordinate	180.0000
Min. Y co-ordinate	-90.0000
Max. Y co-ordinate	90.0000
Grid ID reference	1 – 9331200, (32 bit integer)
Grid ID surface area	Real, km^2

* *Depending on the information to be stored data formats are either 16-bit integer or floating-point (real). The range limits of integer values is -32768 and +32767, while it is 1.0E-38 to 1.0E+38 with 7 significant digital for data in floating-point format (IEEE 754 single; Goldberg, 1991). A 24-bit real number stores approx. 7 digits. The corresponding rounding error for the global land cover corresponds to 13.4 km^2, not including the Antarctic.*

The grid size of 5 arc min. was chosen in response to the spatial characteristics of the various thematic layers to be integrated.

- ***Soil***

  The soil data, although distributed with a nominal resolution of 1km, are derived from data at scale 1:5,000,000 for some parts. This could reasonably be mapped to a raster size of 5 km for a mapping accuracy of ±0.5mm.

- ***Climate***

  The meteorological data defining the climate regions are mapped to different scales, ranging from 30 arc sec. (approx. 1km at Equator) to 10 arc min. (approx. 18.5 km at Equator)[14].

- ***Land Cover***

  Land cover data from satellite imagery are available at various grid sizes. The products considered use a grid size of 300 m (GlobCover) or 1 km (GLC2000). The McGill M3 Cropland and Crops data set[15] from McGill University are available at 5 arc min. resolution.

- ***Ancillary Data***

  The global land suitability maps of the Food Insecurity, Poverty and Environment Global GIS Database (FGGD) are available as 5 arc min. layers through the FAO GeoNetwork site[16]. Other data used in support of the main thematic layers, such as the "*Land Use Systems of the World*" or the "*Global Agro-Ecological Zones*" are largely available at a grid size of 5 arc min. or lower resolution (0.5 deg.).

Under those circumstances a raster size of 5 arc min. was considered a practical compromise when integrating the assorted data sets.

- **Common Land/Sea Mask**

To avoid arbitrary results in coastal areas all spatial layers were adjusted to a standard land/sea mask. The mask was generated from the global GISCO country coverage at scale 1:1,000,000. Coastal areas in the thematic data layers were revised by using a distance function to allocate layer attributes to the common mask. The importance of a common land/sea mask should not be underrated when performing computations with spatial layers as overlays. For example, the total ILUC area for the IFPRI scenarios is less than the size of Crete. Where changes are comparatively small the effect of misalignments is correspondingly high.

- **Area Computations**

The model for distributing crop land processes data in tabular format. To allow exchanging data between the model and the spatial data a layer with unique identifiers for each grid cell was generated. The IDs start at the top-left corner with 1 and count along the rows the bottom-right corner. To reduce the amount of redundant information

[14] http://www.worldclim.org/current

[15] http://www.geog.mcgill.ca/~nramankutty/Datasets/Datasets.html

[16] http://www.fao.org/geonetwork/srv/en/main.home

the land/sea mask is applied to the grid IDs. For an analysis of the areas affected a layer with the surface area in km^2 was generated using a function of the GIS package Idrisi[17].

- **File Size Management**

The size of a file in original resolution with global coverage can render processing the data a resource-intensive task whichever method of reducing the spatial resolution is used. The size of the file on a hard disk can be misleading when a storage format with compression is used. For example, the GlobCover data are store in a file of 300Mb in a GeoTIFF format using compression. For processing the data are decompressed, which leads to a file size of approx. 9Gb. Depending on the GIS package used such files may require dividing the area into 2 or more subsets for processing. The final layers are then produced by merging the processed sub-areas into a single layer.

- **Re-Scaling of Layer Geometry**

When a spatial layer is available at a resolution higher than 5 arc min. the geometry of the data needs to be adjusted to the standard parameters. For reducing the spatial resolution of the data several options are available:

a)	Grid sampling, majority	⇨	single data layer	class, value
b)	Aggregation (mean, max)	⇨	single data layer	value
c)	Proportional distribution	⇨	multiple data layers	class

The grid sampling method is equivalent to systematic sampling of every n^{th} grid in the original layer. The resulting information is therefore biased against classes with a low representation in the data. Similarly, sampling the majority can introduce a bias in the distribution of values in the data with reduced spatial resolution. Aggregating data to a statistical indicator is only applicable for data values of a continuous range. The method can lead to a loss of the dynamic range in the lower-resolution data. The third method maintains the information on the proportional distribution of the classes and thus also includes those with a low occurrence, but has higher requirements for processing and data storage.

The first two methods lead to a single data layer to represent the original data. Those methods are relatively rapid to generate and provide considerable savings in data storage. Depending on the type of data to re-scale, either discrete classes or continuous values, some methods may not be applicable. All methods have in common that any information on the position of an attribute within the re-scaled grid cell is lost.

For the project it was considered preferable to conserve the representation of classes in the LC layer rather than saving on processing time and storage requirements. Therefore, the method of aggregating to the proportional distribution of LC classes was chosen, where the spatial resolution of the original data was reduced to the project grid cell size

[17] Clark Labs, Clark University 950 Main Street, Worcester MA 01610-1477 USA
http://www.clarklabs.org/

of 5arc min. by recording the proportional distribution of all classes. This results in a composite of 22 layers, each containing the relative occurrence of a class within 900 pixels of the original image for the GlobCover data.

- **Land Cover: Harmonization of Thematic Content**

The land cover classes specified by the RED, which could be converted to grow biofuels, are:

- Grassland, incl. degraded pastures
- Forest with <30% canopy cover
- Savannah and wooded savannah
- Degraded land

The categories of the LC data had to be aligned to correspond to these types of potential biofuel areas. The legend contains a combination of distinct and mixed land cover types. For distinct classes an assignment to one of the LC classes of the RED is possible without particular difficulty. Assigning land cover types of the mixed classes is less obvious and to some degree problematic. The main obstruction in aligning the LC types of the image data were the classes containing a mixture of LC types for biofuel production. These mixed classes represent a typical mosaic of several LC types, which could not be separated in the images. Although a proportion of a single class within the mosaic is indicated this proportion at times refers to a group of LC types without further differentiation. The solution adopted was to proportionally repartition the LC types of the mixed classes to the biofuel LC types.

A particular problem is generated by the threshold of a 30% forest cover to distinguish between areas on which could be converted to grow biofuels and forests, which cannot be converted to this purpose. Legend categories for GlobCover, GLC2000 and the LCCS use thresholds of 15% and 40% to classify forests in open or closed areas. According to the LCCS conversion table for GlobCover[18] all classes with >15% forest convert to forest. This does not lead to identifying a class of open forest with <30% cover. The extent of the convertible forest was therefore estimated by proportionally repartitioning the classes of the LC data for forest as for other categories of mixed uses or covers.

2.3.2. GLOBCOVER AND GLC2000 LEGEND ADAPTATION

In order to simplify comparing GlobCover and GLC2000 data a table of correspondence between categories of the two data sets was created. The classes defined in the new

[18] ftp://uranus.esrin.esa.int/pub/globcover_v2/global/GLOBCOVER_Products_Description_Validation_Report_I2.1.pdf

classification scheme are closely aligned to the LC types for growing biofuels and the 5 land use types defined for the IPCC Tier 1 approach to estimate GHG from soils. The correspondence is more detailed in the representation of forest cover in the datasets than for other types to improve the separation of forest types into open and closed fractions. Where no direct correspondence could be established the categories were merged until a reciprocated LC type could be formed. This procedure had to be applied in particular to categories of mixed LC types. It is still to some degree indistinct where a category contains ambiguity in the LC types it contains, i.e. were LC types are listed with an or condition. This is frequently the case in the Level 1 legend of the GlobCover data, but less so in the GLC2000 global legend.

The resulting classes are given in Table 8.

Table 8: GlobCover and GLC2000 Related to Simplified Common Legend

GlobCover Level 1 Legend	Common	GLC2000 Global Legend
Post-flooding or irrigated croplands (or aquatic) Rainfed croplands	10	Cultivated and managed areas
Mosaic cropland (50-70%) / vegetation (grassland/shrubland/forest) (20-50%) Mosaic vegetation (grassland/shrubland/forest) (50-70%) / cropland (20-50%)	11	Mosaic: Cropland / Tree Cover / Other natural vegetation Mosaic: Cropland / Shrub or Grass Cover
Closed to open (>15%) broadleaved evergreen or semi-deciduous forest (>5m)	21	Tree Cover, broadleaved, evergreen (closed > 40% tree cove; open 15-40% tree cover)
Closed (>40%) broadleaved deciduous forest (>5m)	22	Tree Cover, broadleaved, deciduous, closed
Open (15-40%) broadleaved deciduous forest/woodland (>5m)	23	Tree Cover, broadleaved, deciduous, open (open 15-40% tree cover)
Closed (>40%) needleleaved evergreen forest (>5m) Open (15-40%) needleleaved deciduous or evergreen forest (>5m)	24	Tree Cover, needle-leaved, evergreen Tree Cover, needle-leaved, deciduous
Closed to open (>15%) mixed broadleaved and needleleaved forest (>5m)	25	Tree Cover, mixed leaf type
Mosaic forest or shrubland (50-70%) / grassland (20-50%) Mosaic grassland (50-70%) / forest or shrubland (20-50%)	26	Mosaic: Tree cover / Other natural vegetation
Closed to open (>15%) (broadleaved or needleleaved, evergreen or deciduous) shrubland (<5m)	30	Shrub Cover, closed-open, evergreen Shrub Cover, closed-open, deciduous
Closed to open (>15%) herbaceous vegetation (grassland, savannas or lichens/mosses)	40	Herbaceous Cover, closed-open ((i) natural, (ii) pasture, (iii) sparse trees or shrubs)
Sparse (<15%) vegetation	50	Sparse Herbaceous or sparse Shrub Cover
Closed to open (>15%) broadleaved forest regularly flooded (semi-permanently or temporarily) - Fresh or brackish water		Tree Cover, regularly flooded, fresh water (& brackish)
Closed (>40%) broadleaved forest or shrubland permanently flooded - Saline or brackish water	60	Tree Cover, regularly flooded, saline water,
Closed to open (>15%) grassland or woody vegetation on regularly flooded or waterlogged soil - Fresh, brackish or saline water		Regularly flooded Shrub and/or Herbaceous Cover
Artificial surfaces and associated areas (Urban areas >50%)	70	Artificial surfaces and associated areas
Bare areas *Water bodies* Permanent snow and ice	80	Bare Areas Water Bodies (natural & artificial) Snow and Ice (natural & artificial)
No data (burnt areas, clouds, etc)		Tree Cover, burnt

The correspondence of the LC layers thus created was evaluated using a cross-classification of the data and the results of the comparison are presented in Table 9

Table 9: Results of Cross-Classification of GlobCover and GLC2000 Common Legend Layers

		GLC2000												Agree-ment
		10	*11*	*21*	*22*	*23*	*24*	*25*	*26*	*30*	*40*	*50*	*60*	
GlobCover	*10*	**83184**	12273	2916	6432	579	4579	621	725	8339	14303	3848	601	**60.1**
	11	81935	**35982**	12123	9769	4902	5891	1604	2392	21665	33563	14581	1584	**15.9**
	21	5186	11814	**111394**	3747	1828	1767	448	2436	4830	2476	717	1860	**75.0**
	22	11087	4865	3491	**39803**	4307	8791	12092	420	3444	3867	485	1608	**42.2**
	23	1571	1291	1474	3906	**15663**	474	394	2691	7911	1367	353	334	**41.8**
	24	3731	1343	2772	8164	324	**170987**	22211	9115	20404	5151	4810	9174	**66.2**
	25	838	560	37	5796	772	17490	**16435**	2042	3573	573	551	1966	**32.5**
	26	12782	4962	1098	8291	3858	25651	3848	**13398**	41911	29583	19524	2843	**8.0**
	30	9832	9962	6007	6016	12735	4527	720	1671	**48640**	13171	11596	1488	**38.5**
	40	17547	1466	646	2188	545	4331	815	4931	16151	**49134**	19834	793	**41.5**
	50	14637	3787	56	3471	925	10959	3124	7412	29035	32992	**150717**	6311	**57.2**
	60	660	802	3782	1096	295	2952	1308	624	1628	942	1556	**11895**	**43.2**
Agree-ment		**34.2**	**40.4**	**76.4**	**40.3**	**33.5**	**66.2**	**25.8**	**28.0**	**23.4**	**26.3**	**65.9**	**29.4**	**45.1**

Categories as defined in Table 9.

The overall level of agreement between the re-classified GlobCover and GLC2000 data sets was 45.1%. The representation between comparable categories did generally not exceed 75%. It was best for "*Closed to open broadleaved evergreen or semi-deciduous forest*" (Category 21: 76.4/75.0%), followed by the merged category of "*Open and closed needleleaved evergreen forest*" (Category 24: 66.2/66.2%). The LC type "*Shrub*" (Category 30) in the GLC2000 data appears predominantly in forest categories in the GlobCover data. This confusion is more consequential than the confusion between shrub and herbaceous areas because forest areas should not be converted to produce biofuels, whilst areas covered by shrub or herbaceous vegetation are treated correspondingly.

To some degree the spatial variation in the categories between the data sets can be attributed to the procedure of aggregating the data by using the central grid value. This will lead invariably to an amplification of any geometric differences between the spatial layers. Those variations become most notable in areas where the spatial distribution of the categories is patchy. To evaluate the spatial patter of the confusion of forest with other LC types between the two datasets the main mismatches of categories were mapped. The result is shown in Figure 6.

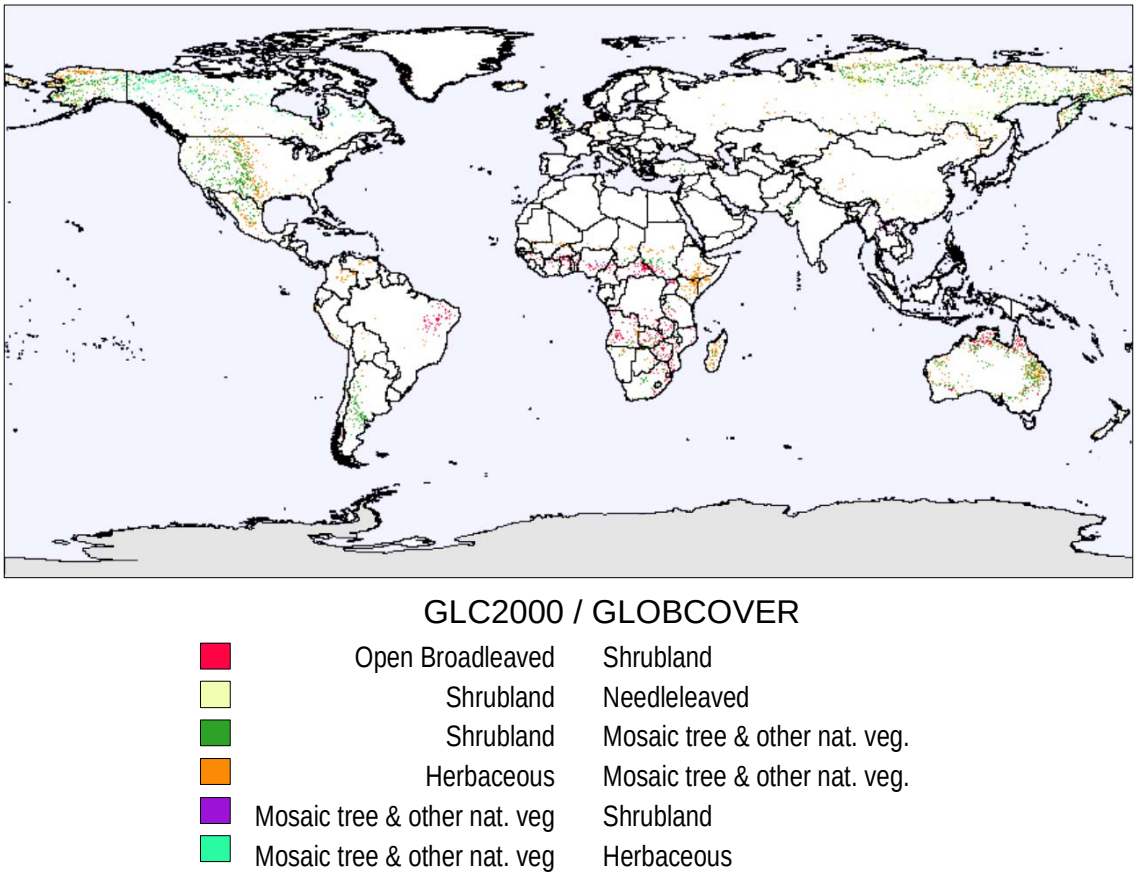

Figure 6: Location of Major Cross-Classification Differences between Forest and Other LC Types in GlobCover and GLC2000 after Reclassification to Common Legend

Open broadleaved tree cover in the GLC2000 data is mainly classified as shrubland in north-eastern Brazil, the savannah regions of Africa and northern Australia. Shrubland in the GLC2000 data classified as needle-leaved tree cover in the GlobCover data is found primarily in areas of boreal forest in Northern America and Siberia. Other cross-classifications of forests relate to categories of mixed classes, in which forests could also be included.

The conclusions drawn from the comparison of the GlobCover data with GLC2000 for mapping forest, and in particular areas of tree cover of <30%, are limited. Both datasets do not indicate the areas of open forest, which could be converted to produce biofuels directly. Categories containing a mixture or mosaic of LC types are inherently difficult to disaggregate because any LC type of the combination could be identified as an individual category in another dataset. There also appears to be some confusion between open forest and shrubland. The consequences of this divergence in classification may not be of great consequence where a high proportion of the open forest with 15-40% tree cover falls into the category of <30% tree cover. The differences in classifying shrubland and areas of herbaceous vegetation are considered largely inconsequential to the project because both can in principal be converted to produce biofuel.

As a practical and still conservative solution to the problem of identifying areas with forest <30% cover it was decided to allocate 60% of the open forest classes to forest with <30% cover and 40% to forest with >=30% cover. A category of shrubland was included as a separate category in the LC data set and not merged with herbaceous vegetation to form a category of "*Savannah and wooded savannah*". Areas of wetland were also identified as separate categories not specifically defined for the conversion to biofuel. The potential changes in organic carbon on wetlands following a transformation of land cover or use are being treated by IPCC using separate conversion factors for example for changes in soil organic carbon. These variations could only be considered by allowing a separate treatment of wetlands.

The proportions assigned to the GlobCover Level 1 legend to generate the LC classes for the biofuel project are given in Table 10

Table 10: Weighting Factors for GlobCover Level 1 Legend to Biofuel LC Categories

Label	Forest <30%	Forest >30%	Cropland	Grassland	Shrub	Sparse	Wetlands	Settlements	Other Land
Post-flooding or irrigated croplands (or aquatic)			1.00						
Rainfed croplands			1.00						
Mosaic cropland (50-70%) / vegetation (grassland/shrubland/forest) (20-50%)	0.10	0.10	0.60	0.10	0.10				
Mosaic vegetation (grassland/shrubland/forest) (50-70%) / cropland (20-50%)	0.10	0.10	0.40	0.20	0.20				
Closed to open (>15%) broadleaved evergreen or semi-deciduous forest (>5m)		1.00							
Closed (>40%) broadleaved deciduous forest (>5m)		1.00							
Open (15-40%) broadleaved deciduous forest/woodland (>5m)	0.70	0.30							
Closed (>40%) needleleaved evergreen forest (>5m)		1.00							
Open (15-40%) needleleaved deciduous or evergreen forest (>5m)	0.70	0.30							
Closed to open (>15%) mixed broadleaved and needleleaved forest (>5m)	0.30	0.70							
Mosaic forest or shrubland (50-70%) / grassland (20-50%)	0.10	0.20		0.40	0.30				
Mosaic grassland (50-70%) / forest or shrubland (20-50%)	0.10	0.10		0.60	0.20				
Closed to open (>15%) (broadleaved or needleleaved, evergreen or deciduous) shrubland (<5m)					1.00				
Closed to open (>15%) herbaceous vegetation (grassland, savannas or lichens/mosses)				1.00					
Sparse (<15%) vegetation						1.00			
Closed to open (>15%) broadleaved forest regularly flooded (semi-permanently or temporarily) - Fresh or brackish water							1.00		
Closed (>40%) broadleaved forest or shrubland permanently flooded - Saline or brackish water							1.00		
Closed to open (>15%) grassland or woody vegetation on regularly flooded or waterlogged soil - Fresh, brackish or saline water							1.00		
Artificial surfaces and associated areas (Urban areas >50%)								1.00	
Bare areas									1.00
Water bodies									1.00
Permanent snow and ice									1.00

An analogous weighting was applied to the GLC2000 classification scheme, as shown in Table 11.

Table 11: Weighting Factors for GLC2000 Legend to Biofuel LC Categories

Label	Forest <30%	Forest >30%	Cropland	Grassland	Shrub	Sparse	Wetlands	Settlements	Other Land
Tree Cover, broadleaved, evergreen (closed > 40% tree cove; open 15-40% tree cover)		1.00							
Tree Cover, broadleaved, deciduous, closed		1.00							
Tree Cover, broadleaved, deciduous, open (open 15-40% tree cover)	0.70	0.30							
Tree Cover, needle-leaved, evergreen	0.20	0.80							
Tree Cover, needle-leaved, deciduous	0.30	0.70							
Tree Cover, mixed leaf type	0.20	0.80							
Tree Cover, regularly flooded, fresh water (& brackish)							1.00		
Tree Cover, regularly flooded, saline water,							1.00		
Mosaic: Tree cover / Other natural vegetation	0.30	0.30		0.20	0.20				
Tree Cover, burnt									1.00
Shrub Cover, closed-open, evergreen					1.00				
Shrub Cover, closed-open, deciduous					1.00				
Herbaceous Cover, closed-open ((i) natural, (ii) pasture, (iii) sparse trees or shrubs)				0.75	0.25				
Sparse Herbaceous or sparse Shrub Cover						1.00			
Regularly flooded Shrub and/or Herbaceous Cover							1.00		
Cultivated and managed areas			1.00						
Mosaic: Cropland / Tree Cover / Other natural vegetation	0.10	0.20	0.60	0.10					
Mosaic: Cropland / Shrub or Grass Cover			0.60	0.20	0.20				
Bare Areas									1.00
Water Bodies (natural & artificial)									1.00
Snow and Ice (natural & artificial)									1.00
Artificial surfaces and associated areas								1.00	

The weighting factors for GLC2000 are aligned to those used for the GlobCover data where comparable classes are defined. There are some notable exceptions for classes of undetermined forest density. Comparing the classification results the class "*Tree Cover, needle-leaved, deciduous*" uses a ratio of 30/70 for open and closed forest, while other classes use a ratio of 20/80. From the occurrence of the class it would appear that deciduous forests tend to be in areas where tree density is lower than for the other forests types. However, this is an observation relative to GlobCover data and not based on ground observations.

2.3.3. MCGILL M3-CROPLAND AND CROP DATA

An inconvenience of the GlobCover data when looking at European agriculture is that the identification of cropland is limited to areas below approx. 57 deg N. This includes most agricultural areas in the Baltic states, but only the coastal areas in Sweden are covered and completely omitted are croplands in Finland. Without additional data on the presence of cropland in those areas the GlobCover data would be of only limited use.

For reasons of compatibility with other applications, such as deposition, the category "*Cropland*" of the biofuel classification scheme was substituted by data from McGill M3-Cropland data sets. The data correspond to the spatial characteristics of the project dataset and were only adjusted to the land/sea overlay. However, the data relate to conditions of the year 2000 rather than 2006. This difference in time was considered acceptable because no extensive changes in the occurrence of cropland or pastures over the period of 6 years were expected.

The global area under cropland extracted from the McGill M3-Cropland layer is 15.1 mil. km^2. The area extracted from the re-classified GlobCover data is 17.4 mil. km^2. This figure is just outside the range given for the M3-Cropland data for a 90% confident level (17.1 mil. km^2). This difference of 15% could probably be accepted if one takes into consideration that the users' accuracy (percentage of land classified as a category actually belongs to that category) for the 3 categories of croplands of the GlobCover data ranges from 60.9 to 84.4%[19]. However, the differences may be unevenly distributed in space and thus lead to significantly conflicting identification of areas which could be converted to grow biofuel.

The difference in the proportion attributed to croplands between the McGill M3 data and the corresponding category of the re-classified GlobCover data has been calculated for the spatial layers and are shown in Figure 7.

[19] This figure for accuracy is derived for the category containing a single LUC type. When taking categories with mixed LUC types into account to compute the overall accuracy for a single LUC category the figure has to be adjusted. For example, from Table 8 in the GlobCover report for the combined categories of croplands (Categories 10+11+14) the users accuracy is computed as 84.9% and the producers' accuracy (percentage of land of a category classified as that category) as 44.2%. Category 10 (Cultivated and managed areas) does not occur in the spatial layer. It appears to have been included in Category 14 (Rainfed croplands).

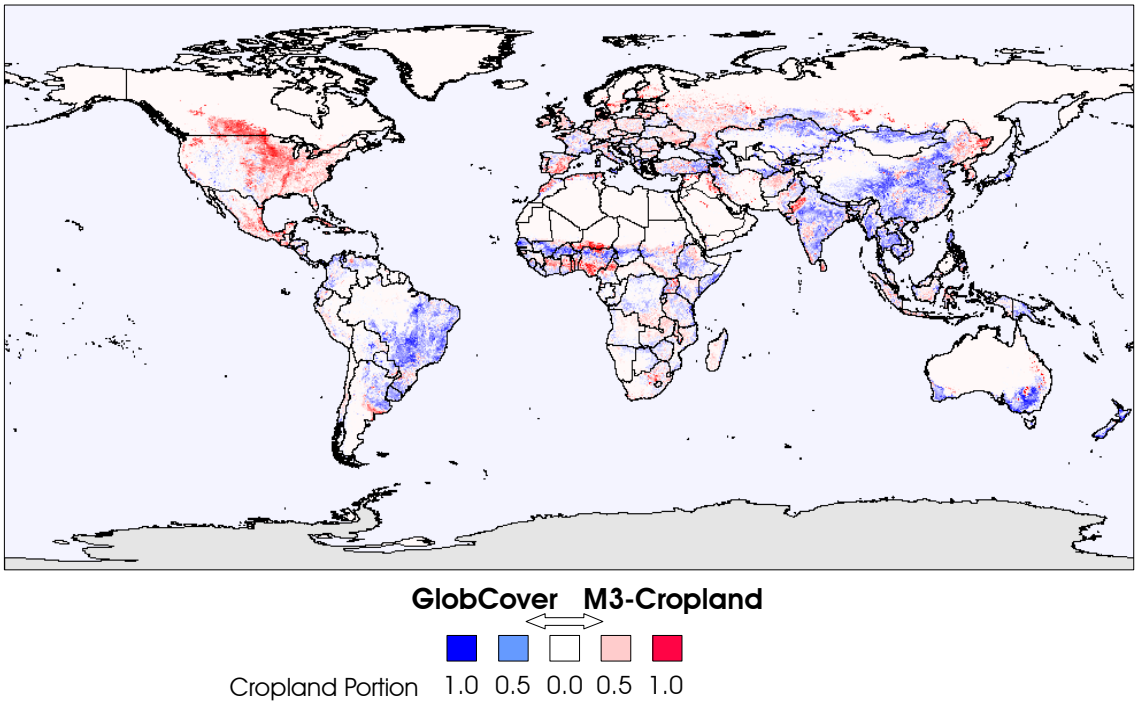

Figure 7: Difference in Proportion by Grid Cell for McGill M3-Cropland and Re-Classified GlobCover Data

Contrary to the differences in the occurrence of forest types between the re-classified GlobCover and GLC2000 data sets the differences in the relative occurrence of croplands in a 5 arc min. grid cell between the McGill M3-Cropland and the GlobCover data show some distinct regional trends. The GlobCover data assigns larger portions of croplands mainly in eastern parts of South America, South-East Asia and southern Australia. The McGill M3-Cropland data show more cropland in northern America and Europe. In Africa the differences are pronounced in sub-Sahelian regions, albeit more localized.

A similar evaluation was performed for the LC type *Pasture*. The differences in the relative proportions assigned to the McGill M3 and the re-classified GlobCover data are presented in Figure 8.

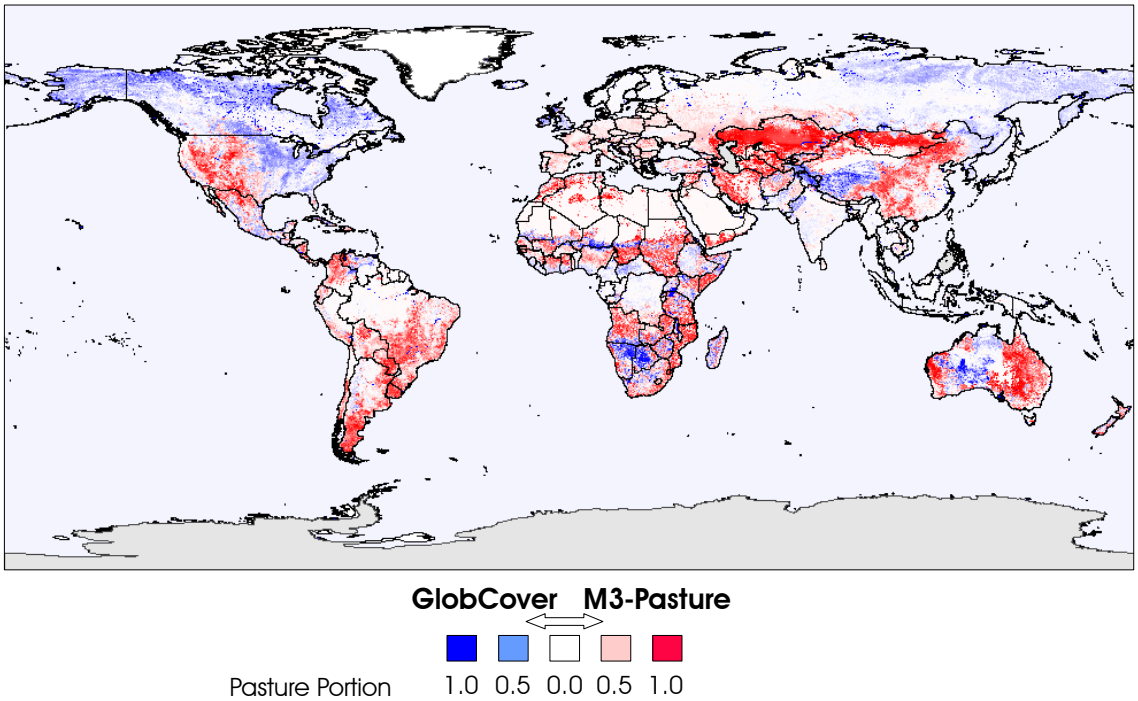

Figure 8: Difference in Proportion by Grid Cell for McGill M3-Pasture and Re-Classified GlobCover Data

The disparity in the allocation of pastures between the two data sets is even more pronounced than for cropland. To assess that the disparity was not caused by the re-classification procedure of the GlobCover data the category containing only herbaceous vegetation (Class 140) was also compared to the McGill M3-Pasture layer. Also for those data the regional differences were as prevalent as for the re-classified data.

When comparing the distribution of the differences for cropland to those for grassland an inverse trend in the identification in the GlobCover data by region is notable (see also Figure 7). Grassland in northern America is defined as cropland in the M3 data while for southern America the inverse relationship is found. A similar trend can be noted for eastern Asia. Another condition leading to the differences is the uncertainty in the separation of pastures from shrubland. This confusion dominates the disparity in eastern parts of North America and Africa. The herbaceous vegetation in central Asia and Australia is generally classified as sparse vegetation in the GlobCover data. Also for this LC type the characteristics separating one category from the other fluctuate.

It is not clear whether the differences between the data sets can at least in part be attributed to variations in the definition of pasture and grassland. The disparity in the distribution of croplands and the likely confusion of cropland with pastures or shrubland poses a problem to the identification of the LC type for the application of the IPCC Tier 1 GHG coefficients.

2.3.4. MERGING LC LAYERS WITH M3-CROPLAND AND M3-CROPS DATA

The statistical basis of the M3-Cropland and Crops Data suggests merging the M3 data with the GlobCover data. For all other LC classes GlobCover data were used. Following the large disparities in the location of pastures and grasslands the GlobCover grassland layer was retained and not replaced with the McGill M3-Pasture data.

The LC types identified in the Renewable Energy Directive are more generalized than the classes used in the economic models. The output from IFPRI-MIRAGE distinguishes the biofuel LC types, but models the development of changes for the following crops and crop groups:

- maize
- wheat
- rice
- sugar crops
- oilseed crops
- vegetables and fruit
- other crops

Information on the distribution of those crops is not available in the satellite-based LC products. The McGill M3-Crops Data layers provide an estimate of the spatial distribution of 175 crops based on FAO statistical data. Contrary to the McGill M3-Cropland data and other sources on LC the data for individual crops contains the proportion of harvested area instead of surface area. The harvested area takes into account multiple crops per year, which may be of the same or following a system of crop rotation. While the use of harvested area retains the proportion for crop yields when computed from production figures the change in LC is based on the surface area the crops use. Therefore, the harvested area of the McGill M3-Crops Data is expressed as surface area by adjusting the data for multiple cropping systems.

The number of crops grown on an area per calendar year is estimated as:

$$AREA_{harvested} = AREA_{surface} \times No_of_Harvests$$

where

$AREA_{harvested}$	represented by the McGill M3-Crops Data;
$AREA_{surface}$	from McGill M3-Cropland layer.

Hence, for the number of harvests the ratio $AREA_{harvested}$ / $AREA_{surface}$ is used.

While the number of harvests on a given location can only be an integer value the ratio figure is used because not all areas within a grid cell may follow the same crop system.

When it is known that no more than 2 crops are grown on a field within a year the portion of single and double cropping can be computed. In places where next to single cropping systems there also exist systems with 2 or 3 crops, the proportion cannot be computed without ambiguity. One approach to better define the number of crops in an area would be to use the occurrence of crops in multiple cropping systems. The maximum proportion of the harvested areas of crops and crop groups within a grid cell of the M3-Crops Data set is given in Table 12.

Table 12: Proportion of Harvested Area for Selected Crops and Crop Groups in M3-Crops Data

Crop Group	Harvested Area *Max. Proportion in Grid Cell*	Crop	Harvested Area *Max Proportion in Grid Cell*
Cereals	2.032	Maize	1.726
Fibre	1.909	Rice	1.930
Forage	1.027	Wheat	1.165
Fruit	1.531		
Oil Crop	1.628		
Other Crops	1.135		
Pulses	1.285		
Roots&Tubers	1.026		
Sugar Crops	1.626		
Tree nuts	0.810		
Vegetables&Melons	1.321		
Total Group	**2.975**	**Total Crop**	**2.032**

The proportion of harvested area in the McGill M3-Crop Data crop groups is highest for cereals (2.032) and lowest for tree nuts (0.810). The proportion of the harvested area of all crop groups indicates that at least triple cropping systems are practiced in some regions. Within the cereal group, the crop most widely used in multiple cropping systems is rice (1.930) while the occurrence of wheat is relatively low (1.165).

In the procedure applied to estimate the crop surface area from the harvested area the information on the maximum proportion of a crop or crop group indicating the presence in multiple cropping systems was not used. Apart from the complexity in the computations it was found that the areas of the McGill M3-Crops Data did not total the surface area of the McGill M3-Cropland in many regions. This discrepancy was attributed to a lack of the harvested areas of crops being reported in the statistical data, but also to areas of fallow land. The extent of missing crop areas or fallow land could be estimated when the surface area of the cropland exceeded the harvested area of all crop groups. Where the harvested area exceeds the cropland the extent of non-reported crops or fallow land could not be defined from the data.

The surface area of crop groups and crops was therefore computed depending on the difference between the harvested area and the cropland surface area as follows:

$$AREA_{surface} = AREA_{harvested} \qquad \text{for } \sum AREA_{harvested} < \sum AREA_{surface}$$

$$\left.\begin{array}{l} \\ AREA_{surface} = AREA_{harvested} \times \dfrac{\sum AREA_{surface}}{\sum AREA_{harvested}} \end{array}\right\} \qquad \text{for } \sum AREA_{harvested} \geq \sum AREA_{surface}$$

The difference [$AREA_{surface}$ - $AREA_{harvested}$] for [$AREA_{surface}$ - $AREA_{harvested}$] > 0 is stored in a separate layer to allow for fallow land.

The classification schemes used in the IPCC Tier 1 approach and the economic models do not fully cover the land surface area and use LC types or crops of different levels of the schemes. An overview of the LC types, groups and crops of the 4 classification schemes is given in Figure 9.

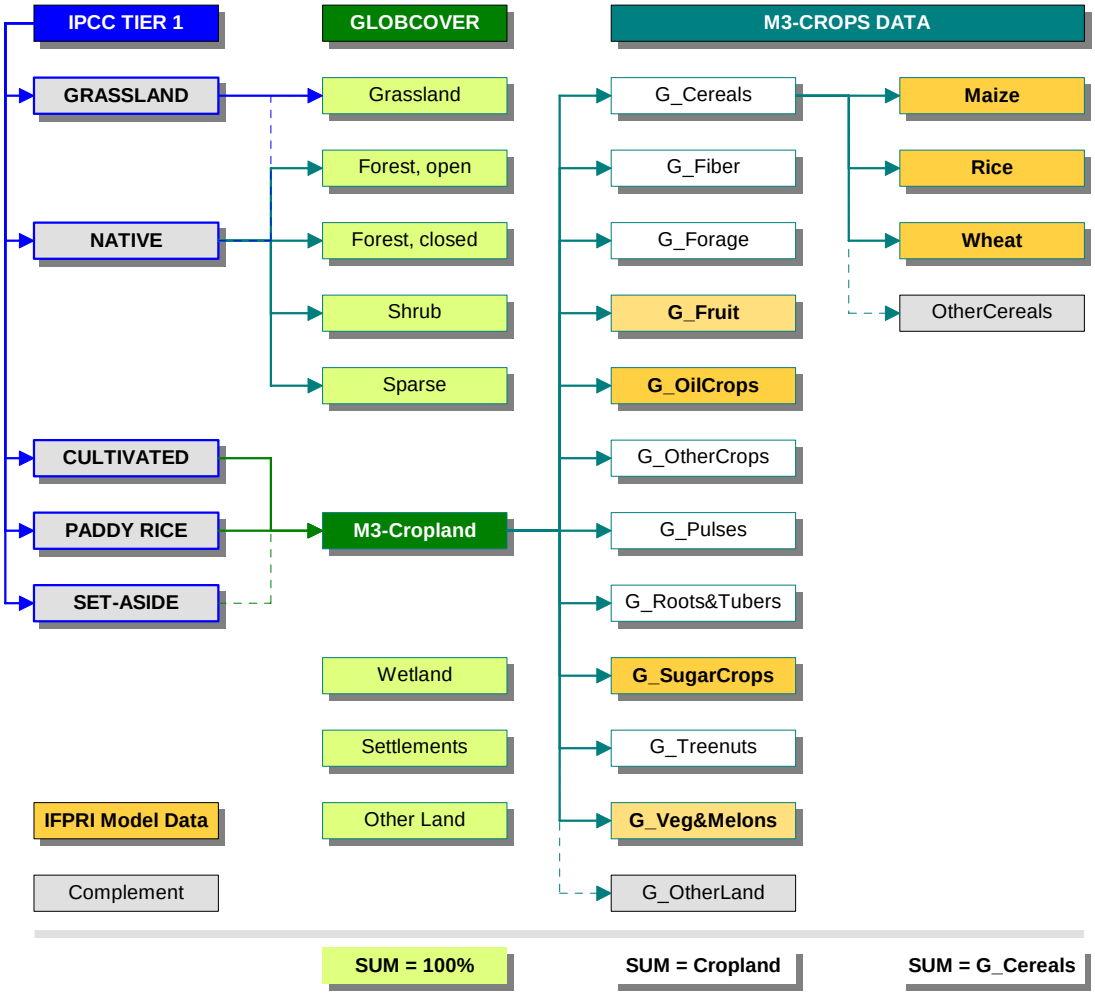

Figure 9: LC Types and Crop Classes of IPCC Tier 1, GlobCover, McGill M3-Crops Data and Economic Model

The LC type "*Grassland*" of the IPCC Tier 1 approach can be directly linked to the corresponding class derived from the GlobCover data. However, grassland can also be part of the "*Native*" LC type, as could be forests, both open and closed, shrub and sparse vegetation. The class "Set-aside" is linked the cropland since it is part of the cropland management system. The economic model uses individual crops, but also groups of crops. The partial use of individual crops, as for cereals, necessitates the creation of a complement class to fully cover the group of crops, as in the case of cereals. The creation of another complement group (*G_OtherLand*) was found to be needed to allow for differences between the sum of the area of crops and the cropland area.

In the preparation of the data for the spatial dispersion model the various crops and groups were arranged to sum to the total of the cropland area. To ensure data consistency all crop surface areas not identified as maize, wheat, rice, sugar crops, oilseed crops or vegetables and fruit were assigned to a complement class named "*Other_Crops*".

The distribution of the surface areas of the crops is processed in the spatial extent of the cropland LC type using the spatial layers directly. This procedure establishes spatial coherence between the cropland and the crop surface areas, but also simplifies the integration of the M3 data into the GlobCover layers. Only the cropland layer needs to be merged, because the layers for individual crops are already harmonized with the M3 cropland layer.

Merging the M3-Cropland data with the GlobCover data is achieved by substituting the cropland layer of the re-classified GlobCover data with the M3-Cropland layer. The proportions are adjusted to fully cover an area with LC types and keeping the M3 layer data constant, as presented in the equation:

$$LUC_{M3_adj} = \frac{1 - LUC_{M3-Cropland}}{\sum LUC_{GC} - LUC_{GC_Cropland}}$$

where

$LC_{M3_Adjusted}$	LC type proportion adjusted for McGill M3 cropland
$LC_{M3_Cropland}$	McGill M3-Cropland proportion
LC_{GC}	LC cover type proportion in GlobCover data
$LC_{GC_Cropland}$	Cropland proportion in GlobCover data

In land areas without data the proportions of the LC classes were estimated based on the distribution found in the neighbouring areas using an inverse distance function. This step ensures that all land areas are covered with data. The procedure was extended to include inland water surfaces, which were not part of the original M3 data. The areas are accounted for in the class "*Other Land*" of the GlobCover layers.

Because the spatial re-sampling of the various thematic layers can introduce shifts in the position of a grid cell the LC types "*Settlements*" and "*Other Land*" are used as defined in the GlobCover data and were excluded from the spatial allocation procedure.

The proportions of the LC types and crops within a grid cell of the raster data were transferred from the spatial layers to a database format. (Tables BASE_LCSA and BASE_CROPS). These tables form the base data from which the spatial distribution of the crops is modelled in response to changes coming from the economic models.

2.3.5. Soil Types for IPCC Reference Values

The Tier 1 approach of IPCC to estimating soil organic carbon is based on defining default reference values under natural vegetation and then modifying those values by coefficients. The default reference values are defined for the combination of 9 soil types and 6 climatic zones. The coefficients are defined for changes in land use, agricultural

practice and applications of fertilizer, both mineral and in the form of manure. Default reference values are defined for mineral soils only and the topsoil layer (0-30 cm).

The reference values are defined for soil typologies following the classification schemes of the *United States Department of Agriculture* (USDA) soil taxonomy and the *World Reference Base for Soil Resources* (WRB). The HWSD provides for the primary soil typological units of a mapping unit the soil class according to WRB. For sub-units soil classes according to FAO74 or FAO90[20] are recorded in the database. These have to be mapped to the classes of the IPCC reference values using a separate procedure.

- **Harmonized World Soil Database**

Soil data were extracted from the Harmonized World Soil Database V1.1 as released in March, 2009. It is a compilation of several global and regional soil databases to a standard structure and harmonized thematic content.

The principal structure of the HWSD is depicted in Figure 10.

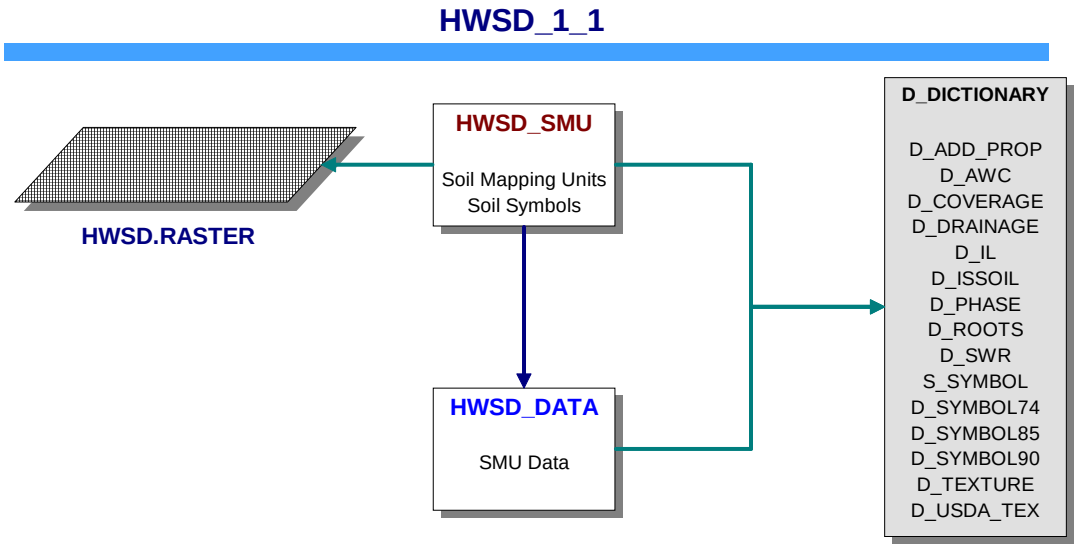

Figure 10: Main Tables of Harmonized World Soil Database v.1.1

The database comprises the spatial mapping units (SMU) as a raster layer (HWSD.RASTER) and the data characterizing to the SMUs in form of combination of properties forming the soil typological units (STU) (HWSD_DATA). In the HWSD a soil mapping unit is composed of up to 10 typological units, all with different soil properties. SMUs and STUs are linked by a table which also contains the dominant STU in an SMU (HWSD_SMU). Meta-data is provided by a number of dictionary tables.

In a deviation from the data model used for the *Soil Geographic Database of Eurasia* (SGDBE) the HWSD does not contain a separate table for the STUs. The corresponding

[20] FAO85 is used at times, but complemented by FAO90 codes.

data is recorded in the HWSD_DATA table for each SMU without a further link table. The arrangement is shown in Figure 11.

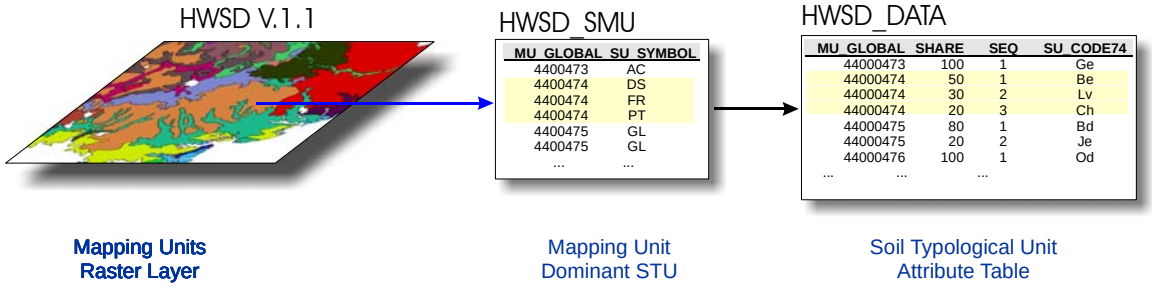

Figure 11: Spatial and Typological Units in Harmonized World Soil Database

A 1:n relationship exists between the HWSD_SMU and the attributes of the HWSD_DATA table. This condition makes mapping the complete range of attributes characterizing a mapping unit a non-trivial task. One approach to the problem is to link only the attributes of the dominant STU, as identified in the HWSD_SMU, to the spatial layer. Mapping all data pertaining to an SMU can be achieved for measured data by computing a weighted average for the area. For classified data a translation of the table data into a spatial database requires generating 10 spatial layers for each of the class attributes. This can considerably increase storage requirements of the spatial data.

- **Assigning IPCC Soil Types**

Several processing steps and data adjustments were taken to assign the mapping units to an IPCC soil type with a default reference value.

- ***Separation of Soil from "Other Areas"***

  "Other Areas" are all non-soil areas, such as rock outcrops, glaciers, sand dunes or inland water surfaces. The separation of soils from other areas is coded in the database in more than one table. Most explicitly areas of soils are given for the typological units through the field [HWSD_DATA.ISSOIL]. However, this information does not uniformly identify the soils. In 5 instances *fibric Histolos* (*Hfs*) were also classified as non-soil. Soils could also be separated from non-soils by using the dictionary table SU_SYMBOL linked to the HWSD_SMU table. For reasons which could not be established some typological units were declared non-soils, in particular as sand dunes and rocky outcrops.

  An overview of the entries in the field [HWSD_SMU.SYMBOL] with the field [HWSD_DATA.ISSOIL] gave the combinations given in Table 13.

Table 13: Classification of Soil and Surface Types of [HWSD_SMU.SYMBOL] to Field [HWSD_DATA.ISSOIL]

SU_SYMBOL	VALUE	ISSOIL ENTRY	
		NON_SOIL	SOIL
AC	Acrisols	1	2334
AL	Alisols		112
AN	Andosols	2	471
AR	Arenosols	8	3095
AT	Anthrosols	2	151
CH	Chernozems	6	711
CL	Calcisols	27	1882
CM	Cambisols	38	5794
FL	Fluvisols		1560
FR	Ferralsols		1847
GL	Gleysols	45	2325
GR	Greyzems	1	165
GY	Gypsisols	2	194
HS	Histosols	20	589
KS	Kastanozems	6	826
LP	Leptosols	84	6985
LV	Luvisols	5	4567
LX	Lixisols		1884
NT	Nitisols		967
PD	Podzoluvisols	11	905
PH	Phaeozems		1276
PL	Planosols		713
PT	Plinthosols		401
PZ	Podzols	91	1765
RG	Regosols	72	2868
SC	Solonchaks	11	594
SN	Solonetz	3	751
VR	Vertisols		1163
*DS**	*Sand Dunes*	*48*	*104*
*GG**	*Glaciers*	*9*	*2*
*IS**	*Island*	*1*	
*NI**	*No data*	*14*	*1*
*RK**	*Rock Outcrop*	*68*	*103*
*ST**	*Salt Flats*	*3*	
*UR**	*Urban, mining, etc.*	*6*	
*WR**	*Water Bodies*	*40*	

** Symbols referring to areas where no soils are defined.*

When classifying the records in the 3 soil classification dictionary tables (D_FAO74, D_FAO85 and D_FAO90) into soil and non-soil and linking the information with the corresponding fields in the HWSD_DATA table the combinations shown in Table 14 were found.

Table 14: Soil and Non-Soil Combinations for FAO Soil Classes

ISSOIL	FAO_74	FAO_85	FAO_90	COUNT
0			False	153
0			**True**	4
0		False	False	409
0		**True**	**True**	1
0	False			57
1			True	26,325
1		**False**	**True**	9
1		True	True	11,389
1	True			9,384

The table shows a consistent result in the separation of soil from non-soil classes between the tables only for the FAO 74 field. For FAO 85 and FAO 90 entries inconsistencies were found with the [ISSOIL] field in the data table and the classified soil entries in the dictionary tables in 5 cases. All cases concern *Histosols* and the reason for their classification as non-soil in the [HWSD_DATA.ISSOIL] field is not evident.

Also found were 9 cases of inconsistent classifications with respect to soil / non-soil between the FAO 85 and the FAO90 data. All cases relate to entries indicating "*No data*" in the FAO 85 field, while the FAO 90 field indicates a soil type (8 for "*ATa*" and 1 for "*ATc*").

Those inconsistencies between the field [HWSD_SMU.ISSOIL] and the dictionary tables diminish the use of the field to separate soil from non-soil records in the data table.

Coherence between the entries in the dictionary tables and the data table was assessed by analyzing data integrity for the [SYMBOL] field in the dictionary table and the corresponding fields in the data table.

- ***D_SYMBOL74***

  All entries in the field [HWSD_DATA.SU_SYM74] had corresponding entries in the field [D_SYMBOL74.SYMBOL]. Conversely, 7 entries in the field [D_SYMBOL74.SYMBOL] ("*??*", "*Cg*", "*D*", "*M*", "*Mg*", "*Pf*" and "*Wx*") did not occur in the corresponding field of the data table.

- ***D_SYMBOL85***

  Correspondence between the field [HWSD_DATA.SU_SYM85] and the linked field in the dictionary table could not be established for the entry indicating "No data" ("ND", 9 occurrences). The code in the dictionary table [D_SYMBOL85] for "*No data*" is "*NI*", while the data table uses "*NI*" and "*ND*", of which the latter is not defined in the dictionary table. The inverse relationship was not complete, because for 9 entries in the field [D_SYMBOL85.SYMBOL] ("*Bf*", "*Bm*", "*Dgd*", "*Eu*", "*Gms*", "*H*", "*MA*", "*NS*" and "*Uk*") no correspondence in the data table was found.

- ***D_SYMBOL90***

  The situation for the field containing the FAO 90 classification codes was more confusing. There were 21 codes in the dictionary table without correspondence in the data table. There were also two codes ("*Glu*", 1 case and "*NI*", 12 cases) in the data table without corresponding entries in the dictionary table. The entry "*Glu*" is most likely a typing error for "*Umbric Gleysols*", for which the code is "*GLu*".

The differences in coding non-soil surfaces between the 4 dictionary tables together with the confusion of coding the condition in the data table does not allow to establish full data integrity between the data and the dictionary tables. For this end the data would have to be modified. Instead, a more coherent approach is to establish a link using the [CODE] field. This approach did not result in the inconsistencies in linking data to the dictionaries described above.

- **Spatial Representation of Soil Types**

The IPCC Tier 1 soil categories for default values are defined using the USDA soil taxonomy and the WRB classification schemes. The relationship for the WRB data of the HWSD and the IPCC soil types are given in Table 15 .

Table 15: Relating HWSD.SYMBOL Entries to IPCC Tier 1 Soil Type

Harmonized World Soil Database *D_SYMBOL.VALUE*	IPCC Soil Type *Name*
Arenosols	Sandy
Gleysols	Wetland
Andosols	Volcanic
Podzols, Podzoluvisols	Spodic
Alisols, Anthrosols, Calcisols, Cambisols, Chernozems, Fluvisols, Greyzems, Gypsisols, Kastanozems, Leptosols, Luvisols, Phaeozems, Regosols, Solonchaks, Solonetz, Vertisols	High Activity Clay soils (HAC)
Acrisols, Ferralsols, Lixisols, Nitisols, Planosols, Plinthosols	Low Activity Clay soils (LAC)
Histosols	*Organic**
Glaciers, island, rock outcrop, salt flats, sand dunes, urban, mining, water bodies, no data	*Other**

** Not defined in IPCC Classification Scheme*

When assigning IPCC soil types to the dominant typological unit 14 mapping units were identified for which no soil data were available. The units cover desert areas (Sinai, Namibia) and lakes (Sweden). The areas concerned were considered of no consequence to the analysis and no substitute soil types were introduced for the land areas.

- ***Classification of Sandy Soils***

  The first rule identifying sandy soils (Sand content >70% and Clay content <8%) could by applied directly to the data. In the dataset 1,692 mapping units were classified as sandy soils. The simple query procedure was possible because the database does not contain entries with empty records for texture[21]. In case of empty field entries the condition defined by the query would not have been met for those fields and the area attributed to one of the other soil classes.

  For the condition set to identify sandy soils the complete set of typological units for the mapping units was also used to allow an evaluation of the differences in the methodology. When using a weighted texture analysis 942 mapping units are classified as sandy soils. This constitutes quite a marked difference in the number of mapping units classified as sandy soils and demonstrates that taking the weighted mean of all typological units to characterize a mapping unit can introduce an element of bias to the distribution of a soil property, although the weighted value better represents the mapping unit. Since all other conditions of the classification scheme act on the categorical parameters (soil type), for which

[21] Only one mapping unit with an organic soil (HSf) was found without soil texture data.

mathematical methods of interpolating between values are not applicable the mapping units were classified according to the properties of the dominant soil type also to identify sandy soils.

Not included in the category of sandy soils were sand dunes. Those areas not classified as soils and in the majority of cases no soil types are attached to the typological units in the database. However, of the 48 typological units recorded as sand dunes, for 20 units a soil type was also recorded. Of those 9 cases had a value of <70% (between 39 and 47%) recorded for the sand texture property. The typological units where a soil type was recorded were included in the query to define sandy soils, while the units without soil type information were treated as sand dunes.

The re-classification used the soil class Arenosol to identify sandy soils rather than the texture conditions. This approach was preferred to using the conditions to be consistent in the methodology. Using conditions to define sandy soils could lead to excluding from the result typological units classified as Arenosols, but with a lower sand fraction or higher clay fraction. Because no other conditions are set in the classification scheme those soils could be excluded from being classified. The outcome depends on the implementation of how "Low Activity Clay Soils" are identified. Adhering strictly to the classification scheme LAC soils cover the areas not defined by any other soil type. Therefore, any areas of Arenosol would end in this category. In practice this involves removing all areas of non-soil first since the database also contains areas of rock, water, glaciers, etc.

- ***Classification of Wetland, Volcanic, Spodic, LAC and HAC Soils***

A wetland soil was the dominant typological unit for 821 mapping units. Mapping Unit 31531 uses "*Gl*" instead of "*GL*" as the symbol for Gleysols, which has to be considered when defining the query conditions. Classified as volcanic soils were 169 mapping units and 429 were classified as spodic soils. The separation of low-activity clay (LAC) soils from high-activity clay (HAC) soils was performed based on the soil types specified in the IPCC.

- ***Treatment of Anthrosols***

A separate treatment not specified in the IPCC procedures had to be applied to 124 cases where an Anthrosol was given for the dominant typological unit. These soils are defined by their anthropogenic influence rather than a soil property and may occur in any of the other classes. According to the recommendations of the SINFO study (Baruth *et al*., 2006) the 18 cases of *aric Anthrosols* (*ATa*) are converted to *aric Regosols* (*RGai*) and 104 cases of *cumulic Anthrosols* (*ATc*) were converted to *terric Anthrosols* (*ATtr*) in WRB98. The latter are regularly found in areas of wetland soils or of acid and unfertile soils (Driessen *et al*., 2001). As a consequence all *Anthrosols* were classified as HAC soils.

Also classified were areas of organic soils and those where no soils are present. For organic soils no default values are defined by IPCC. Under Tier 1 gaseous emissions from those areas are quantified using measurements methods instead of changes in carbon content.

- **Mapping IPCC Tier 1 Soil Types**

The IPCC soil types for SOC default values for mineral soils under native vegetation could be mapped directly to the spatial layer by using the dominant STU. Using only the information of the dominant STU for an SMU greatly simplifies data processing. It allows generating a single spatial layers for regardless of the value type of the soil property and without the need of computing aereal weights or other methods of aggregating properties.

The advantages in data management are balanced by reduced information content and susceptibility for introducing bias in the data. When a soil property is generally present as a sub-dominant typological unit the use of only the properties of the dominant unit introduces a bias against the representation of the sub-dominant soil type. Although demanding a much more involved processing task using the information of all STUs of the HWSD could produce a more detailed result.

The distribution of soils according to the IPCC classification scheme applied to the dominant typological unit of the HWSD is presented in Figure 12

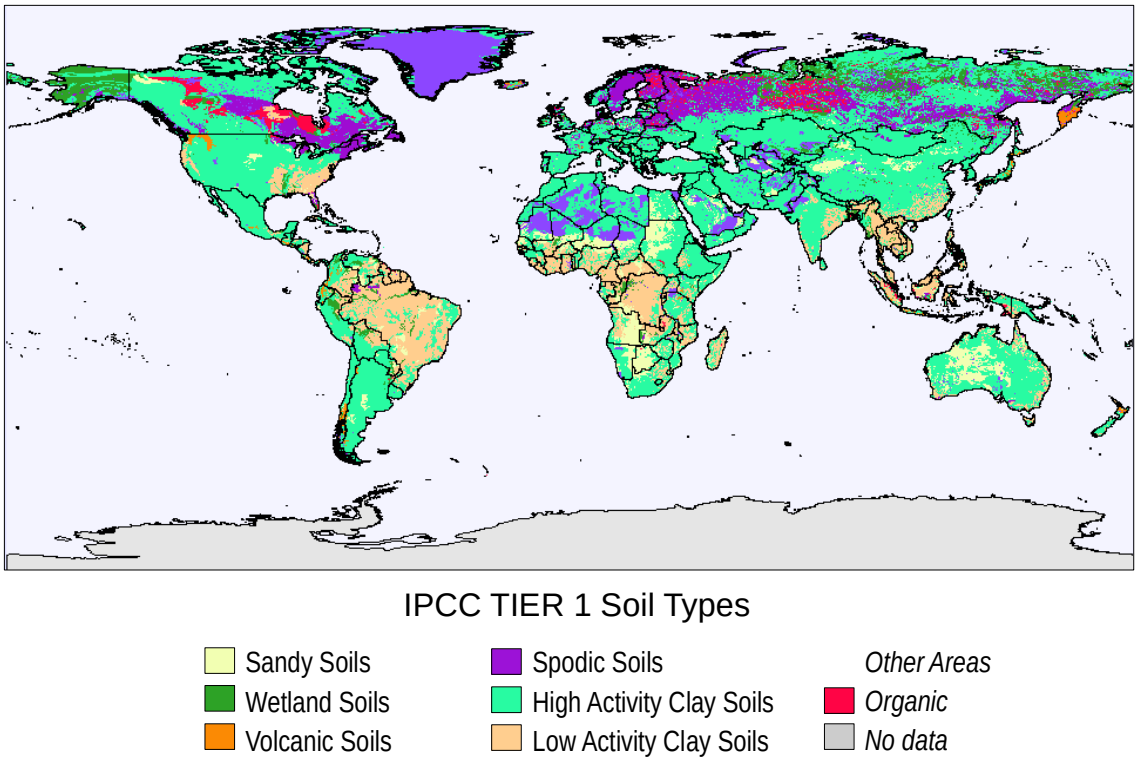

Figure 12: IPCC Soil Classification applied to Soil Type of Principal Mapping Unit of HWSD

The largest number of mapping units (9,939) are classified as HAC, followed by 2,525 mapping units classified as LAC. The distribution of the soil classes across the global land mass is given in Table 16.

Table 16: Distribution of IPCC Soil Classes Across Main Land Mass

IPCC Soil Category	Area	
	mil. km²	*%*
Organic	*2.65*	*2.0*
Sandy Soils	9.60	7.2
Wetland Soils	6.21	4.6
Volcanic Soils	0.97	0.7
Spodic Soils	9.10	6.8
High Activity Clay Soils	74.31	55.4
Low Activity Clay Soils	22.43	16.7
Other Areas	8.75	6.5
Total*	**134.01**	**100.00**

** Land area without Antarctica: 134,540,000 km²*

According to the classification organic soils cover just over 2% of the land surface while more than half of the land surface is covered by HAC soils. Most of the areas not classified into one of the soil types are caused by areas without data in the database. Those areas are mainly located in desert areas, such as the Sahara, and the Sinai Peninsula. Some areas are also not considered soils, such as glaciers, snow fields or bare rock. A specific condition is presented by sealed surfaces or urban areas. For larger urban areas the soil database does not contain information of the soil type. In the course of the project those areas were processed as found in the database. The total area defined as land in the spatial layer differs from the total land area because smaller islands are not included at the resolution of the spatial data layer.

- **Mapping IPCC Default Reference Values of SOC Stocks**

The Tier 1 approach of IPCC for estimating changes in carbon emissions from mineral soils is based on defining default reference values of SOC stocks under natural vegetation for specific soil types and depending on climatic zones. The default reference values are defined for the combination of 9 soil types and 6 climatic zones. Of the 54 possible combinations a default value is defined for 39 cases. For the 15 combinations without a default value it is assumed that the combination does not exists or is sufficiently rare to define a default value.

When using the IPCC soil type layer developed from the HWSD data and overlaying the climate zones combinations are found for which no default values are specified. The areas are comparatively small, as shown in Figure 13.

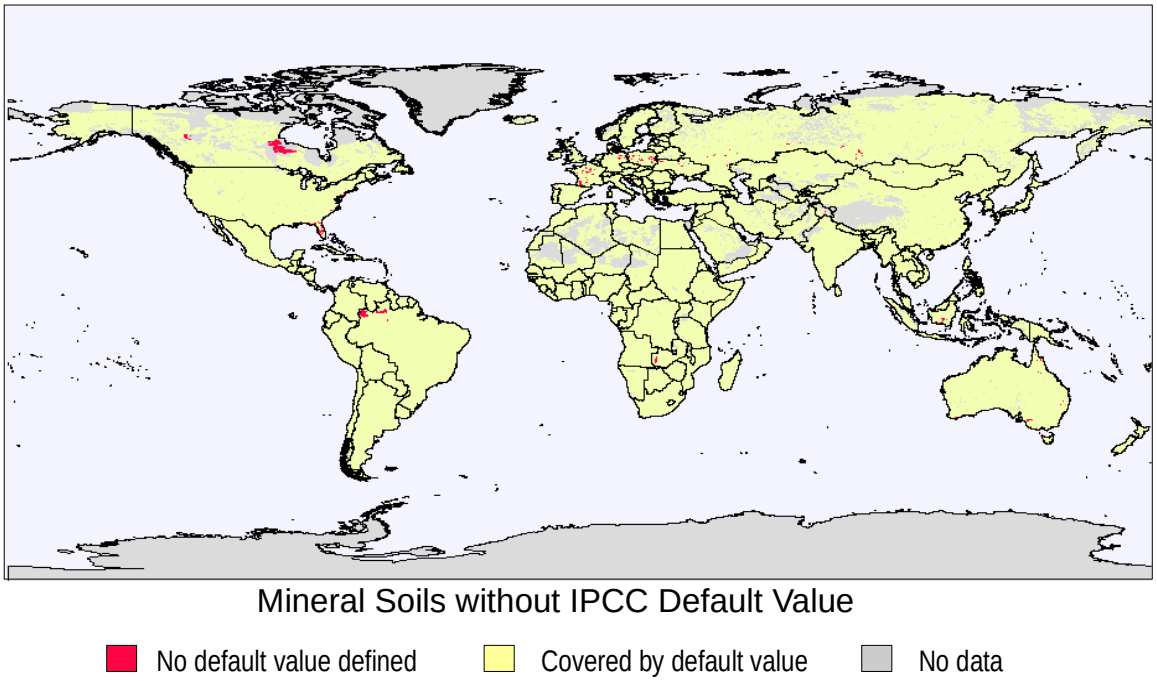

Figure 13: Areas without IPCC Default Values for SOC Stock in Combination of HWSD and Climate Zones

The areas not covered by an IPCC SOC stock default value in the data used are scattered on all continents. Larger SMU are found in Canada and Brazil. To include the areas in the GHG estimation suitable default values were estimated from the topsoil SOC stock developed from the HWSD. A layer of native vegetation was generated from the GlobCover and GLC2000 data by integrating the classes of forest, grassland, shrub, sparse and wetlands to represent native vegetation. In the combination of classes the original classification scheme was used. Classes containing mosaics were not used when they contained cropland, urban areas or other areas. Only those areas were used in the analysis for which the classes representing native vegetation exceeded a threshold of cell coverage.

The SOC stock data were processed in the database for SMUs using all STUs. The SMU SOC stock values were computed by integrating the area-weighted values of the STUs. The 5 arc min. layer of SOC stock was generated using two different methods of aggregating the data to the layer resolution:

- The SOC value is assigned directly to the SMU of the re-sampled 5 arc min. raster reference value.
- The SOC value is assigned to the SMU of the HWSD at full resolution and data are spatially integrated to the 5 arc min. layer.

The differences between aggregation methods are generally small and lower than the differences between LC layers. The greatest differences were found for organic soil, which are not covered by default values. The SOC stock values of the SMU in the re-

sampled data are generally higher than those from the spatially integrated layer, with differences ranging from 11 to 77 kg for 90% coverage (11 to 96 for 95% coverage). Other soil/climate combinations showed distinctly lower variances with a tendency for lower values in the SOC layer of the re-sampled SMU for sandy soils and higher values for volcanic soils.

Also investigated was the influence of the proportion of native vegetation in a grid cell. Thresholds of 90 and 95% were used to accept a cell in the analysis. For both LC layers the mean SOC stocks generally increased with a higher portion of native vegetation in the cell. However, the changes were, however, small and did not exceed 4 kg for mineral soil. A reverse trend was found on wetland soils, where the mean SOC stocks decreased with an increase in native vegetation cover. This tendency was present for both the GlobCover and the GLC2000 data.

The IPCC SOC default values were compared to the values of the HWSD using GLC2000 data to specify areas of native vegetation with a coverage of >95% of a grid cell. The GLC2000 data was given preference over GlobCover data because the data were used in the preparation of the HWSD.

A difference in the mean SOC stock values in the soil database between forest and herbaceous cover was evaluated only for the GLC2000 data. For a native vegetation coverage of >95% the SOC value for soils under herbaceous cover was lower than under trees in 50 soil/climate combinations, while it was higher under herbaceous vegetation cover for 23 combinations.

The comparison between the IPCC default values and the SOC values of the soil/climate layer using GLC2000 to define forest and herbaceous vegetation was performed with a vegetation coverage minimum of 95% instead of 99%. The lower threshold was used because for a limited number of classes the sample size was at times too small, leading to spurious results. Given the spatially aligned differences in SOC stocks between soils under forest and grassland the maximum value for either LC type was extracted.

The resulting mean SOC stock values for the topsoil layer and the IPCC default values for the soil/climate combinations are given in Table 17.

Table 17: Comparison of SOC Stock in Topsoil from HWSD / Climate Zone Data to IPCC Default Values (GLC2000, 95% Coverage)

Climate Zone	Sandy		Wetland		Volcanic		Spodic		HAC		LAC	
	IPCC	SOIL/Clim	IPCC	SOIL/Clim	IPCC	SOIL/Clim	IPCC	SOIL/Clim	IPCC	SOIL/Clim	IPCC	SOIL/Clim
Warm Temperate Moist	34	37	88	60	80	101		70	88	47	63	46
	+3		-28		+21				-41		-17	
Warm Temperate Dry	19	20	88	52	70	85		63	38	28	24	36
	+1		-36		+15				-10		+12	
Cool Temperate Moist	71	36	87	64	130	93	115	76	95	49	85	52
	-35		-23		-37		-39		-46		-33	
Cool Temperate Dry	34	21	87	62	20	91		65	50	40	33	46
	-13		-25		+71				-10		+13	
Polar Moist		23		79		103		80		40		50
Polar Dry		24		86		19*		64		49		52**
Boreal Moist***	34	26	146	79	20	99	117	77	68	48	63	82
	-8		-67		+79		-40		-20		+19	
Boreal Dry***	19	25	146	84	20	-	117	64	68	50	60	70
	+6		-62				-53		-18		+10	
Tropical Montane	71	19	86	53	80	94		93	88	35	47	44
	-52		-33		+14				-53		-3	
Tropical Wet	34	42	86	75	130	109		91	87	49	35	49
	+8		-11		-21				-38		+14	
Tropical Moist	21	29	86	67	70	114		75	65	41	63	40
	+9		-19		+44				-24		-23	
Tropical Dry	22	22	86	51	50	76		67	53	27	60	32
	+0		-35		+26				-26		-28	

* *For with >70% native vegetation cover.*
** *For with >85% native vegetation cover.*
*** *IPCC does not distinguish between Boreal, moist or dry.*

The SOC stock value of the soil/climate layer deviate at times significantly from the IPCC default values. For 34 cases the values are lower than the IPCC default value, while in 14 cases it is higher. The mean of the difference is -11.8 t ha^{-1}. Only for volcanic soils does the soil/climate data provide generally higher estimates than IPCC for default values. The differences between the data merits a more in-depth investigation, in particular the delineation of zones with native vegetation. It would also be preferable to include data from measured soil profiles in the analysis. However, such a study was outside the scope of this work.

The consequences of the differences on estimating emissions of carbon from the soil depend on the distribution of the soils. As shown in Figure 12, the most prevalent soils are of type HAC, followed by LAC. For HAC soils the IPCC default values are largely

higher than the SOC stock values extracted from the soil/climate data. Conversely, the SOC stock values from the soil/climate layer are mainly higher for LAC soils than the IPCC default values.

For further processing of the soil data the IPCC default values were used where available and the values extracted from the soil/climate layer for combinations for which no default values were defined. The areas covered by the substitute values are very limited, as shown in Figure 13.

Although the method of estimating carbon emissions from peat is fundamentally different in the IPCC Tier 1 approach from estimating carbon emissions from mineral soils the average SOC stock values for organic soils were also extracted from the soil/climate layer. The stock of OC in the 0-30cm of organic soils was relatively stable across climate zones and ranged from 193 (Tropical Montane) to 276 t ha^{-1} (Cool Temperate, dry).

The default reference values were mapped to the combination of the HWSD soil class layer and the climate zones. The resulting spatial layer of default reference values for the depth interval of 0-30 cm of mineral soils under native vegetation and applied to the dominant STU is presented in Figure 14.

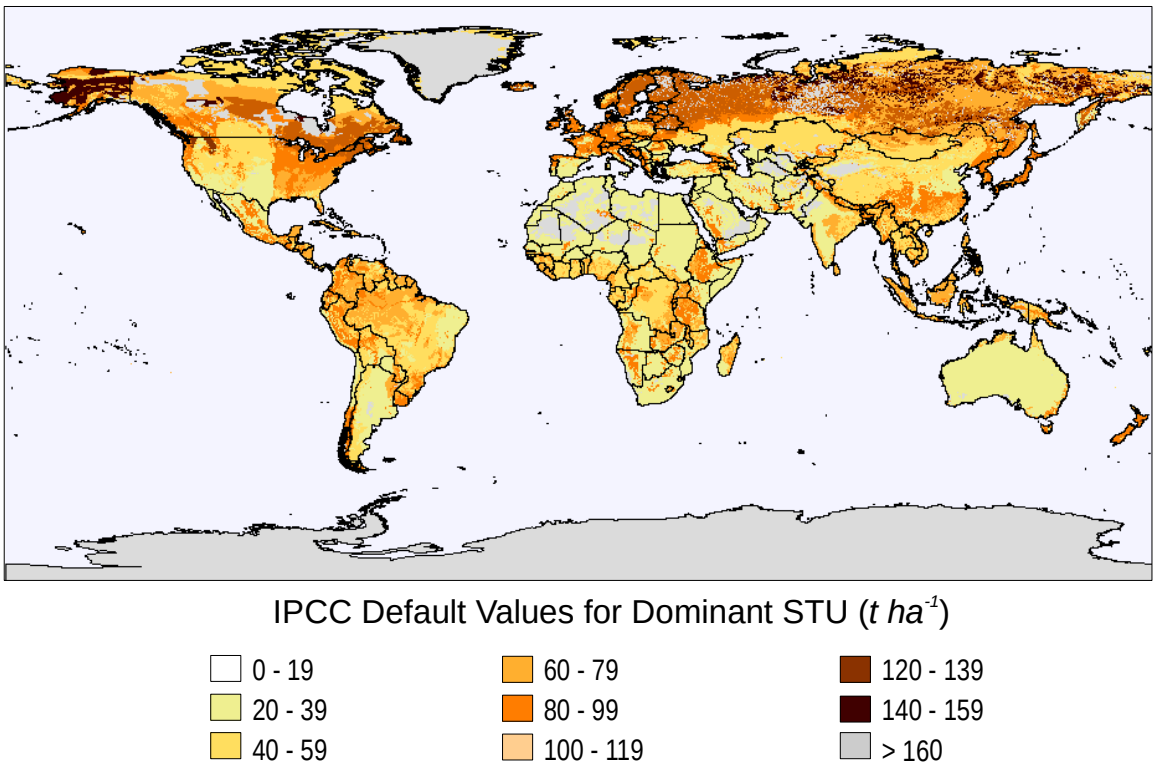

Figure 14: Mapped IPCC Default Reference Values of Soil Organic Carbon under Native Vegetation and Applied to Dominant STU

The default values were also applied to the soil type classification of all STUs and then spatially weighted to provide a single value per grid cell. The resulting SOC stock layer is presented in Figure 15.

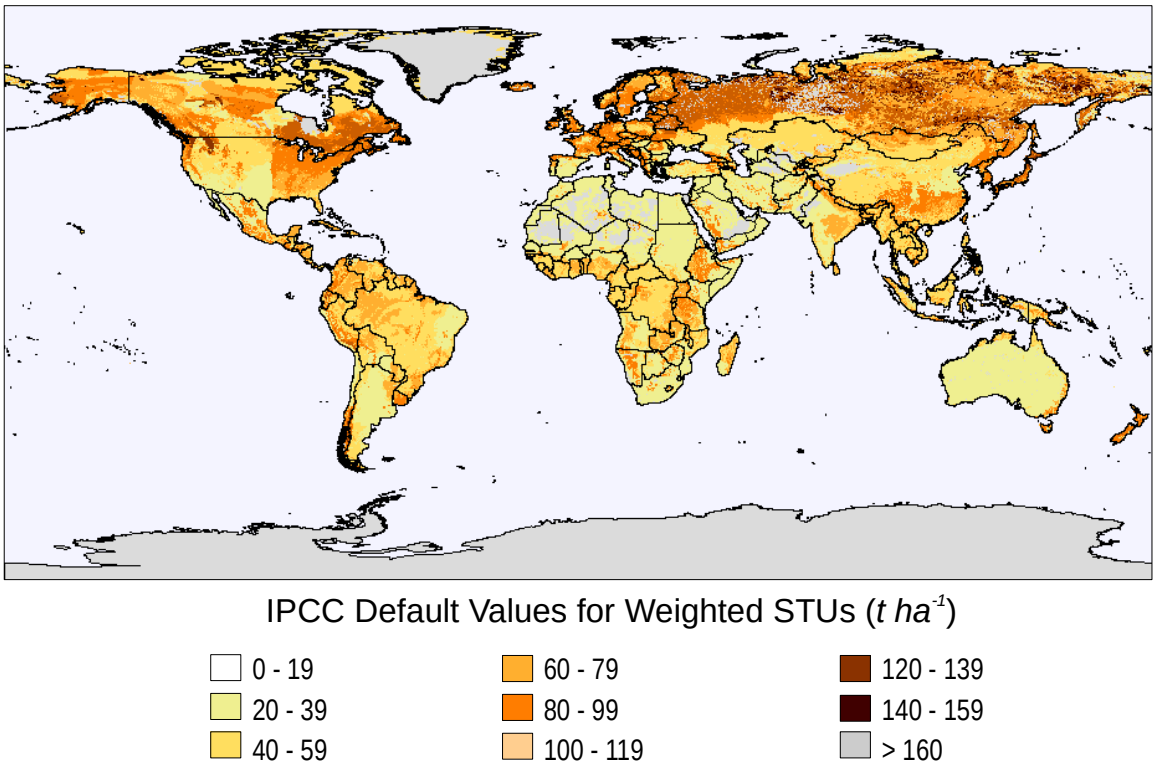

Figure 15: Mapped IPCC Default Reference Values of Soil Organic Carbon under Native Vegetation and Applied to all STUs after Spatial Weighting

Differences in the distribution of the default values are not immediately evident in the layers. A difference map of SOC stock between the dominant STU and integrating data from all STUs is shown in Figure 16.

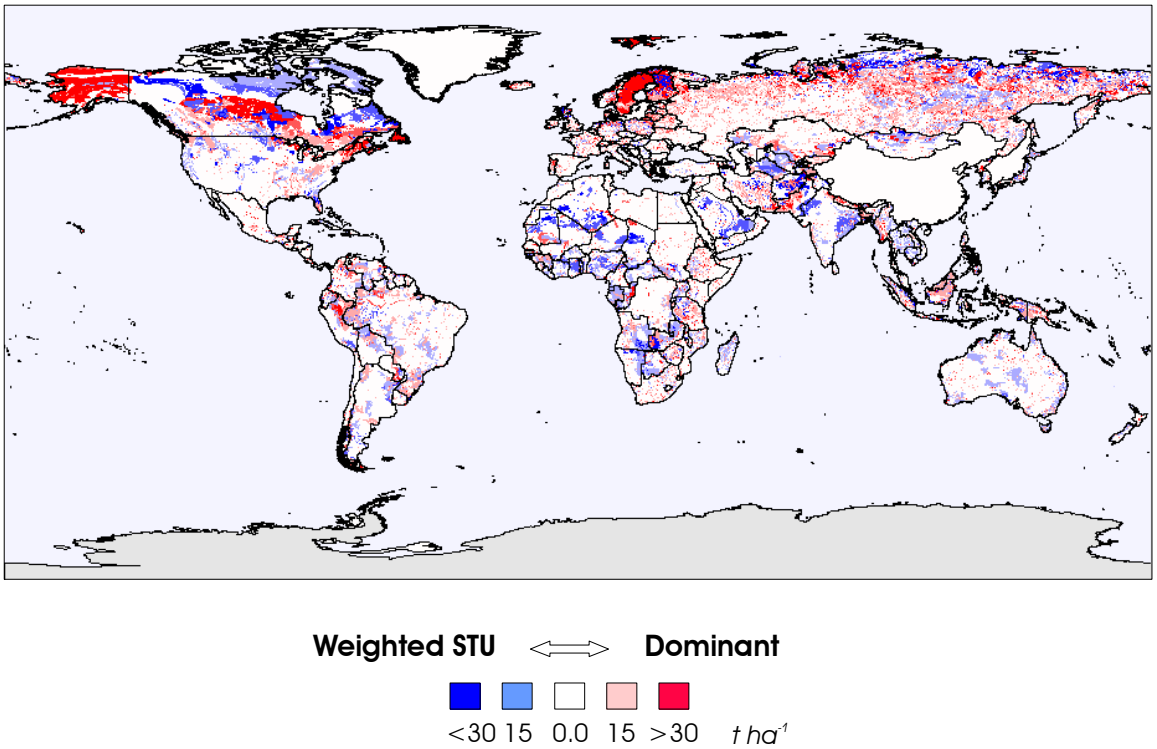

Figure 16: Difference in Mapped IPCC Default Reference Values of Soil Organic Carbon under Native Vegetation between dominant STU and integrating all STUs

The difference map shows lower as well as higher SOC stock values in most areas. A notable exception is China, where the SMU is characterized by one STU. Hence, there is no difference in the values. Larger areas of default values > 30 t ha^{-1} for the dominant STU mapping method are found in areas of organic soils in Alaska, Canada and Sweden. Canada also shows larger areas with default values lower by 30 t ha^{-1}, which are otherwise prevalent in Africa and India.

The global SOC stock for mineral topsoils (0 - 30 cm) using IPCC default values results in 743 Pg when applied to the dominant STU of the HWSD. Integrating data from all STUs results in a global figure of 735 Pg. This compares to estimates for SOC of 684 - 724 Pg of C in the upper 30 cm (1462 - 1548 Pg of C in the upper 100 cm) (Batjes, 2005). It should be noted that the estimates of actual SOC stocks include C from organic soils. From the area of organic soils (2.65 M km^2) the amount of C in the top layer 0 – 30cm can be estimated at 159 Pg (C content: 60%; bulk density: 0.1 g cm^{-3}). The total stock of C under native vegetation in the soil layer 0 – 30 cm could then be estimated at 894 Pg. This is a theoretical figure with actual values expected to be lower.

2.3.6. CLIMATE REGIONS

The IPCC Guidelines for National Greenhouse Gas Inventories defines rules for the classification of 12 climate regions (IPCC, 2006). The graph is reproduced in Figure 17 .

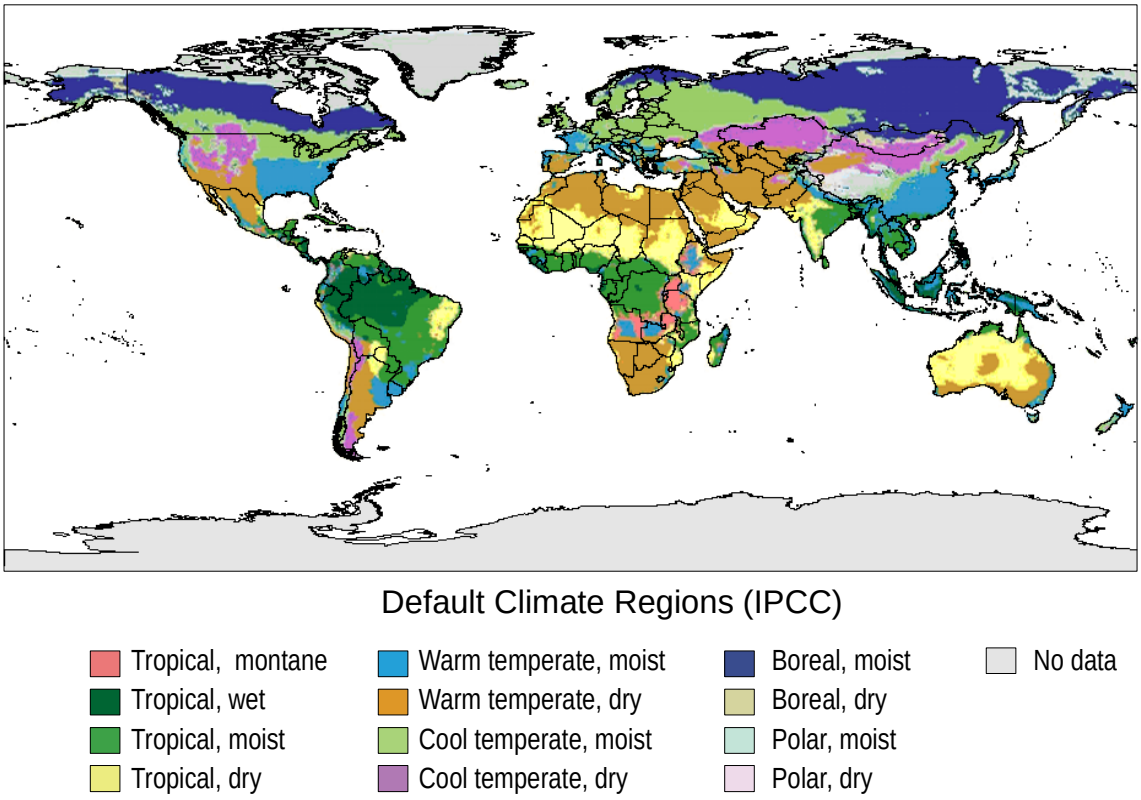

Figure 17: IPCC Default Climate Regions, Figure 3A.5.1, (reproduced IPCC, 2006)

The zones are separated based on the annual mean daily temperature, the total annual precipitation, the total annual potential evapo-transpiration (PET) and elevation. Including PET in the classification scheme separates classification from other commonly used classification systems, such as the system from Köppen-Geiger (Peel, *et al*., 2007).

The classification presented as "*Figure 3A.5.1 Delineation of major climate zones, updated from the 1996 IPCC Guidelines*" (IPCC, 2006) could not be accessed in electronic form as a spatial layer and alternative sources of the data had to be used. The classification scheme applied by IPCC resembles the delineation of life zones developed by Holdridge (1947). A dataset of the life zones was compiled by the International Institute for Applied Systems Analyses (IIASA) in Laxenburg, Austria (Leemans, 1990) and is available e.g. as the GNV5 dataset through the UNEP GRID web-site[22] or the

22 http://www.grid.unep.ch/data/summary.php?dataid=GNV5&category=biosphere&dataurl=http://www.gri

NOAA Global Ecosystem Database (Global Ecosystems Database Project, 2000)[23]. Most similar to the IPCC classification appears the version where the original classes were aggregated with Olson's ecosystem classes.

One of the main disadvantages of using any similar existing datasets is the lack of the base data, to which the classification scheme was applied. This will inevitably lead to inconsistencies when integrating the data in modelling tasks. Furthermore, the data from Leemans is available at 30 arc min. grid spacing, while the other layers are generated at 5 arc min. grid spacing.

The IPCC classification scheme was therefore applied to an independently developed set of base data layers. Climatic information on temperature and precipitation was provided by the 5 arc min dataset Version 1.4[24] from the WorldClim project (Hijmans *et al*., 2005). The data summarized climatic conditions between the years of 1950 to 2000. In the absence of a monthly mean temperature the parameter was computed from the minimum and maximum temperatures. The elevation data was taken from the same source for reasons of consistency with the climate parameters.

PET is not readily available in the dataset. A layer has been computed following two different approaches.

- **PET Modelled for Mean Daily Temperature**

A simple model for PET using as temperature input only the mean daily temperature was developed for modelling rainfall runoff by Oudin *et al.* (2005) and used by Kay and Davis (2008) as:

$$PE_T = \frac{R_e(T_a + 5)}{\lambda \rho_w \times 100} \text{ m day}^{-1} \text{ for } T_a + 5 > 0$$

where

R_e	extraterrestrial radiation (J m^{-2} s^{-1})
T_a	mean daily air temperature (°C)
λ	latent heat flux (2.45 MJ kg^{-1})
ρ_w	density of water (1000 kg m^{-3})

The computation of the extraterrestrial radiation R_e was based on Duffie & Beckman (1991) and Allan *et al*. (1994). The formulas were supplemented by the information provided by the "Solar Radiation Basis" Web-page of the University of Oregon (http://solardat.uoregon.edu/SolarRadiationBasics.html)

d.unep.ch/data/download/gnv005.zip&browsen=http://www.grid.unep.ch/data/download/gnv005-1.gif#preview

[23] http://www.ngdc.noaa.gov/ecosys/cdroms/ged_iia/datasets/a06/lh.htm

[24] http://www.worldclim.org/current

The IPCC classification scheme applied to the data was only modified to read in the first rule "<7 days of frost". The rule could not be fully implemented because daily data were not available, only monthly averages. Therefore, the rule was adjusted to exclude any areas where the mean temperature was less than 0°C.

The result of the re-calculation of the IPCC Climatic Regions compared to the map published in the IPCC 2006 report, Figure 3A.5.1 is presented in Figure 18.

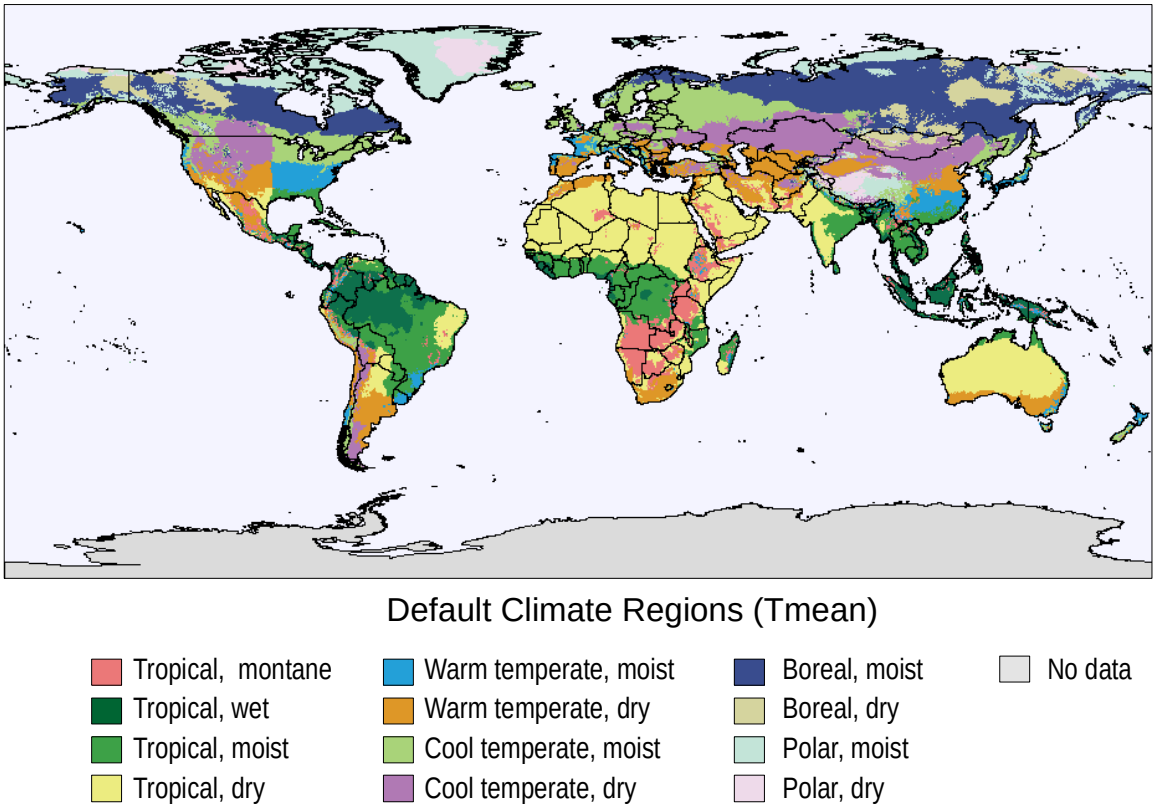

Figure 18: IPCC Default Climatic Regions from PET Modelled for Mean Daily Temperature

The figure shows a general correspondence between the layers, in particular for the American continent. Differences concern the delineation of the "*Tropical Dry*" zone from the "*Warm Temperate Dry*" zone in the Sahara and the separation of the "*Boreal Moist*" from the "*Boreal Dry*" zone. The latter is almost non-existent in the IPCC map. However, the zone does appear in approximately the same areas in the aggregated Holdrige life zone data presented by Oak Ridge National Laboratory Distributed Active Archive Center (ORNL DAAC)[25] and the UNEP Division of Early Warning and Assessment / Global Resource Information Database (DEWA/GRID-Europe) site[26].

[25] http://daac.ornl.gov/NPP/html_docs/hold2_npp.html

[26] http://www.grid.unep.ch/data/summary.php?dataid=GNV5&category=biosphere&dataurl=http://www.gri

One reason for the difference in the boreal zone could be that the formula for PET is only applicable for conditions where $T_a + 5 > 0$ or else PE_T is set to 0. Under this constraint and with the parameters set as given in the equation PE_T does not become negative. It was found that this condition did not change the delineation of the condition except for central Greenland, where the "*Polar Dry*" zone could have been classified as "*Polar Moist*". The source of the different delineation for the boreal zones could not be established and the re-computed layer was used in further analyses.

- **PET Modelled by Hargreaves ET_0**

Application of the IPCC classification scheme to a dataset where PET is computed from the widely used equation for ET_0 by Hargreaves (1985)[27] was investigated.

$$ET_0 = 0.0023 \times (T_{mean} + 17.8) \times (T_{\max} - T_{\min})^{0.5} \times R_a \text{ (mm day}^{-1}\text{)}$$

where

R_a	monthly extraterrestrial radiation (J m^{-2} s^{-1})
T_{mean}	mean daily air temperature (°C)
T_{max}	maximum daily air temperature (°C)
T_{min}	minimum daily air temperature (°C)

The equation was also used by the Consultative Group on International Agricultural Research (CGIAR)[28] to compute a global aridity index from the same WorldClim data used in this project, except that the temperature difference was replaced by the monthly mean of the diurnal temperature range. The resulting PET layer is presented in Figure 19.

d.unep.ch/data/download/gnv005.zip&browsen=http://www.grid.unep.ch/data/download/gnv005-1.gif#preview

[27] http://www.fao.org/docrep/X0490E/x0490e07.htm#radiation

[28] http://csi.cgiar.org/aridity/Global_Aridity_PET_Methodolgy.asp

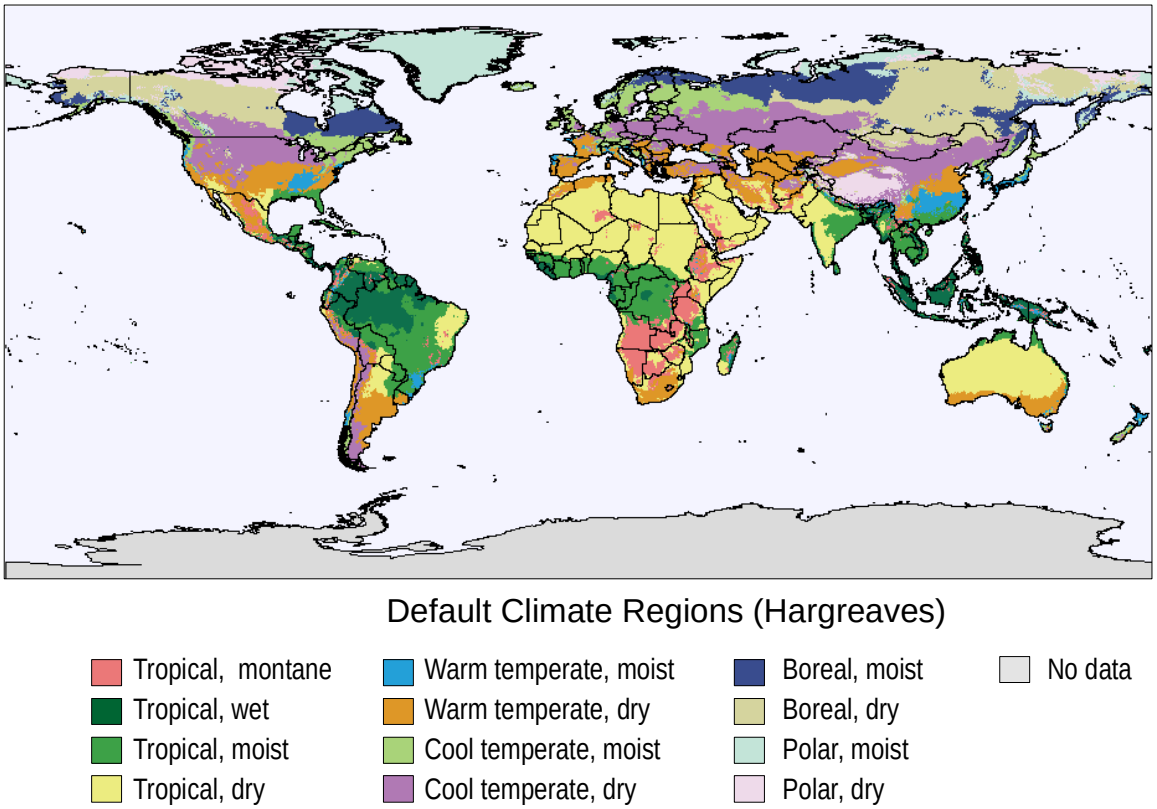

Figure 19: IPCC Default Climatic Regions from PET Modelled after Hargreaves

From the data the aridity index was also computed and compared to the results obtained by CGIAR to support the identification of any faults in the data processing. The data matched for the aridity index because it is readily computed from PET and precipitation it was presumed that the PET layer was computed correctly.

The delineation of the various climatic zones showed greater differences to the IPCC layer than when using the mean daily temperature model. Zones of "*Boreal dry*" are largely expanded, mainly at the expense of "*Cool temperature moist*" and "*Boreal moist*" areas. Using the same input data the shift is indicative of the difference in PET of the two models, which separates the dry from the moist variation of a climate zone.

- **Generation of Ecological Zones Layer**

For the estimation of biomass changes IPCC uses ecological zones. These zones are not identical to the climatic regions. The definition of the ecological zones is described in *Chapter 4 – Forest Land* of the *2006 IPCC Guidelines for National Greenhouse Gas Inventories* rather than in *Chapter 3 – Consistent Representation of Lands*. The map of global ecological zones given in Figure 4.1 of the report originates from *Global Forests Resources Assessment 2000* (FAO, 2001), FRA2000. Spatial layers of ecological zones

and domains can be downloaded from the FAO GeoNetwork server[29]. The definition of the ecological zones is described in Table 4.1 (IPCC, 2006).

While in Table 4.1 reference is made to Climate Regions the domain criteria cited are not those used in the classification scheme for default climate regions (Figure 3A.5.2, IPCC (2006)) and are not exclusive. In the table the subtropical domain is equated with the warm temperate climate region and the temperate domain with the cool temperate region. The defining criterion is the number of months (≥ 8)with a mean temperature > 10°C. For the delineation of the default Climate Regions a criterion of Mean Annual Temperature > 10 is specified without the additional criterion on the duration.

The criteria defining ecological zones are not as strictly defined as those used to delineate the default Climate Regions. An example is the criterion used to separate dry from semi-arid zones, where an area could belong to both zones. The extent of the ecological zones also depends on the order in which the criteria are applied to a climate region. As a consequence, the layer of default Climate Regions cannot be further detailed to result in a layer of Ecological Zones without introducing inconsistencies.

To maintain compatibility with the Climate Region map a spatial layer of Ecological Zones was generated with the minimum of modifications.

- The tropical, boreal and polar zones of the Climate Region layer were maintained.
- The temperate climate regions were first combined and then subdivided according to the domain criteria. Moist and dry regions were defined using the Climate Region criteria.
- The order for applying zone criteria was:
    1. Altitude
    2. Arid
    3. Semi-arid

A schematic classification scheme of the procedure used to generate the Ecological Zone layer is presented in Figure 20.

[29] http://www.fao.org/geonetwork/srv/en/main.home

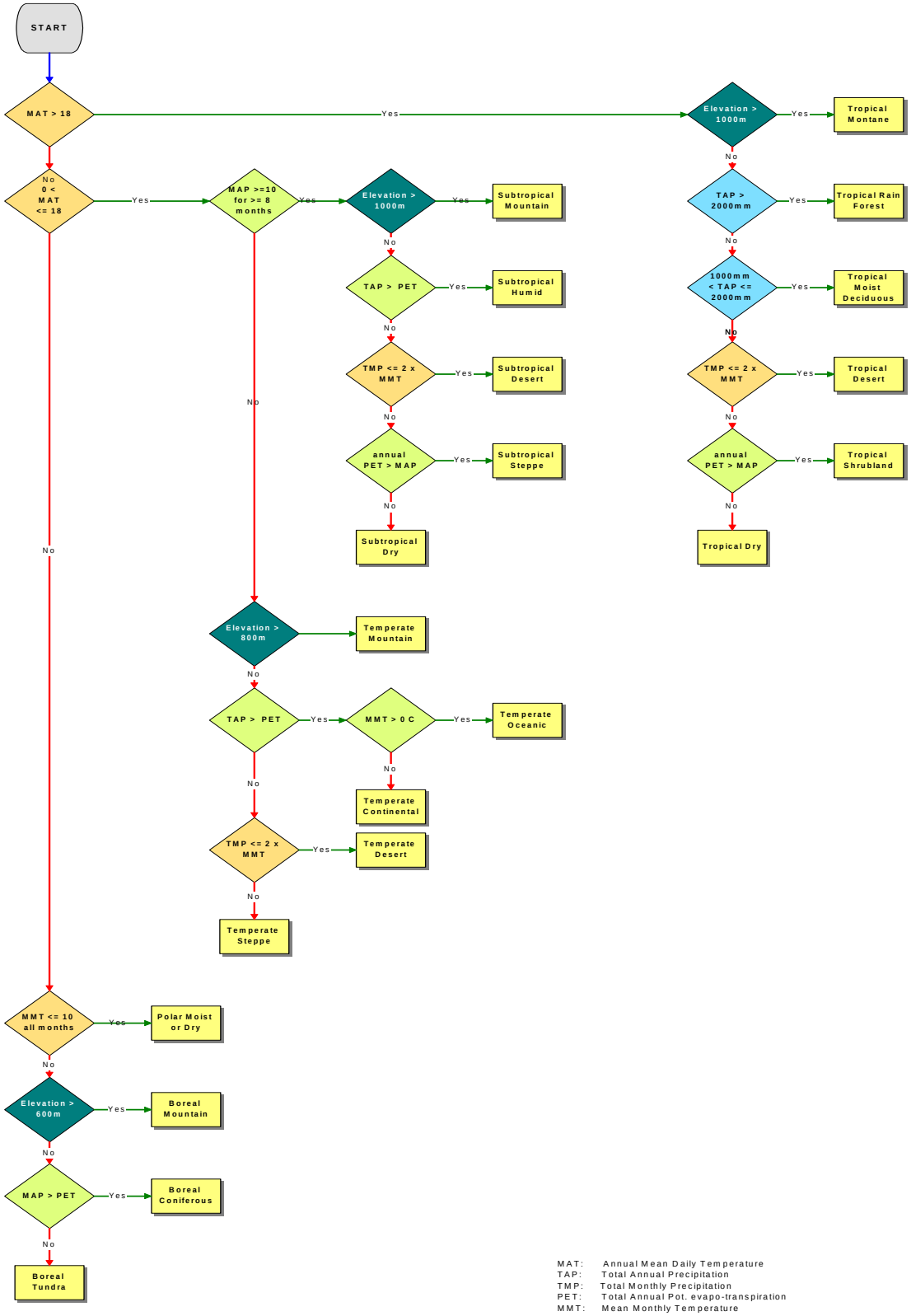

Figure 20: Classification Scheme for Ecological Zone Layer

The effect of using a modified definition for delineating the warm and cool temperate regions and the subtropical and temperate zones on the spatial distribution in the corresponding maps is shown in Figure 21.

The maps show that the Warm Temperate region extends further north than the Subtropical zone. The ecological zone extends into the North American Mid-West and France. The Cool Temperate region largely agrees with the Temperate ecological zone, with the latter extending slightly to the south in the northern hemisphere into the Warm Temperate region. Differences in the southern hemisphere are by comparison limited.

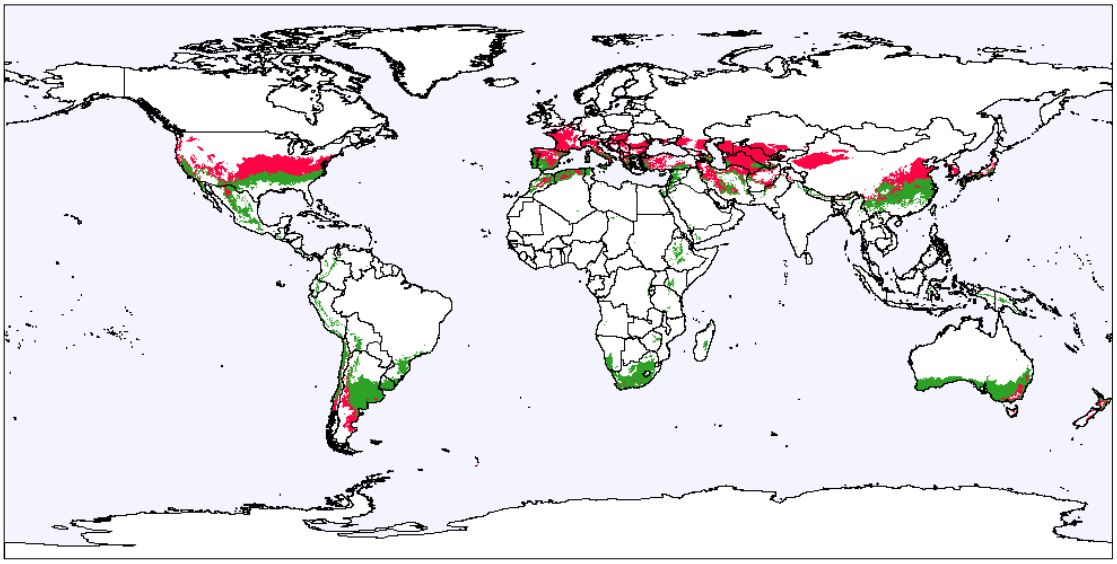

Distribution of Warm Temperate Climate Region vs. Subtropical Ecological Zone

Warm Temperate Climate Region

Subtropical Ecological Zone

Warm Temperate Climate Region and Subtropical Ecological Zone

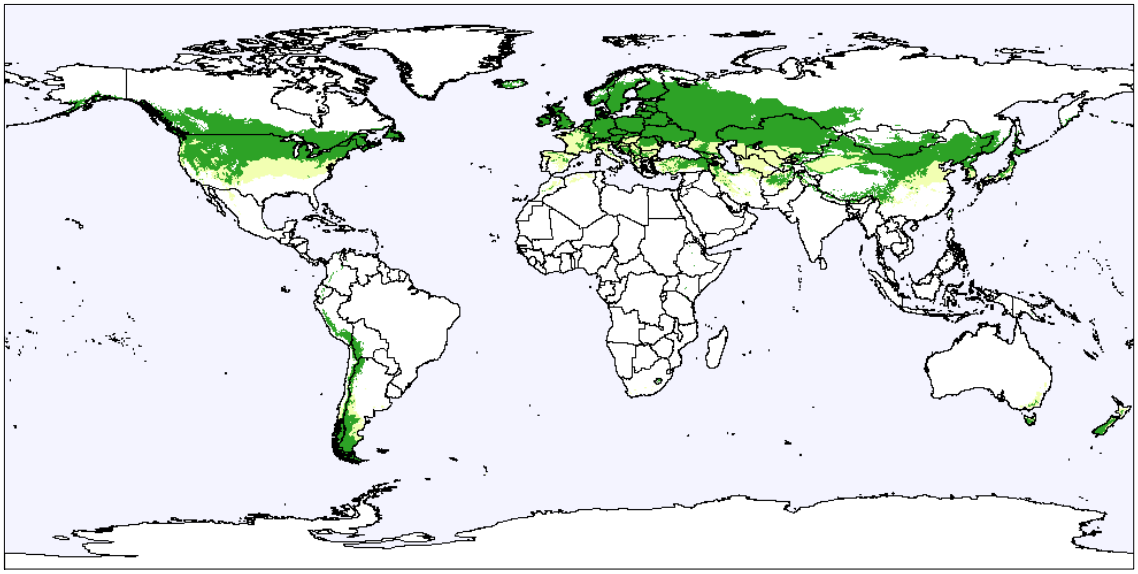

Distribution of Cool Temperate Climate Region vs. Temperate Ecological Zone

Cool Temperate Climate Region

Temperate Ecological Zone

Cool Temperate Climate Region and Temperate Ecological Zone

Figure 21: Differences in Spatial Distribution of Warm and Cool Temperate Regions vs. Subtropical and Temperate Zones

The Ecological Zone data is an approximation of the FAO map on Global Ecological Zones as prepared for the Global Forest Resource Assessment (FAO, 2000). The main

difference in the definition of the ecological zones between the two maps is the use of only climatic data to guide the classification in the study data and not incorporate information on the vegetation pattern. This difference is of some significance because the layer is employed to map the carbon estimates in above and below ground vegetation by land cover type.

The resulting layer for the reduced ecological zones is given in Figure 22.

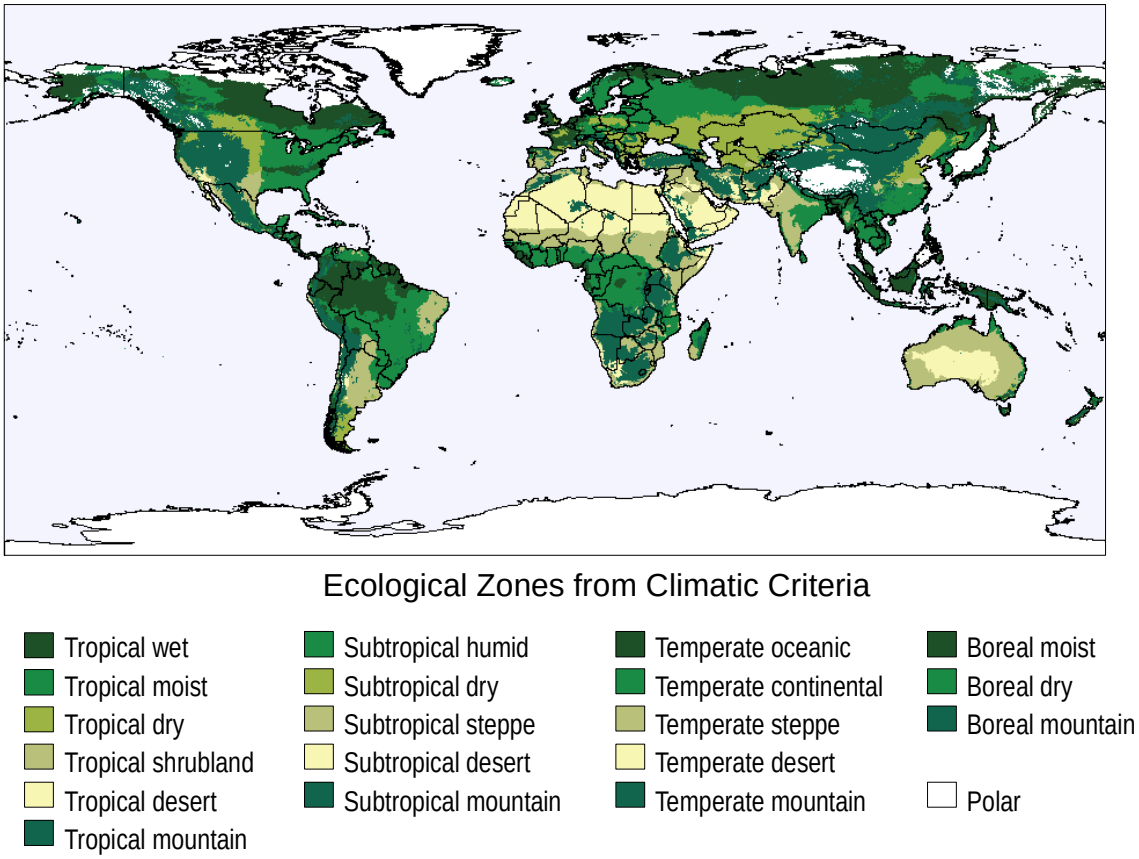

Figure 22: Ecological Zones from Climatic Criteria

Compared with the ecological zone map of FRA2000 the map generated for this study indicates a shift towards drier zones, in particular at higher altitudes. This can be a result of the processing applied, because arid zones are defined before semi-arid and dry zones, the absence of a vegetation layer as a criterion or the climatic data used. This leads to the Tibetan high plateau being classified as polar (all months < 10°C).

The extent of the climate regions and ecological zones depend to a large degree on the base data used, but also on the particularities of the processing applied. In spite of this, generating the derived layers from a single base layer provides consistent delineations and avoids conflicts when estimating GHG emissions using several climatic criteria.

2.3.7. LAND MANAGEMENT SYSTEM FACTORS

To account for the modifying influence of land use and cover on soil organic carbon the IPCC Tier 1 uses defined factors based on the status of the components comprising the land management systems (LMS). The components of the LMS are:

- Land use / cover type
- Management practice
- Input (fertilizers etc.)

Variations in the amount of SOC as a consequence of changes in the status of one or more components of the LMS are defined for LC types croplands and grasslands. The management practices considered by the LMS depend on the LC type. For croplands a further distinction is made for set-aside areas (< 20 years) and paddy rice. All other areas are covered by the LC type "*native ecosystem / nominal management*". Indicators for the status of components are provided to assist in classifying the land. A summary of the LMS components and attached factors is given in Table 18.

Table 18: Land Management System Components and Factors

Land Use / Cover		Management		Inputs		LMS	
Type	***Factor***	***Type***	***Factor***	***Type***	***Factor***	***Type***	***Factor***
Grassland	1.00	Nominal / non-degraded	1.00			*1.1.0*	1.00
		Improved	1.14	Medium	1.00	*1.2.1*	1.14
				High	1.11	*1.2.2*	1.27
		Moderately degraded	0.95			*1.3.0*	0.95
		Severely degraded	0.70			*1.4.0*	0.70
Long-term cultivated	0.82	Full tillage	1.00	Low	0.92	*2.1.1*	0.75
				Medium	1	*2.1.2*	0.82
				High - without manure	1.07	*2.1.3*	0.88
				High - with manure	1.34	*2.1.4*	1.10
		Reduced Tillage	1.03	Low	0.92	*2.2.1*	0.78
				Medium	1.00	*2.2.2*	0.84
				High - without manure	1.07	*2.2.3*	0.90
				High - with manure	1.34	*2.2.4*	1.13
		No tillage	1.1	Low	0.92	*2.3.1*	0.83
				Medium	1	*2.3.2*	0.90
				High - without manure	1.07	*2.3.3*	0.97
				High - with manure	1.34	*2.3.4*	1.21
Set aside (<20 years)	0.93					*3.0.0*	0.93
Wetland (paddy) rice	1.10					*4.0.0*	1.10
Native ecosystem / nominal mgmt.	1.00					*5.0.0*	1.00

To better refer to the LMS types a coping scheme has been introduced. It combines the 3 components as a number code of structure *LC.MANAGMENT.INPUT*. Where *INPUT* and/or *MANAGEMENT* specifications are not used, a “0” is employed to complete the code.

As shown in the table the LMS factors are formed by merging the individual factors for land use / type, management. They are applied to the layer of C-default values from the combination of climatic conditions and soil type.

The various components defining the LMS factors are not readily available as spatial layers. For the analysis they were estimated using information from other related data (proxy).

The thematic data used as proxies in defining and spatially positioning the LMS factors are presented in Table 19.

Table 19: Proxies for Land Management System Components and Factors

	Indicator							OR Function	Indicator			
	AND Function								AND Function			
LMS Type	Land Use / Cover	Irrigation	Mod. Grazing	Intens. Grazing	Tropical Dry	Arid	N Fertilizer		Multiple Crops	Mod. - Intens. Grazing	N Fertilizer	N Manure
1.1.0	x											
1.2.1	x	x									>30	
1.2.2	x	x					>30					
1.3.0	x		x		x							
1.4.0	x			x		x						
2.1.1	x				x							
2.1.2	x											
2.1.3	x	x	not	not					x		>30	
2.1.4	x	x	x				>30		x	x		>30
2.2.1	*											
2.2.2	*											
2.2.3	*											
2.2.4	*											
2.3.1	*											
2.3.2	*											
2.3.3	*											
2.3.4	*											
3.0.0	**											
4.0.0	x											
5.0.0	x											
	Source											
	LC	AQUASTAT	LADA	LADA	CLIMATE	ARIDITY	McGill N-FERTILIZER		LC	LADA	McGill N-FERTILIZER	McGill N-MANURE

* No data or proxy found with sufficient coverage.
** Computed as part of cropland.

The method is based on combining two sets of indicators with conditions set by an AND function. The indicator can be Boolean (x or -) or use a threshold value, as for fertilizer application rates. The two exclusive sets of conditions are combined by an OR function to identify the area for a LMS type.

Several ancillary data sources were used as proxy to define the LMS factors and their spatial distribution.

- ***Project LC***

  The basic information on the distribution of the biofuel land use and cover types are taken from the corresponding thematic layers. The only exception is the layer for set-aside. Set-aside or fallow land comes in various forms and the McGill M3 source data does not include set-aside or fallow land. In an approximation the set-aside layer was computed as the difference of the sum of all crop surface areas and the total cropland area. The crop surface area is the proportion of a crop within a grid cell derived from the harvested area corrected for multiple cropping.

- ***FAO / IIASA LADA***

  Data from the *Land Degradation Assessment in Drylands* project were mainly used to identify the grazing intensity from the thematic layer of *Land Use Systems of the World*. The data are available in raster format and 5 arc min. grid size with a single attribute for each grid cell.

- ***FAO AQUASTAT***

  From FAO's Aquastat[30] information system the global map of irrigation areas was used in Version 4.0.1 (Siebert, *et al*., 2007). The data were integrated into the LADA layer in the form of 3 classes of irrigation intensity. In the definition of the LMS factors the original map data were used instead of the classified data from LADA. This procedure would allow more flexibility when merging or updating the thematic data set.

- ***Project CLIMATE***

  Information on climatic conditions was taken from the layer of climatic regions prepared according to IPCC specifications.

- ***Project ARIDITY***

  A layer of the global distribution of arid areas was generated from the climatic data used to produce the climatic regions and eco zones layers. Comparable data have become available as the *CGIAR-CSI Global-Aridity and Global-PET Database* (Trabucco & Zomer, 2009) from the *Consortium for Spatial*

[30] ftp://ftp.fao.org/agl/aglw/aquastat/gmia_v4_0_1_pct_asc.zip

Information (CGIAR-CSI) within the *Consultative Group for International Agriculture Research* (CGIAR-CIS)[31]. However, the data uses the Penman-Monteith equation for the estimation of PET. The results of using the equation were found to differ too much from the IPCC data when producing the map of climatic regions. For consistency a global aridity layer was therefore computed using the same PET layer as employed to classify the climatic regions.

- ***McGill N-FERTILIZER***

  The amount of nitrogen fertilizer applied to crops was based on *Global Fertilizer and Manure Application Rates*[32] data from McGill University, Montreal, Canada. The data layer uses a much coarser spatial resolution (0.5 arc deg) the project layers, but was used for reasons of consistency with the crop area data from the same source.

- ***McGill N-MANURE***

  The amount of nitrogen from husbandry was based on the same data as the N-Fertilizer application rates.

By combining the AND and OR conditions of the proxy layers the LMS factors are generated as spatial layers. The first layer in the process is given by the LC default conditions, all other layers are added by using overlay functions.

No LMS factor layers could be produced for the reduced and non-tillage scenarios for cultivated areas. The areas of reduced tillage can be notable, but vary appreciably between countries. In Portugal reduced tillage is applied on 1.3% of the arable land, while it is estimated to be applied on 40% in Switzerland (van Lynden & Lane, 2004). Data are generally only available at national level and no thematic data could be identified which could be used as a proxy.

[31] http://www.cgiar-csi.org/

[32] http://www.geog.mcgill.ca/~nramankutty/Datasets/Datasets.html

3. CALCULATING GHG EMISSIONS FROM ILUC USING SPATIAL ALLOCATION PROCEDURE

This section describes the methodology used to spatially allocate agricultural land demand and the estimation of land carbon stocks and GHGs.

The general function of the spatial allocation procedure is to distribute the marginal cropland resulting from the implementation of different biofuel policy scenarios, according to the results of the economic models run at regional level. The land is allocated over either existing or new cropland, given the LC and crop distribution in the reference layers. Allocation criteria are the land suitability for agriculture and the distance from cropland.

The spatial allocation of agricultural land demand is performed a two step process:

- ***Spatial analysis:***

  database creation, combining different data sources into a single database.

- ***Simulation:***

  based on cropland demands from agro-economic models.

Details on the steps of the spatial allocation and specific considerations are presented hereafter.

3.1. DATABASE CREATION

The input database includes the following tables which provide data referred either to the reference grid layer (see Chapter 2) or to the tables containing the countries and the economic regions:

- **Administrative** table, containing the identification code, the country code, the economic region name and the surface in hectare for each grid cell.

- **Region** table, assigning world countries to the regions defined by each economic model.[33]

- **JRC Crop Share** table, containing the adjusted share (see Chapter 2.1.1 Land Use and Cover Layers) of the following crop groups:

[33] Only a few countries are neglected.

  - wheat
  - maize
  - rice
  - sugar cane and sugar beet
  - oilseeds (including soybean, rape seed, sunflower and, if available, palm oil)
  - vegetables and fruits
  - other, calculated as the difference between total and the sum of the other crops
  - sum of all crop groups, total production

- **JRC Land cover** data, storing the information on land cover share by grid cell of the raster layer according to the specific LC classification described in Section 2.1.2 Cropland and Individual Crop Data.

- **Land demand** table, storing the land demand calculated by economic models for different biofuel policy scenarios by regions and crop groups.

- **Conversion to cropland** table, providing the surface of Forest, Shrubland, Savannah and Grassland (aggregation of IGPB classes) supposed to be transformed in cropland by country. This table is inspired by the EPA report (EPA, 2009) and based on trends for land conversion to cropland between 2001 and 2004, deduced from MODIS Land Cover time series (2001-2004) (see 2.2.3 Baseline and Scenario Assumptions).

- **Suitability** table, containing the suitability coefficient deduced from the map on Global Agro-Ecological Zoning, for the following crop groups (see 2.1.5 Global Agro-Ecological Zones (GAEZ)).

  - wheat
  - maize
  - rice
  - sugar cane and beet
  - oilseeds
  - other crops and vegetables and fruits

- **Statistics** tables for each crop, storing the average, the maximum and the standard deviation of surface values by country and by GAEZ zone.

- **Distance** table, containing the distance to area of cropland in 2000. Arbitrarily, a cell has been considered with a significant amount of cropland when the share of cropland in the cell is above 25% compare to the total size of the cell.

3.2. SPATIAL ALLOCATION PROCESS

The spatial allocation is performed by region defined in the economic models, with each region being processed independently from the other. Within a region, through the allocation process data are downscaled to the country and then to the grid cells of the spatial layer.

The spatial allocation process distinguishes three processes to perform the spatial distribution of the cropland demand given by economic model:

a) For each crop the marginal economic demand is split in four buckets according to the trends extracted from MODIS time series. Those buckets correspond to the 4 land cover used in the Winrock study (EPA, 2009), which are Forest, Shruband, Savannah and Grassland.

b) The grid cells candidate for cropland expansion are selected using filters on the MODIS Land Cover classes (to fit with the split in A), on the suitability classes in term of soil and climate provided by IIASA (Fisher, 2002) and on the distance to the cropland class of the Biofuel LUC map at the year of reference.

c) The four buckets of process A are distributed in the grid cells selected by B. When the demand is negative the crop acreage is decreased and when the demand is positive the crop acreage is increased. An adjustment of the non cropland classes of the JRC Land Cover classification is also performed.

A schematic overview of the three processing steps of the spatial allocation process are presented in Figure 23.

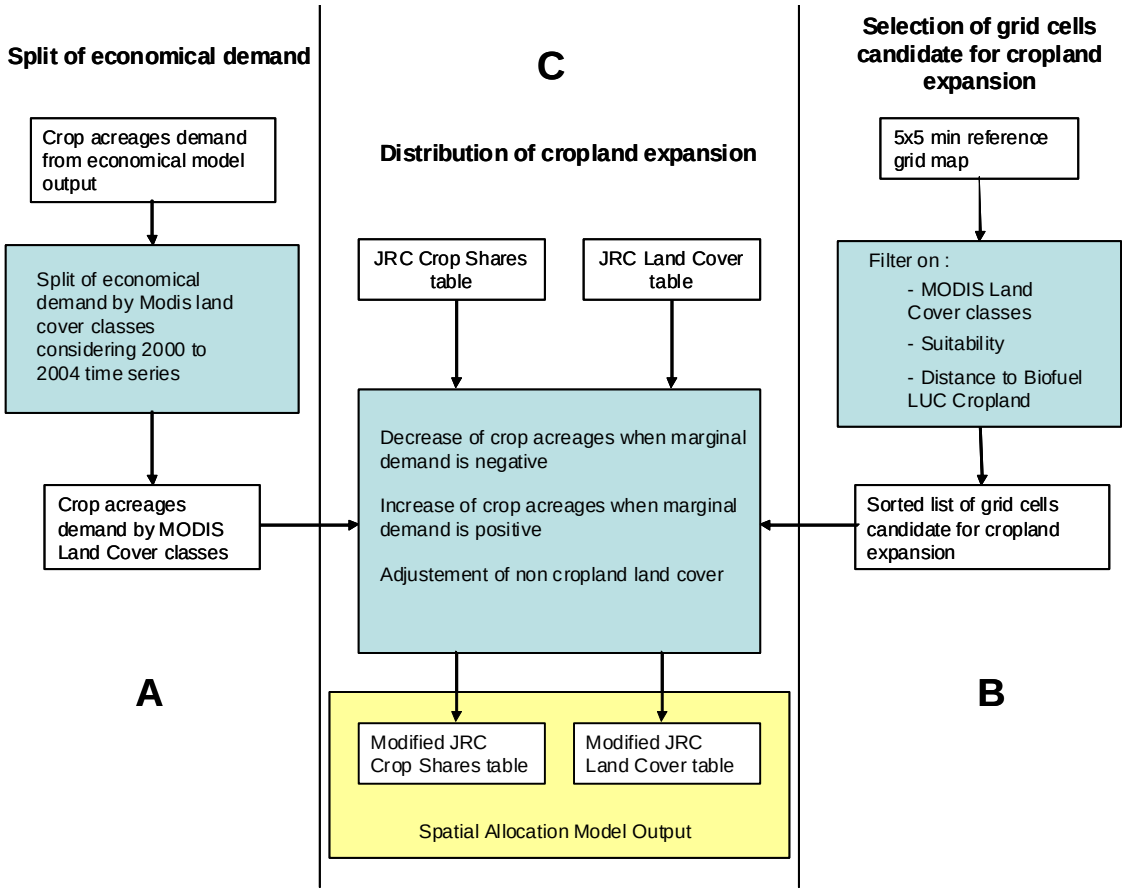

Figure 23: Schematic Representation of the 3 Processes Performed by the Spatial Allocation Procedure

3.3. FILTERING AND SORTING AREAS WITH POTENTIAL FOR CROPLAND EXPANSION

The choice of the grid cells in which land expansion will occur is made by a selection process that takes into account four parameters:

- the land cover change trends deduced by MODIS time series dataset,
- the suitability of the land,
- the distance to current cropland,
- a random factor.

The result of this selection process is a sorted list of candidate grid cells with potential for accommodating cropland expansion. This list of cells is then transmitted to the distribution process which performs the distribution of the economic demand to the candidate cells.

3.4. FILTERING DATA WITH MODIS LAND COVER TYPOLOGY

The MODIS land cover time series allow to compare the land cover distribution in the world for the years between 2001 and 2004. Using this comparison it is possible to extract some trends for the future. This process has been described (EPA, 2009) and the JRC proposes to partially use it in the current study. Basically, it indicates how much of the new cropland is supposed to be taken from the classes Forest, Grassland, Savannah or Shrubland of the MODIS classification if the trends observed between 2001 and 2004 are also followed in the future. The procedure is covered in detail in 3.4 Filtering Data with MODIS Land Cover Typology.

- ***Suitability Criteria***

  One of the drivers for the land allocation process is the suitability of the land for agriculture. This suitability indicates how much the soil and climate characteristics are favourable or unfavourable for agriculture. This suitability can be defined for each crop and gives information on the likelihood of cropland expansion in the different areas according to the type of soil and the climate of the region.

- ***Distance Criteria***

  The grid cells are ranked according to their proximity to the current cropland areas. The land allocation process gives a priority to the cells at a short distance from those areas already devoted to agriculture but it can also handle the apparition of new spots for agriculture.

  The balance between the constraint of distance and the constraint of suitability can be adjusted with the customization of the distribution functions.

- ***Random Factor***

  A random variable has been introduced to spread out, in some contexts, the land expansion uniformly between areas of equal land suitability and equal distance to cropland.

3.5. CROPLAND DISTRIBUTION

The cropland distribution process assigns the cropland demand (derived from the economic models) to the cells selected according to a customizable 3-step process. The first step of the process decreases the acreage of the crops with a negative marginal demand, the second step allocates crops with a positive marginal demand on land released by step one and the third step allocates the remaining cropland demand in new agricultural land. In parallel to the increase of cropland areas a decrease of other types of land cover is performed.

- ***Cropland Decrease***

  In case of negative marginal cropland demand the land allocation process decreases the share of cropland in the cells of the region affected by this cropland withdrawal. This decrease is performed homogenously across all the cells of the region, no specific driver parameters are used for this decrease.

- ***Cropland Increase***

  All the crops with a positive marginal demand are distributed through a unique process: The application checks the suitability for each crop in the region and starts the land distribution with the crop(s).

  The areas where land expansion occurs are selected by order of priority, as defined before. When two or more crops are equal candidates for crop expansion in the same cell, with the same level of suitability for each crop, then the land available in the cell is equally shared between the crops.

- ***Crop Substitution***

  Where marginal cropland demand is negative for some crops and positive for other crops then crop substitution takes place. The crop substitution is simply a decrease in the acreage of some crops followed, in the same cell, by a refill of the land released, i.e. an increase in the acreage of other crops. The land expansion for crop with a positive land demand always starts in these areas released from crops with negative land demand. The cropland expansion in new areas occurs only when land substitution possibilities are exhausted.

- ***Land Cover Adjustment***

  If cropland expansion occurs in a cell, the corresponding amount of hectares must be released from other land covers present in the cells. MODIS time series could, in theory, gives indication about the type of land cover that is converted. As already mentioned, in ENSUS (2009) there are some discrepancies between the MODIS dataset and the statistics provided by FAO. Therefore, to limit the impact of these differences the MODIS time series data are only used to identify areas of change relative to cropland. The share of different land cover classes

converted to cropland is not deduced directly from the MODIS time series trends.

As an alternative, the land allocation model adopts a conservative strategy: the decrease is performed in a way that the shares between the land covers present in the cell and eligible for cropland substitution remains constant (see illustration Figure 24.

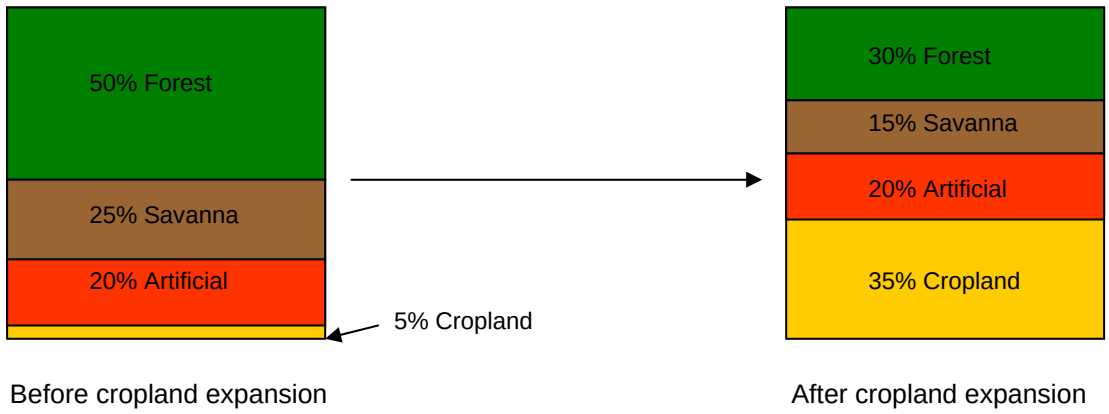

Figure 24: 3,000 ha of Cropland Expansion Homogeneously Distributed between Forest and Savannah in a 10,000 ha Area

3.6. General Comments on Spatial Allocation Procedure

It is important to point out some drawbacks of the process in order to avoid any confusion on the scope and the use of the results coming from the spatial allocation procedure.

Results obtained from the simulation run by the model should not be taken as a true picture of what will be the reality of future cropland distribution in the world: this is beyond the capabilities of any global model at present. Rather, the model provides a best-estimate of the typical areas which would be affected, which is particularly important for the subsequent calculations of the associated soils emissions (compared to assuming all land types are affected equally, or some other gross simplification). Modelling means making assumptions, simplifying and making compromises between the complexity of the model, the computing time and the availability of the data.

- ***Remarks on Data Availability***

  The model presented in this document distributes the cropland using only biophysical criteria as drivers. It means that some very important constraints such as socio-economic criteria are not taken into account. This is due to the lack of data on this issue, for instance global dataset on the land costs or production costs are not available at 5 arc min. spatial resolution. However, some socio-economic criteria are embedded in the agro-economic model providing the crop demand for the future, thus they impact indirectly the land allocation process at macro level.

- ***Difficulties of Calibration***

  Due to the lack of data, and more specifically the lack of time series in term of land cover, the calibration of the model is difficult. Some trends have been extracted from the MODIS land cover between 2001 to 2004 but the time frame is not long enough to process a calibration based on the comparison between the result of the model and an observed situation for a date posterior to 2004.

- ***Data Uncertainty***

  Within the framework of the ILUC estimates there is significant uncertainty and of course it follows that there is uncertainty present in the spatial allocation procedure of extra cropland demand. Each input data source comes with its own inaccuracy that can be difficult to evaluate. This apples not only to the output of agro-economic models but also for the soil, climate and land cover database used as the main drivers for cropland expansion.

Regarding uncertainties in land cover data, Table 20 presents the total amount of hectares allocated to cropland in the world according to different datasets. It highlights the important discrepancies between the datasets even if it only shows global values. Obviously, the spatial distribution of cropland in the world is also prone to strong uncertainties.

Table 20: Cultivated Land in the World According to Different Datasets

Cultivated Land	Year			
	2000	2001	2005	2007
	mil. ha	*mil. ha*	*mil. ha*	*mil. ha*
Global Land Cover	1,995			
MODIS Mixed Cropland/Natural		300		
MODIS		1,305		
GlobCover			1,730	
FAOSTAT (ProdSTAT)	1,185			1,255
FAOSTAT (ResourceSTAT)	1,530			1,555
McGill M3 (satellite dataset)	1,490			
McGill M3 (agric. inventory)	1,250			

3.7. METHODOLOGY FOR ESTIMATING GHG EMISSIONS

GHG emissions estimated in the study are emissions of carbon and N_2O from the soil, carbon from above and below-ground vegetation.

3.7.1. CARBON EMISSIONS FROM SOIL

The method applied to estimate carbon emissions from the soil is to use changes in carbon stock and treat all changes as emissions. The variable factor determining changes in carbon stocks is land use change. All other factors, such as climatic conditions or land management practices, are kept constant. To avoid introducing spurious changes as a consequence of differences in the base data between the project data and the data used to drive the economic model only the variation in crop area between the scenario and the reference data for 2020 is used:

$$C_STOCK_{Change} = C_STOCK_{Projection} - C_STOCK_{Base} \ (t\ ha^{-1})$$

with:

$$C_STOCK_{Base} = C_STOCK(LC_{Base}) \ (t\ ha^{-1})$$

$$C_STOCK_{Projection} = C_STOCK(LC_{Base} + (LC_{Reference} - LC_{Scenario})) \ (t\ ha^{-1})$$

where:

C_STOCK_{Change}	C stock for land use change in economic model ($t\ ha^{-1}$)
$C_STOCK_{Projection}$	C stock for projected data ($t\ ha^{-1}$)
C_STOCK_{Base}	C stock in land use of base data ($t\ ha^{-1}$)
LC_{Base}	Land use area in base data (*ha*)
$LC_{Projection}$	Projected land use area data (*ha*)
$LC_{Reference}$	Land use area in economic model reference (*ha*)
$LC_{Scenario}$	Land use area in economic model scenario (*ha*)

The absolute value of the area change is transferred as the difference between scenario and reference land use, not the relative value. This variation is then applied to carbon stock of the baseline situation. The approach saves modelling conditions for 2020 and assumes that the C emissions from the expansion in cropland in 2020 are not significantly different from those that would be estimated based on the distribution of crops in the base data.

Although the transfer of changes in area rather than total values removes some of the differences between the economic model and the project data some other aspects of data consistency remain.

There some problematic areas in the layers of national boundaries when defining the regions. For example, overseas areas are assigned to the region of the administering country and not to the economies of immediately neighbouring regions. Additionally, no clear attribution to a region can be made for areas under dispute. Since the thematic layers all contain data for those areas the transfer of regional trends from the economic model has to account for those areas. One option is to mask all areas concerned, another to assume no change between the reference and the scenario results. The latter option has been chosen for estimating C stock changes in the soil because the approach does not change the global values for SOC stocks.

3.7.2. N_2O EMISSIONS FROM LOSS OF CARBON IN MINERAL SOILS

For all areas undergoing a land use/cover change as described in the previous chapters the soil N_2O emissions related to mineralised N which results from loss in soil organic C stocks are calculated according the IPCC (2006) guidelines. The guidelines outline: "*Where soil C is lost through oxidation as a result of land-use change ..., this loss will be accompanied by a simultaneous mineralisation of N. Where a loss of soil C occurs, this mineralised N is regarded as an additional source of N available for conversion to N_2O ...*". According to IPCC (2006) the opposite process to mineralization, whereby inorganic N is sequestered into newly formed SOM, is not taken account of in the calculation of the mineralization N source. This is because of the different dynamics of SOM decomposition and formation, and also because reduced tillage in some circumstances can increase both SOM and N_2O emission. The IPCC (2006) Tier 2 approach - taking into account different land uses/covers and disaggregated C:N ratios - was applied to calculate the amount of mineralized N resulting from loss of soil organic carbon. The calculation of direct and indirect soil N_2O emissions is based on the IPCC (2006) Tier 1 method.

The net annual amount of N mineralised in mineral soils (F_{SOM} in kg N) as a result of loss of soil carbon through change in land use is calculated for each grid cell (g) as:

$$F_{SOM,g} = \Delta C_{mineral,g} \cdot \frac{1}{R_g} 1000$$

where:

$\Delta C_{mineral,\,g}$	annual loss of soil carbon (t C) in the grid cell (for calculation methods and results see Chapter 3.7.1)
R_g	C:N ratio of the soil organic matter in the grid cell

Direct N_2O emissions (N_2O_{direct}) as kg N_2O-N yr^{-1}:

$$N_2O_{direct} - N = \sum_g F_{SOMg} \times EF_1$$

where:

EF_1	Emission factor. IPCC (2006) default value: 0.01

Indirect N_2O emissions from leaching/runoff $N_2O_{(L)}$ as kg N_2O-N yr^{-1} :

$$N_2O_{(L)} - N = \sum_g F_{SOMg} \times Frac_{LEACH\text{-}(H)} \times EF_5 \cdot Exfact_g$$

where:

EF_5	Emission factor. IPCC (2006) default value: 0.0075
$Frac_{LEACH\text{-}(H)}$	N losses by leaching/runoff as fraction of F_{SOM}. IPCC (2006) default value: 0.3.
Exfact	Leaching/runoff occurs only in grid cells where soil water holding capacity is exceeded as a result of rainfall, in this case Exfact is set to 1, otherwise Exfact = 0.

Total emissions as kg CO_2eq yr^{-1}:

$$CO_2eq = (N_2O_{direct} \cdot N + N_2O_L \cdot N) \times \frac{44}{28} \times 296$$

The following data were used as input to the computations:

- ***Loss in Soil Organic Carbon due to Land Use/Cover Change***

  The method, input data and the results are described in paragraphs 5.2 and Chapter 6 of this report.

- ***Carbon to Nitrogen Ratio (C:N)***

  IPCC suggests to use a universal default C:N ratio of 15:1 (uncertainty range from 10:1 to 30:1) for situations involving LUC from forest land or grassland to cropland when more specific data are not available.

  In this study spatially variable values of the C:N ratio are used, which are calculated from soil layers prepared for the study (FAO, 2007). The original dataset distinguishes C:N class ranges (see Figure 25) for the dominant and the associated soils in a raster cell.

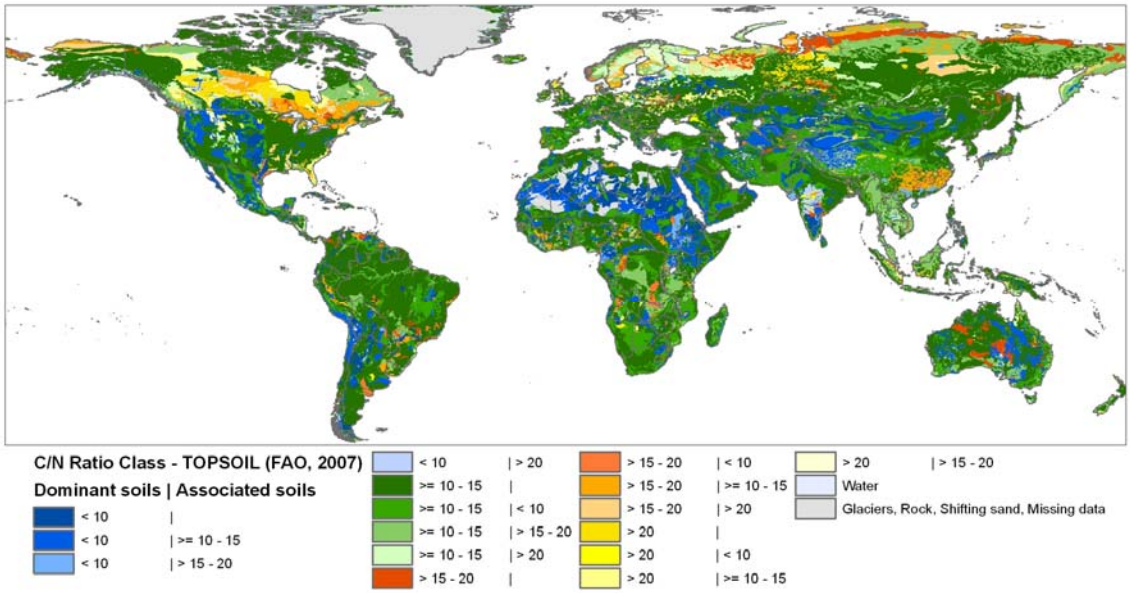

Figure 25: C:N Ratio Classes - Topsoil, Edition 3.6, 2007-02-08 (Source: FAO, 2007)

For the calculations of N mineralised in mineral soils (F_{SOM}) as a result of loss of soil carbon as a consequence of LUC these ranges had to be translated into single values as given in Table 21.

Table 21: Reclassification Scheme of FAO (2007) C:N Ratio Classes into Single Value C:N classes

C:N in Dominant Soil	C:N in Associated Soils	C:N Value Applied
<10	dominant class occurs in >80% of the pixel	7.5
<10	>=10-15	8.5
<10	>15-20	9.5
<10	>20	10.5
>=10-15	dominant class occurs in >80% of the pixel	12.5
>=10-15	<10	11.5
>=10-15	>15-20	13.5
>=10-15	>20	14.5
>15-20	dominant class occurs in >80% of the pixel	17.5
>15-20	<10	15.5
>15-20	>=10-15	16.5
>15-20	>20	18.5
>20	dominant class occurs in >80% of the pixel	22.5
>20	<10	19.5
>20	>=10-15	20.5
>20	>15-20	21.5

- ***Areas with Leaching / Runoff***

  IPCC (2006) defines the area where leaching/runoff occurs as areas where Σ(rain in rainy season) - Σ (PE - potential evaporation - in same period) > soil water holding capacity, or where irrigation (except drip irrigation) is employed. The rainy season(s) can be taken as the period(s) when rainfall > 0.5 * Pan Evaporation.

Calculation of areas where leaching/runoff occurs are based on the data set of long-term average of monthly potential evapo-transpiration (PET) of the reference land use "grassland" and monthly rainfall as described in chapter 2.3.6 Climate Regions. PET is used as an approximation of PE and Pan evaporation required according to IPCC (2006). A detailed description and discussion of PET, PE and Pan Evaporation is available from FAO (http://www.fao.org/docrep/x0490e/x0490e04.htm). Soil water holding capacity data[34] on a 5 x 5 arc min. grid is provided along with the ISRIC-WISE soil properties data set (Batjes, 2006).

Input data and results are shown in Figure 26. The top figure shows the amount of precipitation during the rainy season, the central map gives the soil water holding capacity (Batjes, 2006) and the bottom map depicts the excess of soil water holding capacity in the rainy season. All the areas > 0 mm in the bottom map are subject to leaching or run-off according the IPCC (2006) definition, thus the parameter *Exfact* in the above described equation to calculate indirect N_2O emissions is set to 1.

Within this study the second condition "where irrigation (except drip irrigation) is employed" has not been taken into account. To the knowledge of the authors there is only one source that gives information about irrigated areas in the required spatial resolution on a global scale. Siebert *et al*. (2007) produced a digital map showing the area equipped for irrigation for a global grid of 5 arc min. resolution. However, the type of irrigation cannot be distinguished. Thus drip irrigation cannot be excluded from the total irrigated area. It can be also assumed that irrigation in a region is usually not employed to all crops but predominantly to the crops most sensitive to drought and/or to the economically most valuable ones. Reliable estimates would require a more detailed analysis region by region.

[34] Available water storage capacity (AWC; from -33 to -1500 kPa; cm m^{-1})

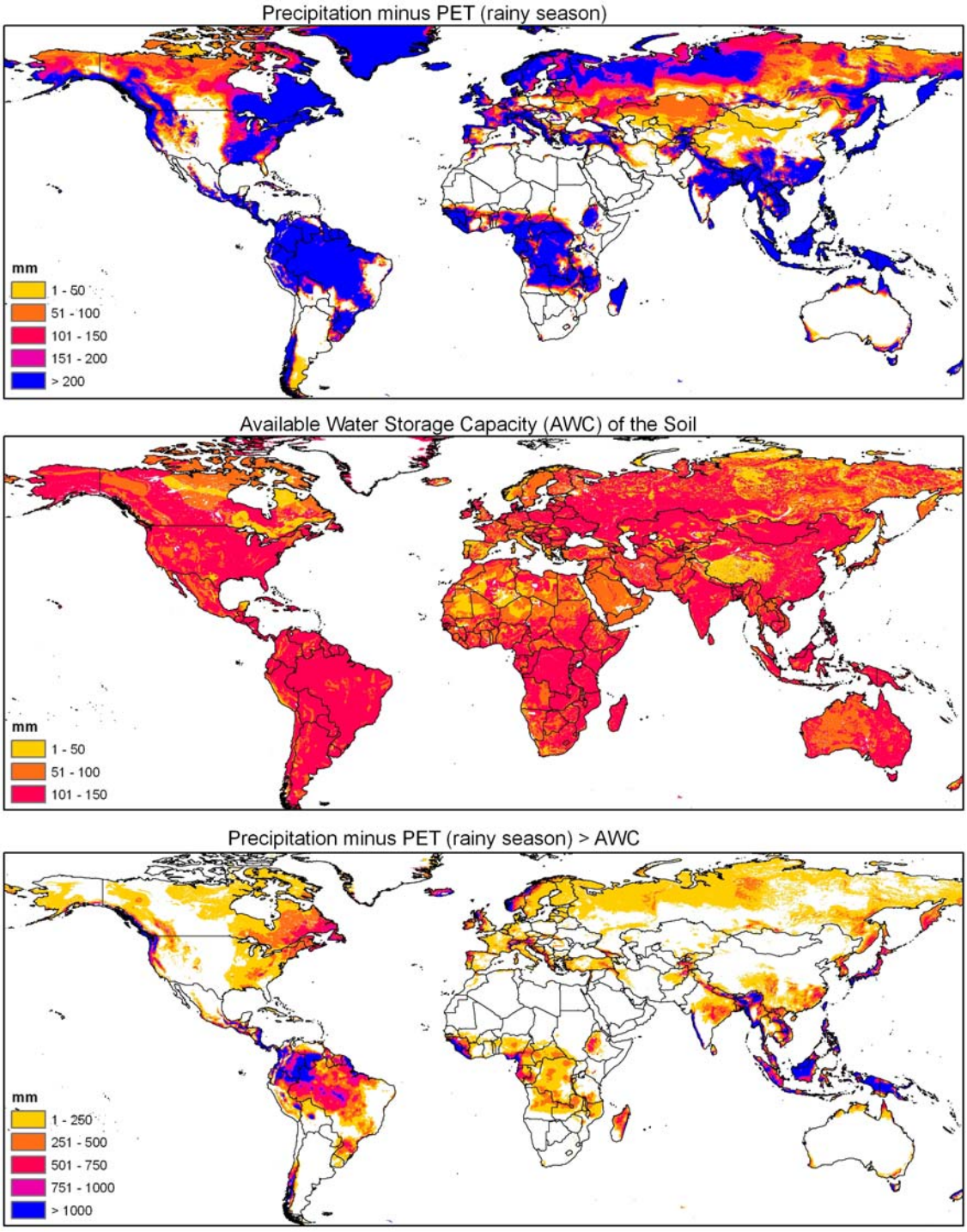

Figure 26: Input Data and Result of the Delineation of Areas where Water Holding Capacity is Exceeded (central map) and Leaching/Runoff Occurs (bottom map)

3.7.3. CO_2 EMISSIONS FROM CHANGES IN ABOVE- AND BELOWGROUND BIOMASS CARBON STOCKS

The spatial allocation procedure provides estimates on the LUC area in the year 2020 at the resolution of the study grid based on the results of the agro-economic models (IFPRI, 2010 and IPTS, 2010) for:

a) a reference case – excluding the effects of the Biofuels target in the RED on global biofuel crop cultivation;
b) one or more scenarios simulating the effects of the RED on global biofuel cultivation and cropland expansion.

LUC as a consequence of the RED (LUCRED) is the difference in land use/cover in a scenario with respect to the reference case, regardless of the direction of change (e.g cropland to forest or forest to cropland). The spatially allocated change in land use/cover in 2020 is compared with the land use/cover at the same place in the year 2000 (LU2000).

Following the approach outlined in IPCC (2006) and Carre *et al*. (2009), the total above and below-ground biomass carbon stock (ABCS) was calculated for LU2000 and the LUCRED for each grid cell (g) as:

$$ABCS_{LUCRED,LU2000,g} = \sum_{lu} ABCS_{lu} \cdot Area_{lu}$$

where

$ABCS_{LUCRED,LU2000g}$	Total ABCS (t C) in a grid cell (g) for LUCRED or LU2000
$ABCS_{lu}$	Average ABCS of a land use/cover class in the grid cell (t C ha^{-1})
$Area_{lu}$	Area of a land use/cover class in the grid cell (ha)

The total change of ABCS is calculated as the sum of the differences in ABCS between LUCRED and LU2000 within each grid cell:

$$\Delta ABCS = \sum_{g} (ABCS_{LUCRED,g} - ABCS_{LU2000,g})$$

where

$\Delta ABCS$	Change of total ABCS (t C) induced by the RED. Negative values indicate a loss in C which is assumed to be released completely into the atmosphere in the form of CO_2.

Thus, total CO_2 emissions (t CO_2) can be computed as:

$$\Delta \text{ ABCS} \cdot \frac{44}{12} .(\text{t } CO_2)$$

The emission balance in the RED refers to annualized values. It is defined that annualized emissions from carbon stock changes caused by land-use change, shall be calculated by dividing total emissions equally over 20 years, despite the fact that the major part of CO_2/GHG emissions from biomass occur at the moment of the LUC (in any case in a very short period), whereas emissions from soil occur over a longer period. Moreover, the current approach only covers CO_2 emissions/removal by the relevant pools, and not the non-CO_2 GHG emissions which are often associated with land conversions (i.e. land conversion technology may involve burning of the existing biomass, which leads to non-CO_2 emissions).

As explained in the previous chapters, the spatial allocation procedure distinguishes 7 agricultural classes and 8 other land use/cover classes. In this context it is important to note the issue of temporal reference. The initial land use/cover data set describes the situation in the year 2000. When considering carbon stock changes associated with land use/cover changes, the RED relies on the methods described in Carre *et al*. (2009), which is based on the IPCC Tier 1 approach. Concerning the temporal issue in land use/cover changes it is stated that:

"…lands might have experienced several successive uses or cover changes before it is finally converted to a biofuel crop. In this case, initial land use in rapport with a reference time or period has to be considered (i.e. x years before the biofuel crop is established), but not the intermediary land uses."

Thus it is assumed that the earlier baseline is conservative from the emission counting perspective.

As outlined in the RED (Annex V C, 7), calculations of changes in ABCS for 2020 requires the comparison of land use/cover in 2020 with the situation in 2008. Global spatial land use/cover data providing the required detail for this work was available only for the year 2000, thus all the following comparisons are based on the reference land use/cover in 2000

Different agro-economic models may use different classifications or aggregations for the crops. Prior to the spatial allocation they have been re-classed into the classification system of the spatial allocation procedure.

- ***Climate Regions and Carbon Stocks in Biomass***

  Carre *et al*. (2009) provide mean values of ABCS in t C ha^{-1} for the land use/cover classes in different ecological zones and climate regions, largely based on the 2003 IPCC Good Practice Guidance for Land Use, Land Use Change and Forestry and other sources (see next chapter). The nominal values for ABCS data of grassland are given for Climate Regions while the values for open and closed forest are given for Ecological Zones und further distinguish geographical aggregations. Total C-stock values for shrubland are listed for climate domains and geographic aggregations.

To map the nominal C-stock values in ABCS to climate regions and geographic aggregations a data set combining the two themes has been generated. Following the specifications of Table 4.1 of Volume 4 of IPCC (2006) the climate regions "Warm Temperate" was substituted by the "Subtropical" domain and "Cool Temperate" by the "Temperate" domain. The resulting map of climate regions and 8 geographic aggregations is presented in Figure 27.

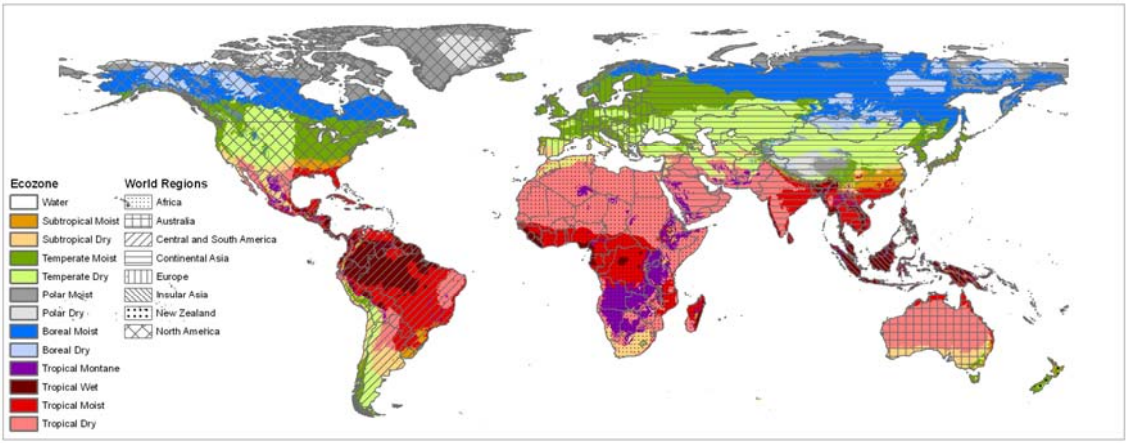

Figure 27: Climate Regions and Geographic Aggregations for ABCS

- ***Above- and Belowground Biomass Carbon Stock for Individual Land Use/Cover Classes***

  The ABCS values given in Carre *et al*. (2009) to calculate changes in carbon stocks are based on the assumptions that for non-cropland vegetation the ABCS amounts to a maximum quantity which is considered constant over time under prevailing natural and management conditions. The entire biomass and dead organic matter is cleared when land use change occurs, thus all C is emitted into the atmosphere as CO_2 after conversion. For annual crops it is assumed that the C stock is zero, while in perennial woody crops a time constant C stock is assumed which is equal to the half of the C stock in biomass reached at the end of the production cycle.

While ABCS for grassland and forest corresponds to the values given in IPCC (2003), additional information from the literature has been taken into account for the ABCS values of shrubland and biofuel crops in Carre *et al*. (2009). For the classes 'sparse vegetation' and 'wetland' no ABCS data is cited in Carre *et al*. (2009). By expert judgment we assume 'sparse vegetation' to have 15% of the ABCS of grassland. For completeness reasons the ABCS for Wetlands are included, although they are not considered as subject to conversion in this work. Wetlands are assumed to consist 60% of grassland, 20% of open forest and 20% of closed forest (no open water was assumed, as at least part of the year the land is generally not covered by water). ABCS for wetlands was calculated from the grassland and open-closed forest ABCS values considering the before mentioned shares.

IPCC (2003) gives uncertainty ranges of 75 - 100% for the ABCS values in forest and grassland ecosystems, the same uncertainty range can be assumed also for shrubland, while for biofuel crops the uncertainty of ABCS was estimated based on available data and conservatively rounded to nearest $5^{th}/10^{th}$.

According to the assumptions mentioned before, no ABCS is assigned to the annual crop classes of maize, wheat, rice and 'other crops'. The remaining agricultural classes considered in our study (sugar crops, vegetables and fruits, oilseeds) are a mixture of annual, perennial shrub and tree crops. The share may differ largely between countries. From the McGill M3 crop data (Monfreda *et al*., 2008) we calculated the shares of the perennial crop sugar cane in the class 'sugar crops', the share of shrub and tree fruits in the class 'vegetables and fruits' as well as the share of the tree crops oilpalm, coconut, olive, karite and tung in the class "oilseed" for each country (see Table 41 in Appendix II), all other crops in these classes are considered as annual. The ABCS for these shrub and tree crops was estimated based on literature research and comparison of the plant size and dimensions (i.e. crown shape, height) with other woody crops existing in the same ecological region (Blujdea, 2010). It was also assumed that the C stock is constant over time and that it is half of the maximum reached at end of a production cycle. The ABCS values (t C ha^{-1}) used in this study are given in Appendix 2 (see Table 42). Based on the shares of the shrub and tree crops, country specific mean ABCS values for the land use classes sugar crops, oilseeds, vegetables and fruits were calculated.

In cases of cropland decrease it is currently supposed that the regional average ABCS developing on these areas corresponds to the regional average ABCS we calculate for the areas where conversion into cropland occurs. This is a preliminary assumption, however. It has to be examined more in detail, which land cover will develop if cropland is abandoned in the different regions of the world.

4. RESULTS OF APPLYING METHODOLOGY

4.1. IFPRI-MIRAGE DATA

The input data for estimating GHG emissions from ILUC were taken from the revised IFPRI data (version of 17.05.2010) and the output of the land allocation model. In the analysis data from the scenarios "*Business as Usual*" (BAU), "*Free Trade*" (FT) and "*Reference*" (REF) for 2020 were processed. All other data originates from base-layer dataset.

The output of the IFPRI model used in this study distinguishes 11 regions. Results are presented by country and as total values for LUC and C emissions. This representation was given preference to mapping regional figures or relative changes because eventually the quantity of GHG emissions per country are relevant.

4.1.1. SPATIAL ALLOCATION AND SOIL CARBON EMISSIONS

The output received from the IFPRI MIRAGE model relates to two different scenarios of world trade.

- **IFPRI BAU Scenario**

The changes in land cover provided by the spatial allocation procedure are used to estimate subsequent changes in C stocks. The distribution of changes in total cropland area by country/region in the BAU scenario according to the spatial allocation is presented in Figure 28.

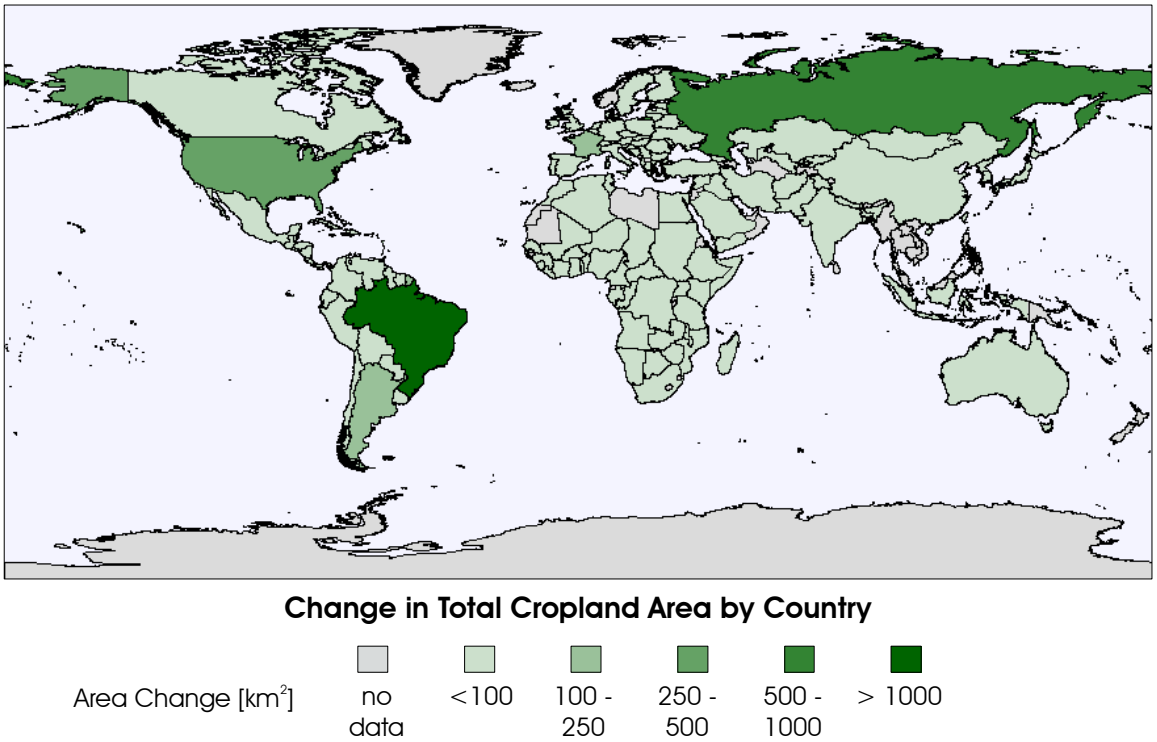

Figure 28: Change in Total Cropland Area by Country / Region from IFPRI BAU Scenario

The total area attributed to additional cropland for producing biofuels in the BAU scenario is 8,209 km^2. Most of the additional cropland is assigned to Brazil and CIS regions. In Europe the strongest increase is modelled for France (118 km^2). The changes in cropland areas in Africa are comparatively small and in the lowest legend category (<100 km^2).

The distribution of changes in soil organic carbon from LC by country / region in the BAU scenario are given in Figure 29.

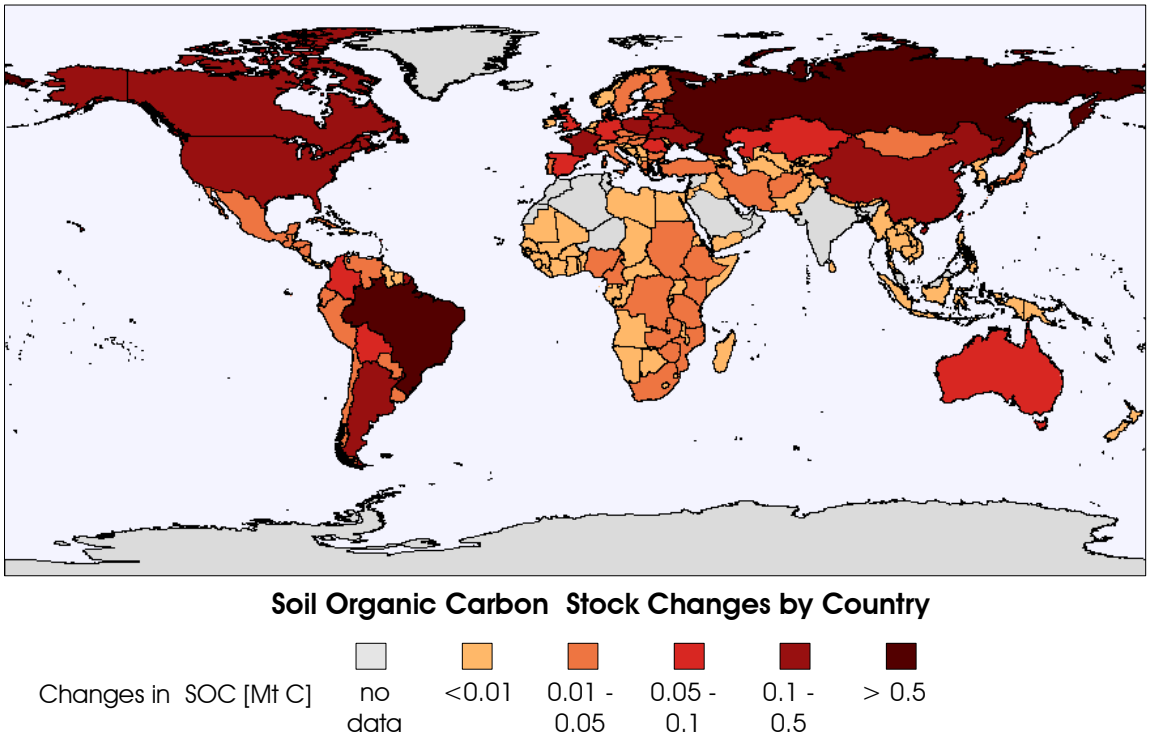

Figure 29: Changes in Soil Organic Carbon Following LUC in IFPRI BAU Scenario

The distribution of losses in SOC closely follow those from LUC. The larger part of losses in SOC are modelled for Brazil and the CIS region. Small changes are modelled for Europe and hardly any changes for Africa (< 100,000 t C in any country).

- **IFPRI FT Scenario**

The distribution of changes in total cropland areas by country/region in the IFPRI FT scenario resulting from the spatial allocation procedure is given in Figure 30

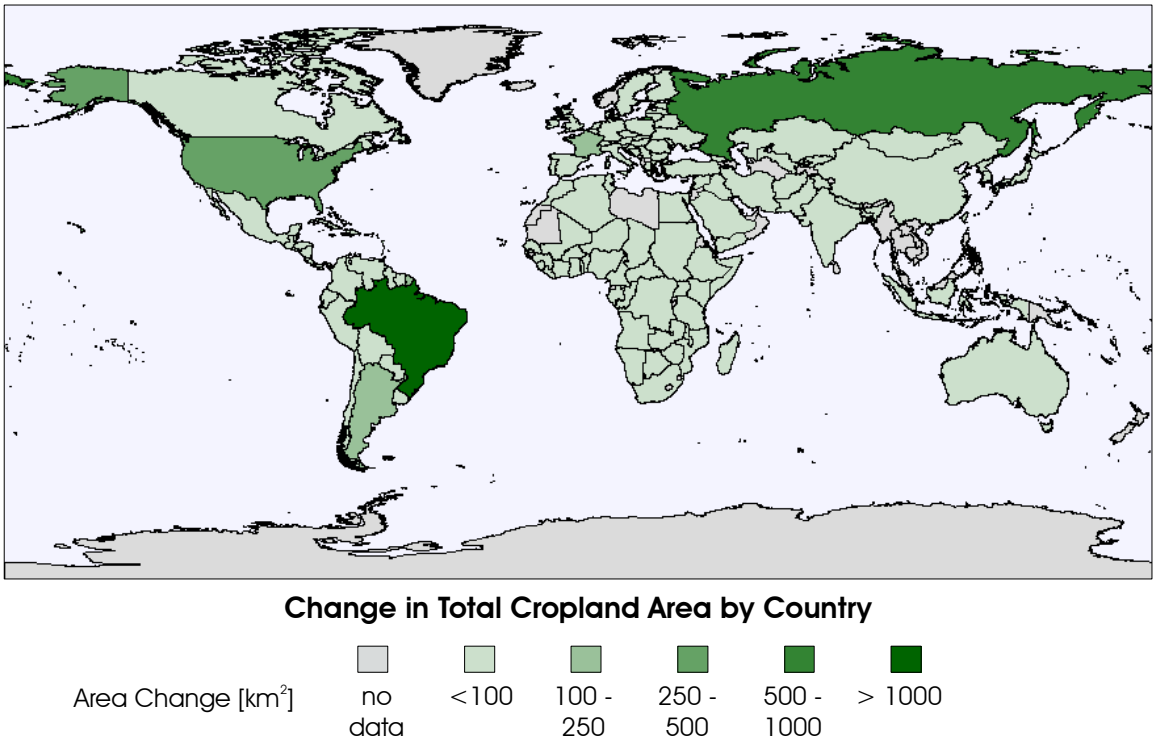

Figure 30: Change in Total Cropland Area by Country / Region from IFPRI FT Scenario

For the FT scenario the additional land demand is 9,759 km^2, slightly higher than for the BAU scenario. No significant changes in the distribution of land use changes between the BAU and the FT scenarios are apparent in figure. This would not be expected given that the global differences in the overall LUC area between the two scenarios is just 1,409 km^2.

When computing the corresponding change in C stock per area the FT scenario shows a distribution by country presented in Figure 31

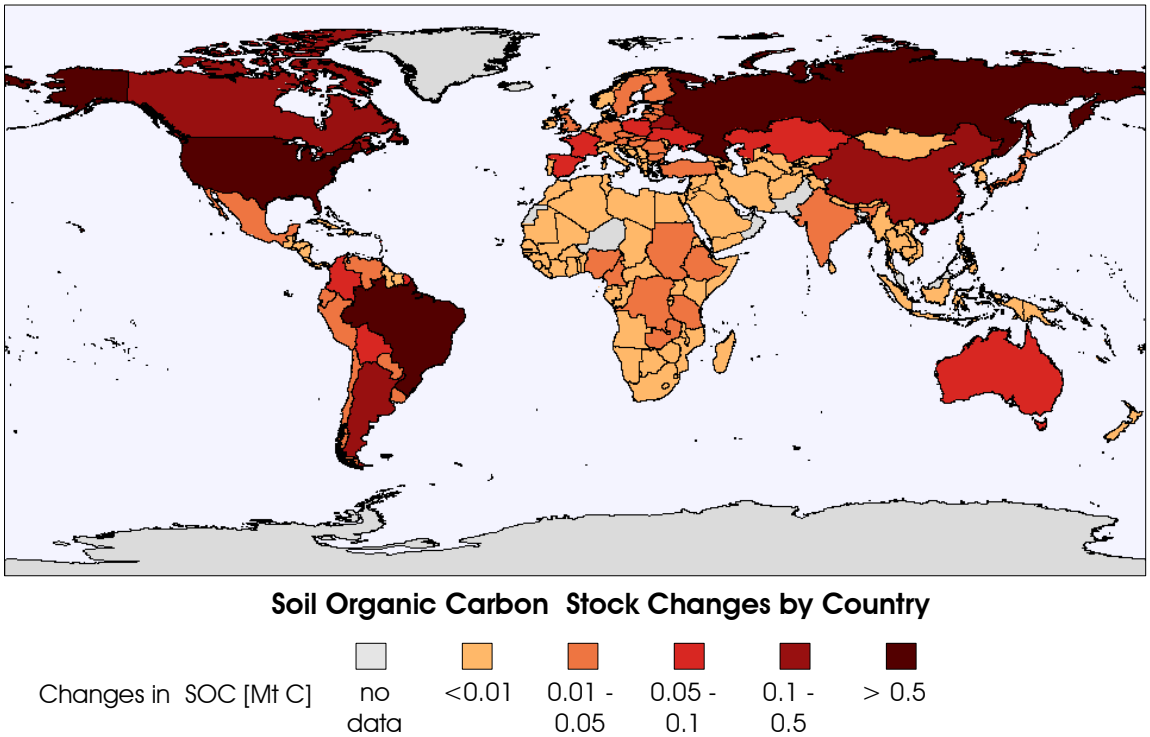

Figure 31: Changes in Soil Organic Carbon following LUC in IFPRI FT2020 Scenario

The map does not indicate significant changes in regional SOC stocks in the FT scenario when compared to the BAU scenario. There are, however, minor changes in some regions, mainly within the African region. In the BAU scenario the SOC losses for the CIS region are estimated at 1.13 Mt, as compared to 1.07 Mt in the FT scenario. The corresponding figures for Brazil are 3.67 Mt and 5.21 Mt, respectively. Those figures illustrate the differences in the crop areas and indicate that the FT scenario positions a significantly larger effect of LUC in Brazil than in the CIS region.

- **Carbon and CO_2 Emission Estimates from Soil**

A summary of the modelled effects of cropland area changes on soil C emissions for the BAU and FT scenarios from the IFPRI economic model is given in Table 22

Table 22: Soil C Emissions from IFPRI Economic Model BAU and FT Scenarios

Scenario	New Cropland	Soil Organic Carbon Stock Changes			CO_2
	km²	*Mt C*	*Relative Change (%)*	*t C ha⁻¹*	*Mt CO_2*
Business as Usual	8,209.0	-7.80	-0.0011	-9.5	28.6
Free Trade	9,758.9	-8.73	-0.0012	-8.9	32.0

In the BAU scenario the total cropland area attributed to ILUC is 8,209.0 km^2. The conversion of land to cropland at this level could be expected to reduce SOC stocks by -7.80 Mt, which would amount to 28.6 Mt of CO_2 emissions from the soil. For the FT scenario cropland expands 9,758.9 km^2. The change in land use modelled to result in a loss of SOC of 8.73 Mt or 32.0 Mt of CO_2 emissions from the soil.

The area of ILUC seems to be very low. In the BAU scenario the additional area for crops for growing biofuels amounts to approx. 90x90 km^2 globally. For the FT scenario the expanded area covers approx. 100x100 km^2.

This low figure suggests that the model allocates biofuels within existing cropland, which includes areas of set-aside, through intensification rather than in expanding cropland areas by land cover conversion. Changes in SOC through intensification on existing cropland are not included in the estimates. Between the FT and the BAU scenario land is converted to cropland increases by 1,550 km. The land conversion is regionally variable. Approximately 2/3 of the increase in land conversion from the BAU to the FT scenario is located in Brazil.

The effect on SOC stocks from the BAU to the FT scenario also shows regional differences. While the area of converted land increases by 18.9% the losses in SOC increase by 16.7%. This indicates that the additional areas converted under the FT scenario may not differ in their characteristics from those converted under the BAU scenario.

4.1.2. N_2O Soil Emissions

According to the JRC study based on IFPRI-MIRAGE (2010) data, the emissions of N_2O related to mineralized N as result of loss in soil organic C stocks are in the range of 5 - 6 Mt CO_2eq ha^{-1} within a period of 20 years (FT and BAU scenario respectively).

Table 23: Global N_2O Soil Emissions over a Period of 20 Years Related to Mineralized N Resulting from Loss of Soil Organic Carbon due to Land Use Change in 2020

Region	N_2O Soil Emissions Related to Mineralized N Resulting from Loss of SOC	
	IFPRI-MIRAGE BAU	IFPRI-MIRAGE FT
	Mt CO_2eq	*Mt CO_2eq*
Global Total	**5.1**	**6.2**

This source is rarely included in studies on GHG emissions from land use change due to biofuel production, but in our study it reaches 10 - 14% of the CO_2 emissions resulting from loss of soil organic C (Figure 33), depending on the soil C:N ratio in the region and the area where indirect emissions from leaching occurs.

For the discussion on the regional differences in emission (Figure 32) please refer to Chapter 4.1.2 Study Background as N_2O emissions are related to loss in SOC and hence follow a similar spatial pattern.

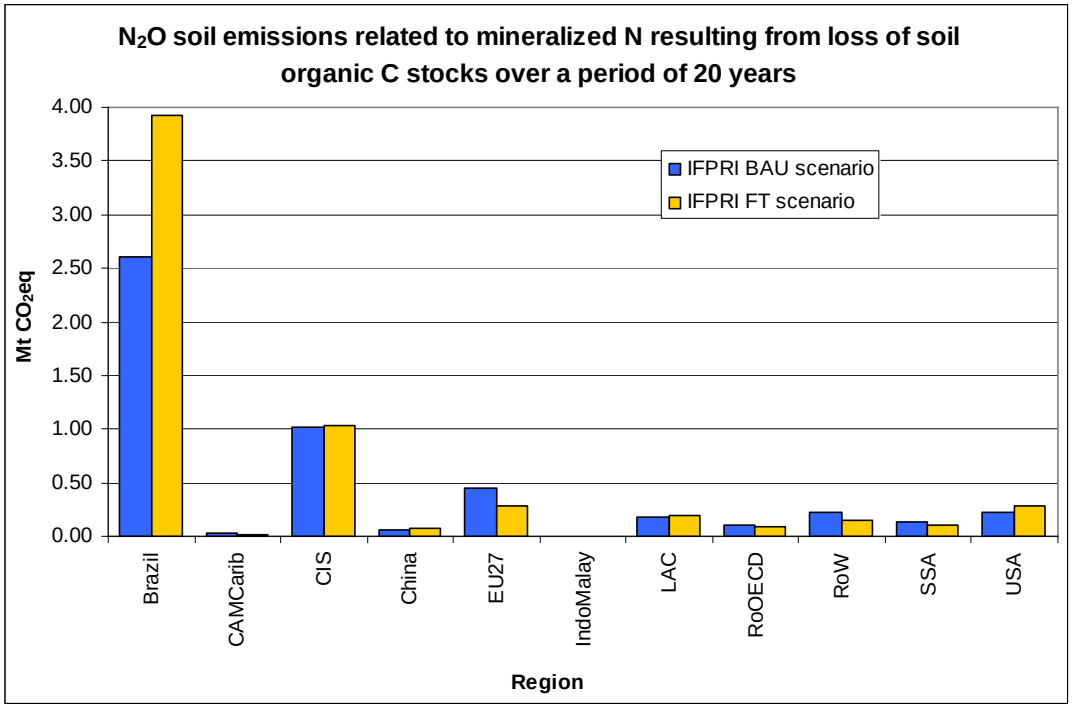

Figure 32: N_2O Soil Emissions over a Period of 20 Years Related to Mineralized N Resulting from Loss of SOC for IFPRI-MIRAGE Regions (BAU and FT scenarios, in Mt of CO_2eq.)

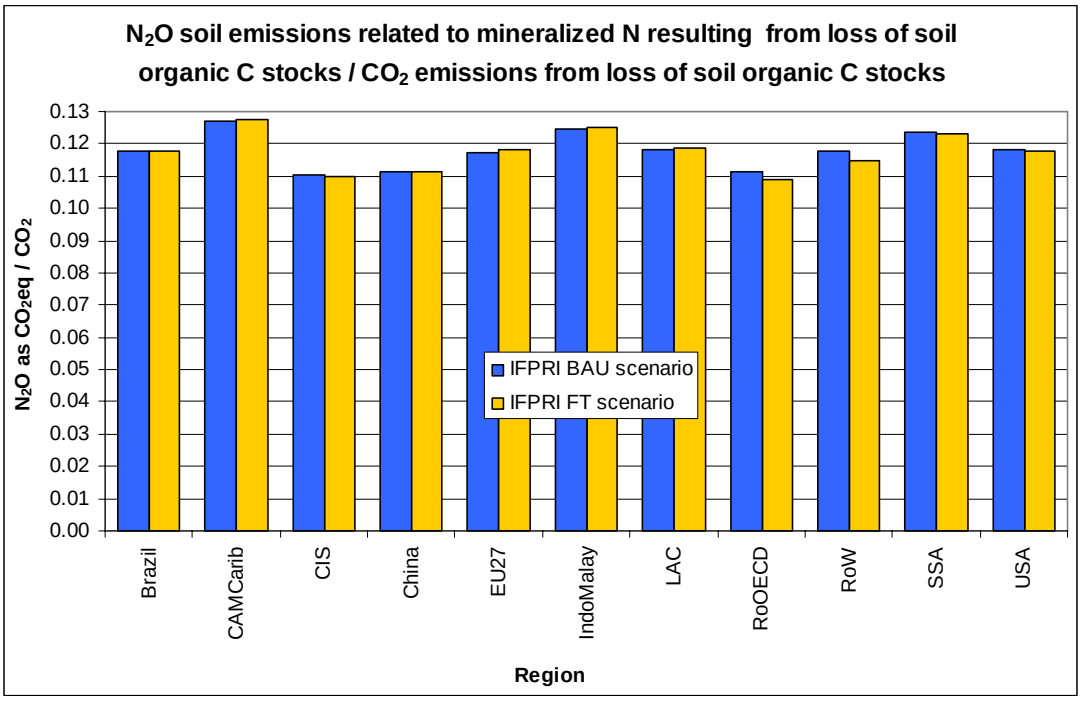

Figure 33: Relationship between N_2O Soil Emissions Related to Mineralized N and CO_2 Emissions from Loss of SOC

4.1.3. CO_2 Emissions from Changes in Above- and Belowground Biomass Carbon Stock

IFPRI (2010) reports total GHG emissions of 43.4 Mt CO_2eq (BAU scenario) and 46.1 Mt CO_2 (FT scenario) from loss of C in ABCS stock in areas subject to land use change. Based on our study the emissions due to change in ABCS result in 167.7 Mt CO_2eq for the BAU scenario and 209.8 Mt CO_2eq for the FT scenario (see Table 25). This large difference is mainly attributed by the fact, that the Spatial allocation procedure results in a higher share of closed forest (32%, see Figure 35) - with the highest ABCS of all land covers - converted into cropland than assumed in the IFPRI study (9% primary forest conversion, see Figure 34). However it is not mentioned explicitly in the IFPRI report which ABCS value was assigned to primary forest, thus it is not known if it is similar to the values for closed forests in our study. In both cases IPCC (2003) served as the basic source for the ABCS values, with additional information for shrublands and biofuel crops in our study as described in Carre *et al*. (2009).

The main land use change occurs in Brazil. It accounts for approx. 60% (BAU scenario) to 70% (FT scenario) of the global land use change modelled by IFPRI (see Figure 36 and Figure 37). Based on our study, the share in terms of CO_2 emissions compared to the global total is even higher (67% BAU scenario, 77% FT scenario) as the main land use/cover classes converted - closed forest and shrubland - show the highest ABCS

values (see Table 42 in Appendix 2) and the conversion rate is above the global mean (see Table 40, left and right graphic).

In our study we consider also the ABCS in permanent crops as sugar cane and tree crops. If land use/cover is converted into a sugar cane plantation, the mean annual carbon stock for sugar cane (4 - 5 t C ha^{-1}) is accounted for in the emission balance. In the case of Brazil the cultivation of sugar cane contributes with a positive carbon stock of 3 -5 Mt C (BAU and FT scenario respectively) to the total balance (see Figure 38 and Figure 39). Also in Europe and the Indo-Malaysia regions ABCS occurs on the positive side of the balance. In the IndoMalaysia region this is mainly caused by the conversion into oil palm plantations with an ABCS of approx. 60 t C ha^{-1} (see Table 42). In Europe the positive values in the emission balance is however mainly an artificial effect of the aggregation of classes. IFPRI predicts an increase of oilseed cultivation area in Europe, composed mainly of rapeseed and sunflower and to a minor extent also soybean. As a result of the spatial allocation procedure the oilseed cultivation area extension occurs mainly in Spain, Germany, France and Italy (see Figure 40). During the spatial allocation oilseeds are considered a single crop class and herbaceous crops are not distinguished from tree crops. As described in Chapter 5.4, a “mean” ABCS per ha was calculated for the oilseed crop class in each country based on the mean composition of oilseed crops in this country. As in Spain and Italy olive trees (ABCS approx. 43 t C ha^{-1}) contribute with 71% and 67% to the oilseed cultivation area, the average ABCS for oilseeds in these countries is about 30 t C ha^{-1}. This ABCS is then attributed to all oilseed extension area within the country, although the IFPRI data predicts an extension only for the 3 abovementioned annual herbaceous crops which should not be assigned any ABCS. In the global emission balance this effect is negligible in the current case, but it will be a point for future improvements.

The land use/cover classes used in the IFPRI study cannot be matched exactly with the classes considered within our study (see Table 24), therefore no detailed comparison using the individual ABCS for a certain land use/cover class of from our study is possible. However, a back-of-the-envelope calculation indicates that most probably at least some of the ABCS values in our study are higher than in the IFPRI study. This has to be examined more in detail. Differences may occur e.g. by including/excluding root biomass and dead organic mater (litter, dead wood). Both biomass compartments are considered in the ABCS values for our study. The share in total ABCS is 25% and more in the case of root biomass and around 5% in the case of dead organic matter in closed forest.

Table 24: Land Use/Cover Classes Available for Cropland Extension

IFPRI	This Study
Pasture	Grassland
Savannah and Grassland	
Managed forests	Closed Forest >30% coverage
Primary forests	Open Forest <30% coverage
Other land (shrubland, mountains, deserts, urbanized areas)	Shrubland
	Sparse Vegetation

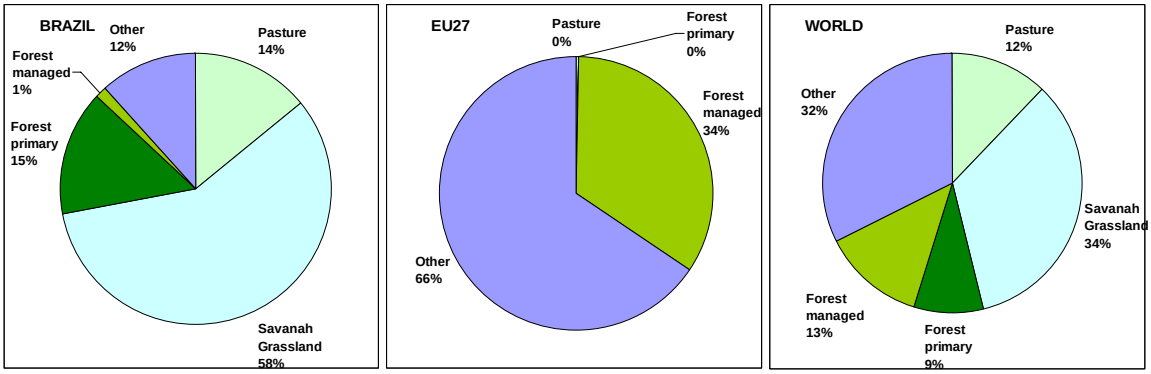

Figure 34: Land Use/Cover Converted to Cropland for IFPRI BAU Scenario According to Table S14 of IFPRI (2010)

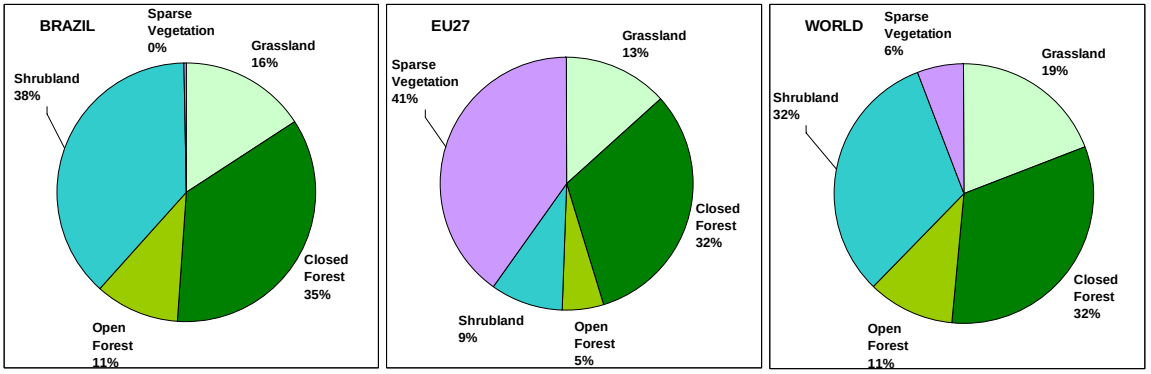

Figure 35: Land Use/Cover Converted to Cropland According to Spatial Allocation Procedure Based on IFPRI LUCRED (BAU scenario) Compared to LU2000

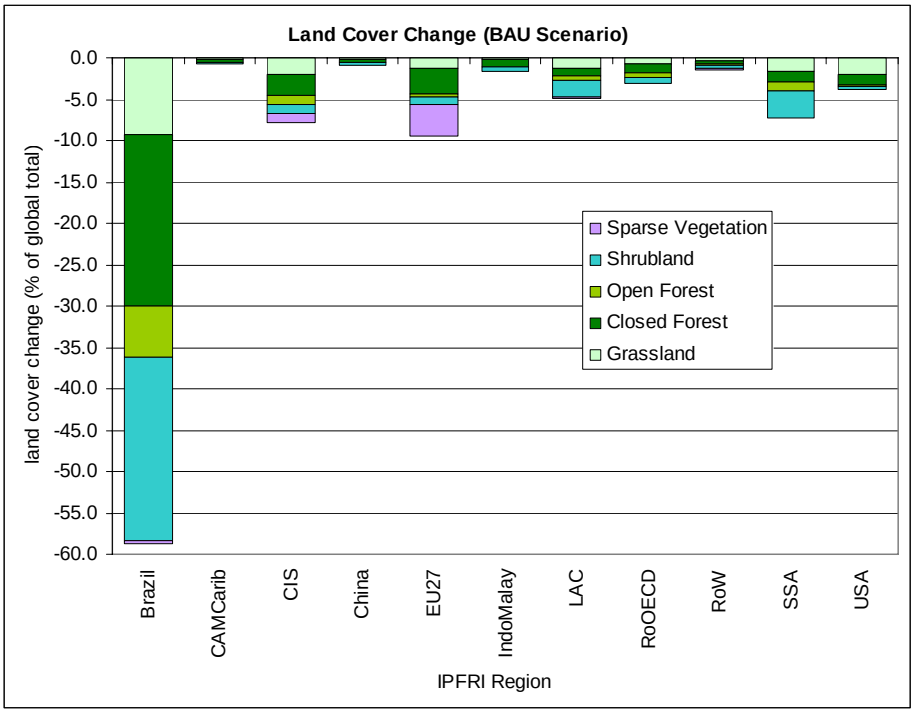

Figure 36: Decrease of Non-agricultural Land Cover (total global decrease = 100%) in Different Regions and Land Cover Types Based on Spatial Allocation Procedure Applied to IFPRI LUCRED (BAU scenario) Compared to LU2000

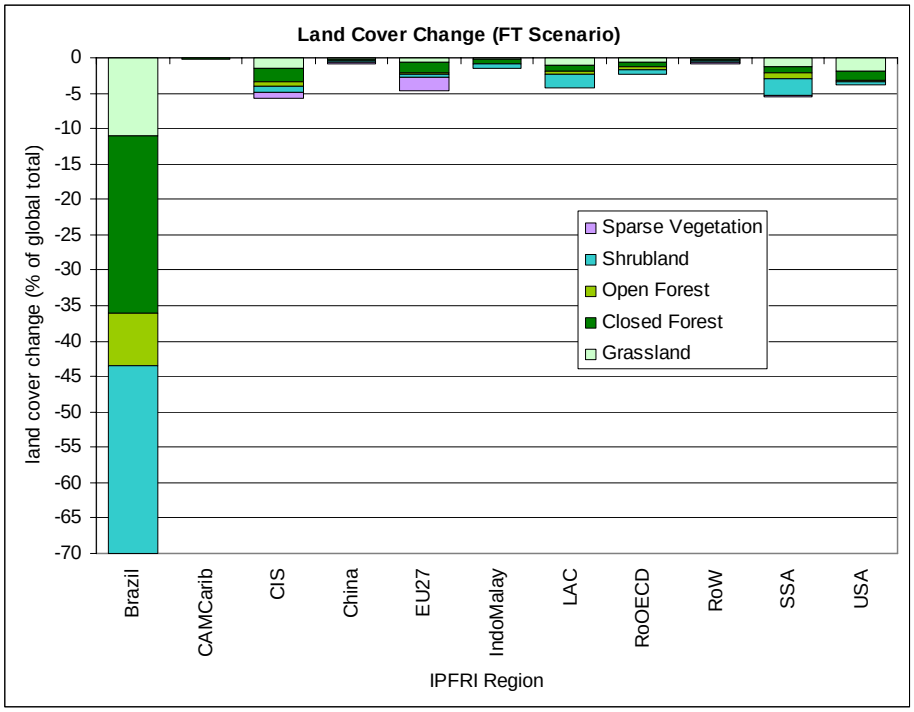

Figure 37: Decrease of Non agricultural Land Cover (total global decrease = 100%) in Different Regions and Land Cover Types Based on Spatial Allocation Procedure Applied to IFPRI LUCRED (FT scenario) Compared to LU2000

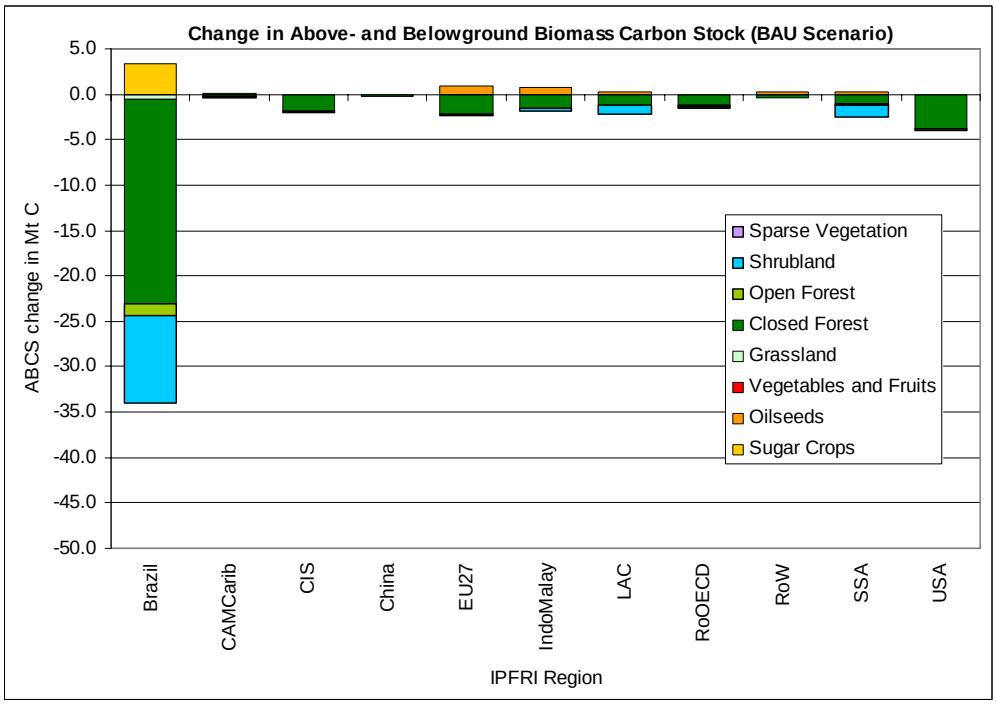

Figure 38: Change in Above- and Belowground Biomass Carbon Stock (Mt C) in Different Regions Based on Spatial Allocation Procedure Applied to IFPRI LUCRED (BAU scenario) Compared to LU2000

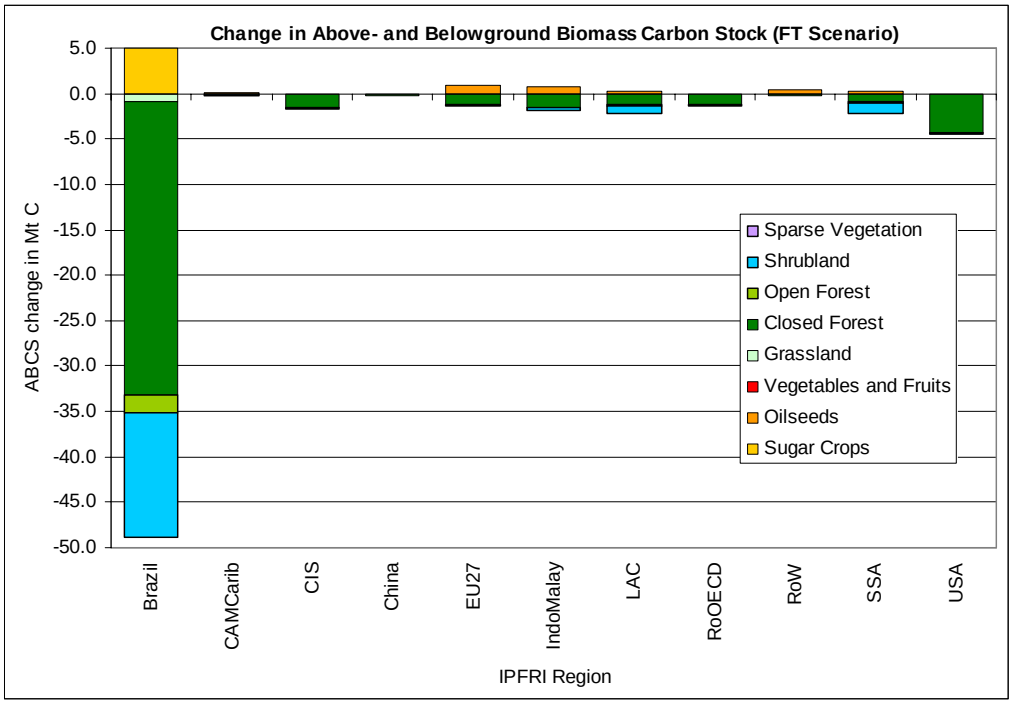

Figure 39: Change in Above- and Belowground Biomass Carbon Stock -ABCS-(Mt C) in Different Regions. Based on spatially allocated IFPRI LUCRED (FT scenario) compared to LU2000

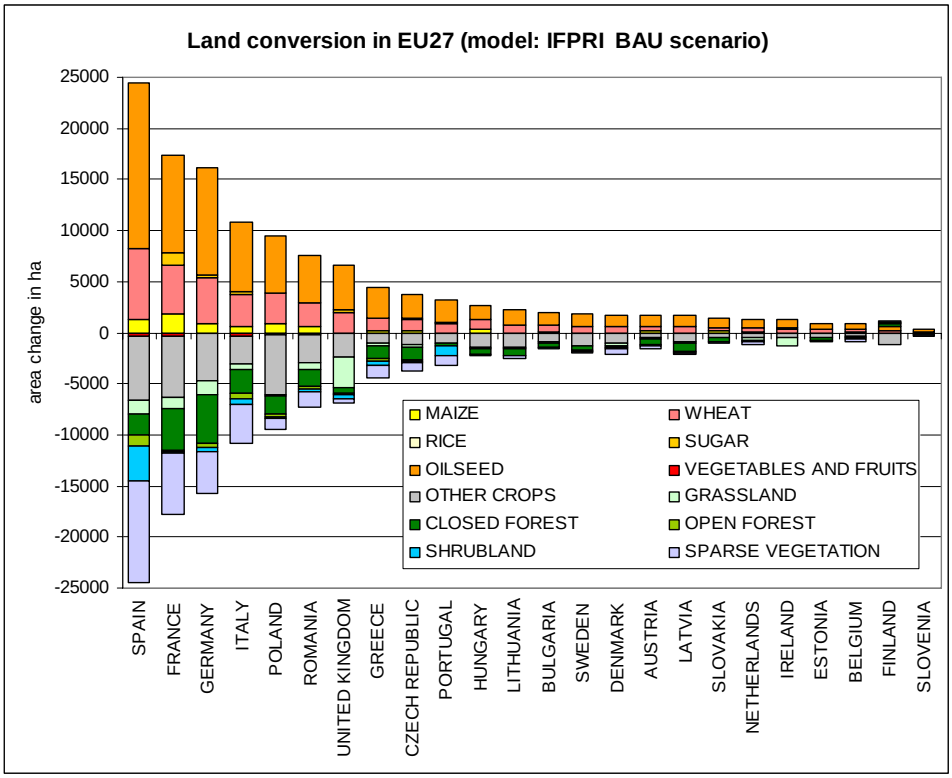

Figure 40: Change in Land Use/Cover in EU Countries Based on Spatial Allocation Procedure applied to IFPRI LUCRED (BAU scenario) Compared to LU2000

Table 25: Emissions from change in Above- and Belowground Biomass Carbon Stock Related to Biofuel Cultivation in 2020 by IFPRI Region

Region	Emissions from Change in Above- and Belowground Biomass Stock			
	Business As Usual (BAU)		Trade Liberalization (FT)	
	IFPRI (2010)*	This Study	IFPRI (2010)*	This Study
	Mt CO_2		*Mt CO_2*	
Brazil	24.0	112.6	28.5	160.8
CAMCarib		1.2		0.5
CIS	3.2	7.3	2.9	6.4
China	1.6	0.9	1.4	0.8
EU27	3.0	5.6	1.8	1.9
IndoMalay	3.4	4.1	3.4	4.1
LAC	2.6	6.8	2.7	7.0
RoOECD	1.1	5.5	0.9	5.0
RoW	1.2	0.7	0.9	-0.3
SSA (Africa)	1.5	8.1	1.4	7.1
USA	1.9	14.7	2.2	16.3
Global Total	**43.4**	**167.7**	**46.1**	**209.8**

* *The table shows IFPRI original results (from IFPRI, 2010 p. 92 Table 9) and spatially allocated IFPRI model results (this work). Positive values are extra emissions.*

CO_2 emissions from change in ABCS based on the spatial allocation procedure results for the IFPRI study (168 - 210 t CO_2eq ha^{-1}) are significantly higher than the values of 43-46 t CO_2eq given by IFPRI for 2020. This is largely attributed to the different shares of land use/cover classes assumed to be converted into cropland: The spatial allocation procedure gives a larger share of land use cover classes with high ABCS (forest and shrubland) to be converted into cropland.

4.2. JRC-IPTS AGLINK-COSIMO DATA

As with all model data received in form of spreadsheet tables the data were transferred to tables of a relation database (RDB). The transfer to the RDB allows evaluating data for consistency and integrity. This transfer also includes an implementation of the data structure. The aggregation of regions in the AGLINK-COSIMO data follows a multi-level approach. Initially single countries and some country aggregates (including EU-15

and EU-12) are calculated and thereafter aggregates are built. A multi-level structure for crops was reconstructed by the authors of this report from a logical arrangement of the countries and regions based on the data received from JRC-IPTS and in a manner that was suitable for the spatial allocation procedure. At Level 1 three regions are defined: AGLINK aggregate, COSIMO aggregate and "*Rest of the World*". Those regions are subdivided into 20 regions of Level 2.

The structure of the crops and their aggregations as used in the project are given in Table 26.

Table 26: Crop Types and Aggregations in AGLINK-COSIMO Model Data

Level 0	Level 1	Level 2	Level 3	Level 4	Level 5
Macroeconomic					
	Crops				
		Cereals and oilseeds			
			Cereals		
				Wheat	
				Coarse grains	
					Barley
					Maize
					Oats
					Sorghum
					Other cereals
					Rye
			Oilseeds		
				Soybeans	
				Rapeseed	
				Sunflower seed	
		Rice			
		Sugar (in raw sugar equivalent)			
			Sugar beet		
			Sugar Cane		
		Vegetables & Fruit			
			Potatoes		
			Dried beans		
			Manioc		
		Special crops			
			Cotton		
			Jatropha		
	Pasture				

Blue: Crops used in emission analysis
Underlined: Crops available for the complete set of countries/regions

According to the interpretation of the structure, Level 2 appeared to be the most practical data to use in the study, with the exception of the groups "Vegetables & Fruit" and "Special Crops". As explained by JRC-IPTS experts, the crop group "Vegetables and Fruit" is not modelled in AGLINK-COSIMO. The special crops cotton and jatropha

are modelled only for those countries for which the commodities are relevant in economic terms.

When preparing the data for the study some additional particulars of the crop aggregation scheme had to be considered. According to the aggregation *Rice* is reported separately from the "*Cereals*" group. "*Coarse Grains*" include maize in the aggregation schema, but is not reported for all regional aggregation levels. Also, there is no group summing all other crops which could be used as a correspondence to the group "Other Crops" used in the study.

Given the importance of coarse grains for biofuels the variability of reporting grain maize depending on the aggregation level and region was dealt with by defining two runs for the emission analysis:

a) data for maize are used where available (GM run);
b) coarse grain areas are used to represent maize areas where they are not reported (CG run).

In practice, these two runs of the spatial allocation procedure delimit a range for a value of a distinct crop of grain maize: maize cannot be more than what is used in CG run, and not less than what is used in GM run. With respect to the total cropland area or any other crop group there is no difference between the data of the two runs.

4.2.1. SPATIAL ALLOCATION AND SOIL CARBON EMISSIONS

The distribution of the area requirements by country of the scenario for the run with grain maize processed where such data are reported is presented in Figure 41.

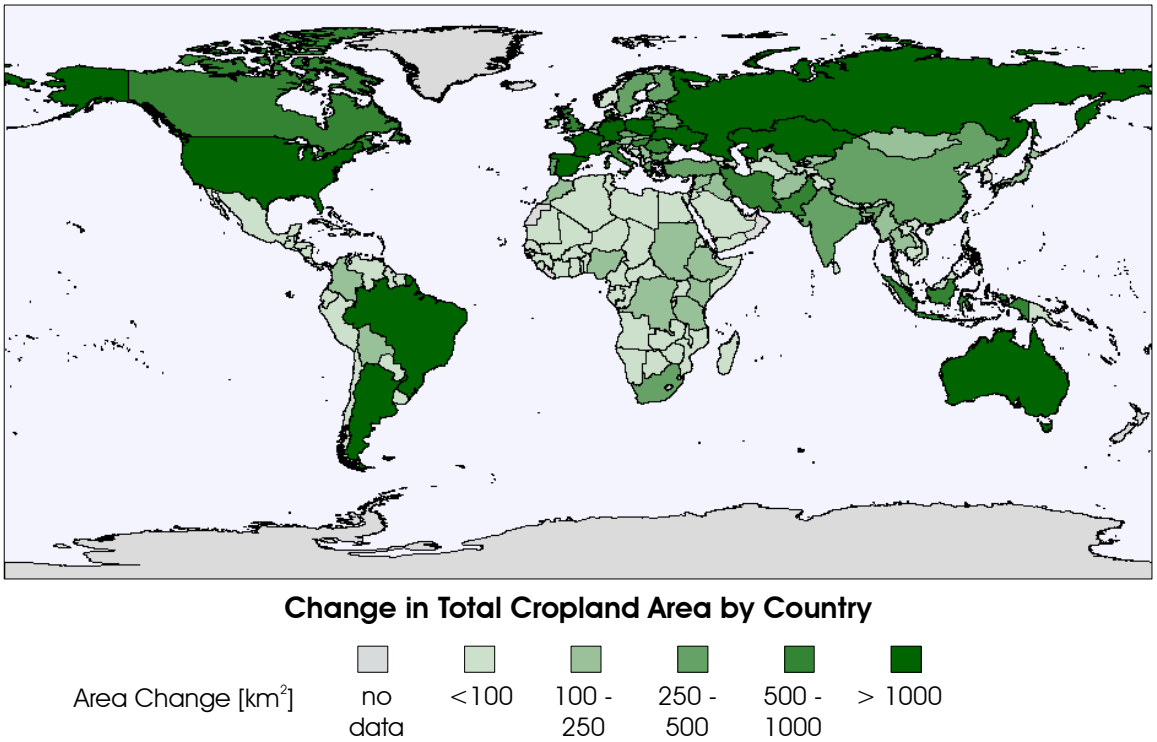

Figure 41: Change in Total Cropland Area by Country / Region from AGLINK Scenario (CG Run)

Only the map for the CG run is shown, because as far as total cropland needs are concerned the runs use identical values. The total area needs of the scenario over the reference data is 52,372.1 km^2.

- **Changes in Soil Organic Carbon Stocks from CG Run**

The changes in SOC resulting from the LUC as defined for the CG run are presented in Figure 42.

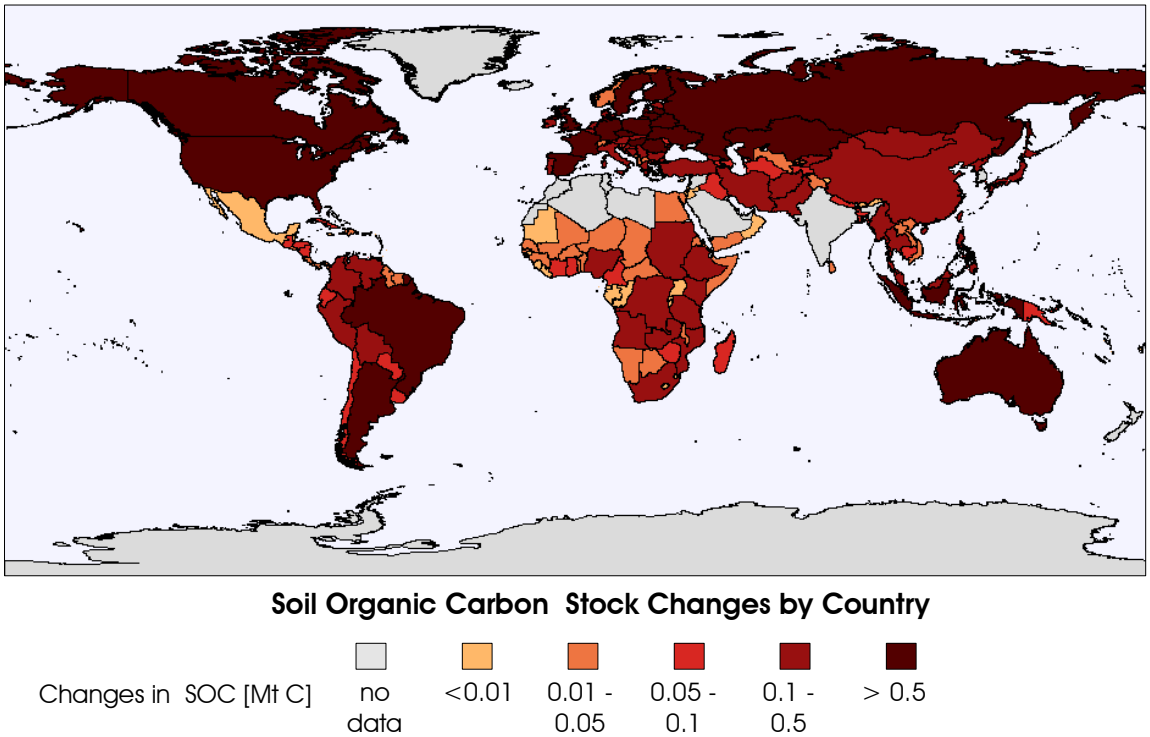

Figure 42: Changes in Soil Organic Carbon following LUC in AGLINK Scenario (CG Run)

The main areas of changes in SOC stocks are found in Argentina, Australia, Brazil, North America, CIS and Indonesia/Malaysia. Within the classification scheme Europe shows a degree of variation with southern and eastern parts of Europe showing lower losses in SOC stocks than central and northern European areas. The situation in Africa is more diverse than in other AGLINK-COSIMO regions.

- **Changes in Soil Organic Carbon Stocks from GM Run**

The corresponding changes in SOC stocks for the GM run are presented in Figure 43.

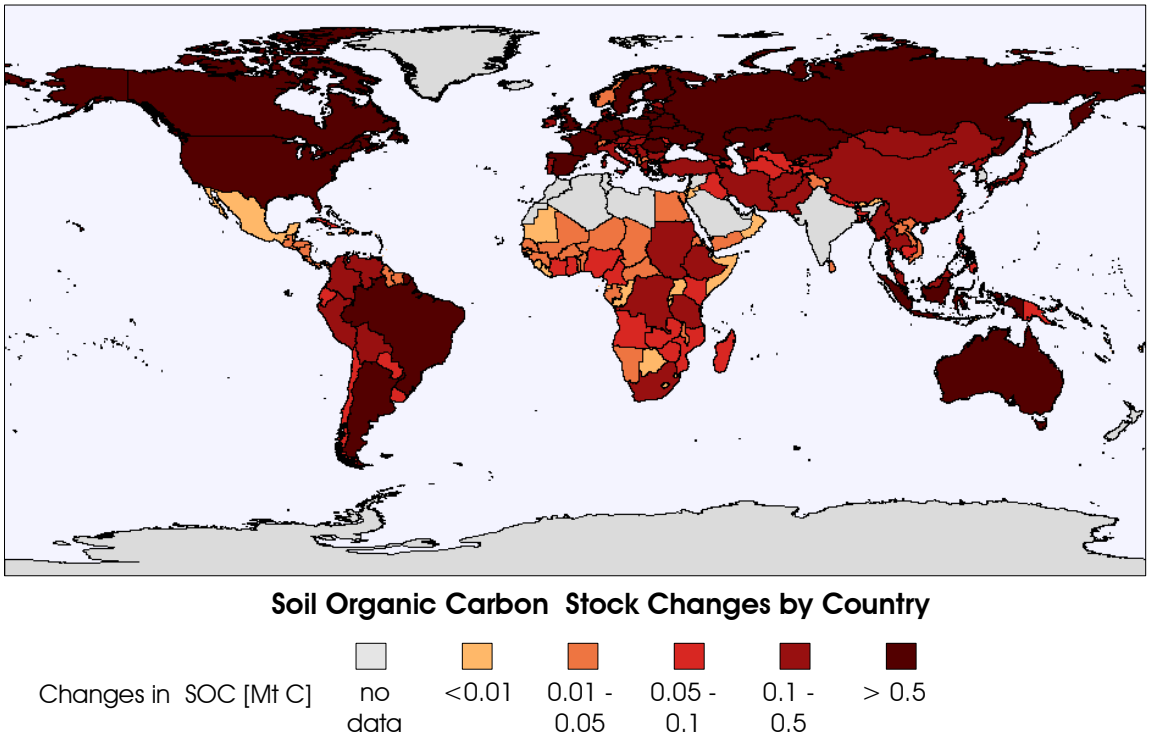

Figure 43: Changes in Soil Organic Carbon following LUC in AGLINK Scenario (GM Run)

The general pattern of changes in SOC stocks is comparable to the CG run for most regions with the notable exception of Africa. Here the merge of grain maize with coarse grains has resulted in a decrease in SOC stocks in some countries, such as Nigeria and Angola, and an increase in others, such as South Africa or Mozambique.

- **Carbon and CO2 Emission Estimates from Soil**

As regards the management and system factors for computing changes in SOC stocks the treatment of grain maize as a distinct crop or including the crop in the group of coarse grains, and therefore as part of the crop group "*Other crops*", is of no consequence. However, with respect to the spatial distribution the areas where grain maize, coarse grains and other crops are found varies. As a consequence, the factors influencing SOC, which are soil type, management practice and system, differ with geographic location of the crop. Globally, the harvested maize area for 2008 is 1,610,165.42 km^2. This amounts to 22.6 % of all harvested area for cereals, or 12.4 % of the harvested area of all primary crops (FAO Statistics Division, 08. July, 2010)[35]. For the CG run the area under change attributed to grain maize is 7,160 km^2 while for the GM run the area is 2,994 km^2. Although the changes are small compared to the overall area under maize the figures differ by a factor of almost 2.5. Thus, changes in the treatment of gain maize in the estimation of CO_2 emissions can be expected to have

[35] http://faostat.fao.org/site/291/default.aspx

some bearing on changes SOC stocks, albeit only as a function of the geographic positioning of the crops.

A summary of the global changes in soil organic C stocks and CO_2 emissions from soil is given in Table 27

Table 27: Soil Carbon Emissions from AGLINK-COSIMO Economic Model Scenario

Scenario	New Cropland	Soil Organic Carbon Stock Changes			CO_2
	km²	*Mt C*	*Relative Change (%)*	*t C ha⁻¹*	*Mt CO_2*
Grain Maize where available, coarse grain as "*Other crops*"	52,372.1	-55.0	-0.0076	-10.5	201.8
Grain Maize & Coarse Grains as "*Grain Maize*"	52,372.1	-59.7	-0.0082	-11.4	218.9

When areas for grain maize are used for regions where such values are available SOC stocks are reduced by 55.0 Mt, corresponding to a release of 201.8 Mt CO_2. In case all areas under coarse grain are treated as grain maize the losses in SOC amount to 59.7 Mt or 218.9 Mt CO_2, an increase of 8.5% over the GM run. The difference indicates that grain maize is spatially associated with other soil types and land management systems than other coarse grains.

4.2.2. N_2O EMISSIONS

Based on IPTS AGLINK-COSIMO scenario, (for CG and GM runs) the N_2O emissions related to change in soil carbon contribute with approx. 28 Mt CO_2eq to the annual GHG emissions in areas subject to land use/cover change (Table 28). Almost 1/3 of the emissions are related to land use/carbon stock change in the EU27 area.

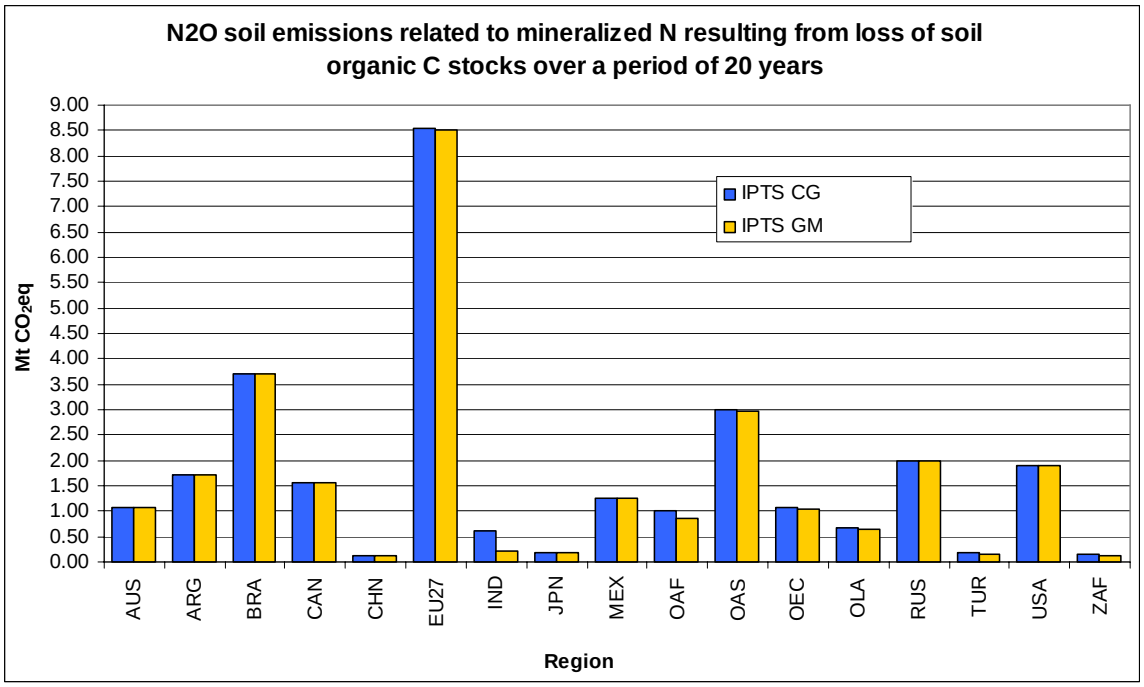

Figure 44: **N_2O Soil Emissions Related to Mineralized N Resulting from Loss of Soil Organic Carbon for IPTS AGLINK-COSIMO Results (CG and GM runs, in Mt CO_2eq. over 20 years)**

Table 28: **Global N_2O Soil Emissions Related to Mineralized N Resulting from Loss of Soil Organic Carbon due to LUC in 2020 over 20 Years**

Region	N_2O Soil Emissions Related to Mineralized N Resulting from Loss of Soil Organic Carbon	
	IPTS AGLINK-COSIMO CG run	IPTS AGLINK-COSIMO GM run
	Mt CO_2eq	*Mt CO_2eq*
Global Total	**28.8**	**28**

4.2.3. CO_2 EMISSIONS FROM CHANGES IN ABOVE AND BELOW GROUND BIOMASS

In this section only the IPTS Biofuel scenario based on the CG crop aggregation (maize is part of the "other crops" class within the spatial allocation procedure) is described as the results are almost identical to the GM run where maize is considered as a single crop class for several countries. For completeness, emissions for both runs are given in Table 29.

The predicted area subject to a land use change is around 5 times higher than in the IFPRI scenarios due to different assumptions for the scenarios as described previously. The major land use change occurs in EU27 (see Figure 46), followed by Brazil, Argentina, and the other Asian countries (OAC delineation). In general the land use change is more scattered over the globe than in the IFPRI study. The share of land use/cover classes converted into cropland in EU27 as output of the spatial allocation is rather similar to the IFPRI result (compare Figure 35 and Figure 45). In Brazil a slightly higher share of shrubland and lower share of closed forest can be observed. For the global average a lower share of shrubland and a higher share of sparse vegetation are subject to land use change based on IPTS results compared to the IFPRI results.

The major contribution to the total CO_2 emission results from land use/cover change in Brazil (see Figure 47). This is due to the fact that ABCS values for tropical closed forests and shrublands are significantly higher than in the corresponding classes in temperate Europe (see Table 42). Further, the area of shrubland subject to conversion in Brazil is more than 2 times higher than in Europe (see Figure 46). Notable are the GHG emissions in Canada and the US, despite the small share of land conversion, the contribution to the global greenhouse gas emissions is high due to ABCS values in North American forests of up to 400 t C ha^{-1}.

Looking at the positive side of the C balance (see Figure 47), the effect of class aggregation - described in the previous section - may lead to an overestimation of the ABCS related to the oilseeds class also in this case.

Global emissions from changes in ABCS based on the spatial allocation of the IPTS-AGLINK-COSIMO biofuels scenario results are calculated to be approx. 865 Mt CO_2eq with a major part of the emissions resulting from land use change in South America and Europe (see Table 29)..

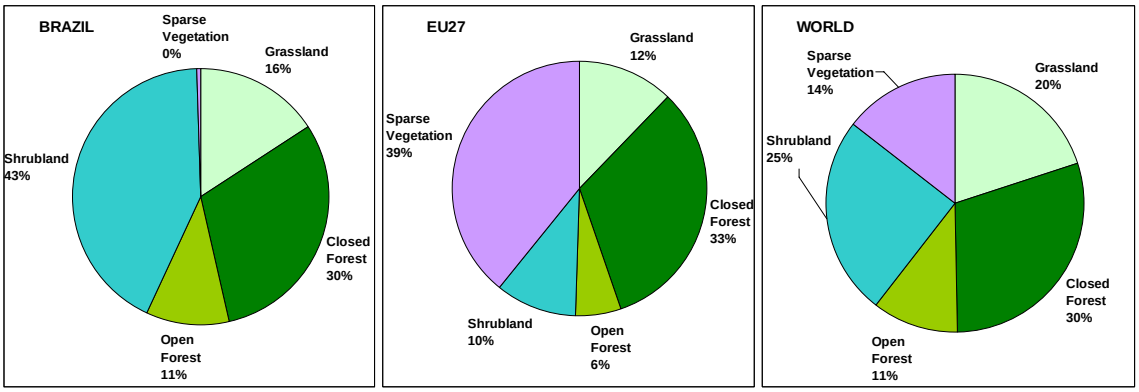

Figure 45: Land Use/Cover Converted to Cropland Based on Spatial Allocation Procedure Applied to IPTS LUCRED (CG Run) Compared to LU2000

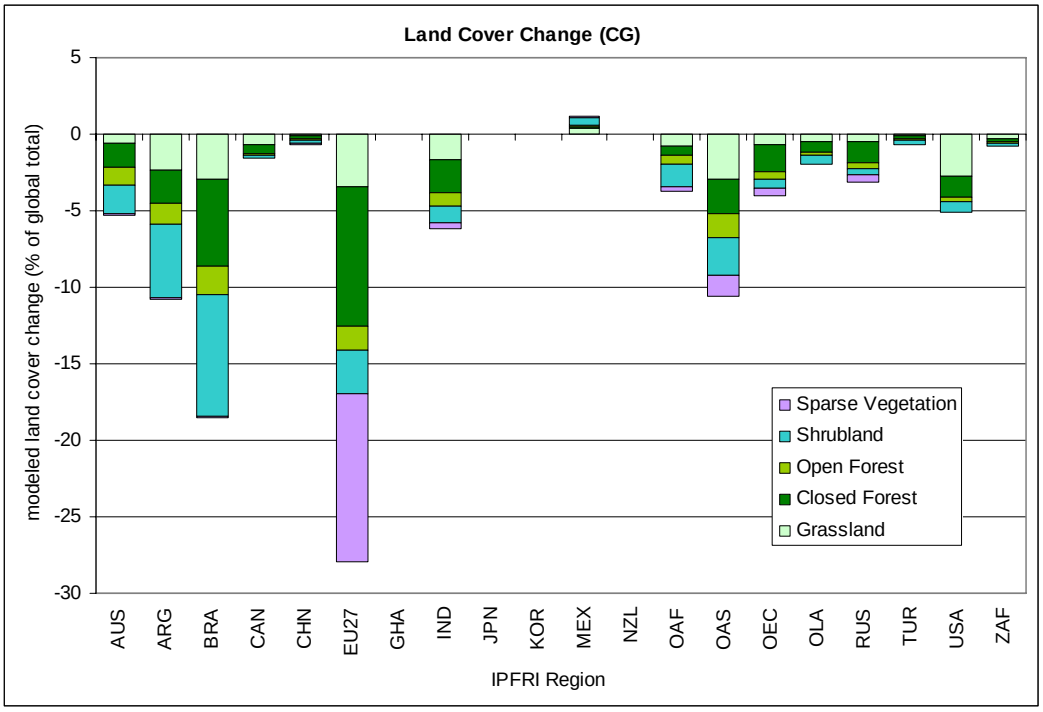

Figure 46: **Change in Non-agricultural Land Cover (total global decrease = 100%) by Region Based on Spatial Allocation Procedure Applied to IPTS LUCRED (CG Run) Compared to LU2000**

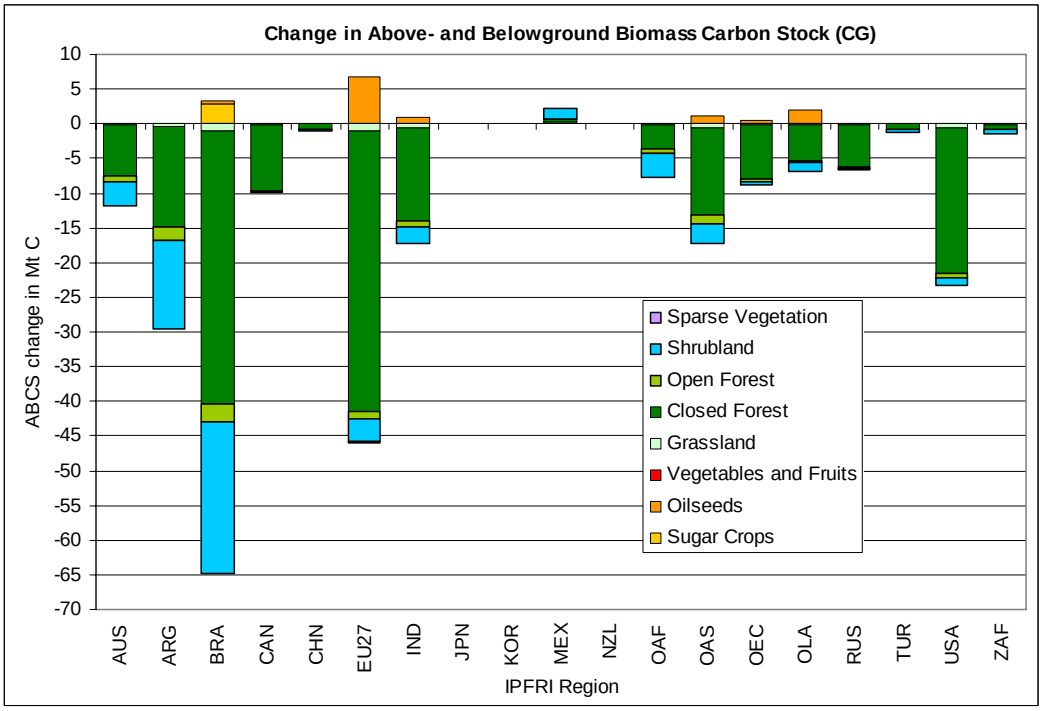

Figure 47: **Change in Above- and Belowground Biomass Carbon Stock by Land Cover and Region Based on Spatial Allocation Procedure Applied to IPTS LUCRED (CG Run) Compared to LU2000**

Table 29: Emissions from Change in ABCS Related to Biofuel Cultivation in 2020 by Region

Region	Emissions from Change in Above- and Belowground Biomass Stock			
	IPTS (2010) CG run		IPTS (2010) GM run	
	Mt CO_2	*Share %*	*Mt CO_2*	*Share %*
AUS	44	5	43	5
ARG	108	12	106	12
BRA	226	26	226	26
CAN	36	4	36	4
CHN	4	0	4	0
EU27	144	17	144	17
IND	60	7	60	7
JPN	0	0	0	0
KOR	0	0	0	0
MEX	-8	-1	-8	-1
NZL	0	0	0	0
OAF	28	3	25	3
OAS	59	7	58	7
OEC	30	4	30	3
OLA	18	2	18	2
RUS	25	3	25	3
TUR	5	1	4	0
USA	85	10	85	10
ZAF	5	1	5	1
Global Total	**867**	**100**	**862**	**100**

4.3. Overall Emissions Estimated from Agro-Economic Models

Total GHG emissions resulting from extra land demand based on IFPRI-MIRAGE and AGLINK-COSIMO model as run by JRC-IPTS are summarized in Table 30. The figures presented are the outcome of this JRC study using a newly developed model to allocate the extra land demand according to a range of criteria such as suitability of the land, proximity to infrastructure etc. Emissions were estimated based on the assumption that no LUC occurred on organic soils as a consequence of growing biofuels. Additional

GHG emissions from intensification are not taken into account at the current stage within the present report.

Table 30: Total Greenhouse Gas Emissions from Changes in Soil and Biomass Carbon Stocks Induced by ILUC

Source	IFPRI BAU		IFPRI FT		IPTS CG		IPTS GM	
	Mt CO_2eq	*%*	*Mt CO_2eq*	*%*	*Mt CO_2eq*	*%*	*Mt CO_2eq*	*%*
Emissions from change in soil C stock	29	15	32	14	202	18	219	20
N_2O emissions related to loss in soil C	5	2	6	2	28	3	29	3
Emissions from change in ABCS	168	82	210	83	862	79	867	78
Total GHG emissions from land use change	201	100	248	100	1092	100	1115	100

Major contribution (~80%) to total GHG emissions follows from the removal of above- and belowground biomass (ABCS). Changes in soil carbon stock contribute with ~15 to 20%, whereas N_2O emissions related to loss in soil C stock have only a small share (2-3%) compared to the other sources.

It needs to be outlined that the emissions from change in ABCS depend strongly on the assumptions about the share of forest to be converted into cropland. A small change in the share may cause a considerable increase/decrease of the emissions as the biomass stock - thus the carbon released due to the conversion - is generally high compared to other land uses as e.g. grasslands.

4.4. ANNUAL GHG EMISSIONS PER AMOUNT OF ENERGY

Emissions based on the model output of the two studies used (IFPRI-MIRAGE and AGLINK-COSIMO used by JRC-IPTS) were compared in terms of emissions per amount of energy produced as the initial assumptions on energy demand in the year 2020 differ between the models. A summary of the values is given in Table 31.

Table 31: Annual GHG Emissions from Changes in Soil and Biomass Carbon Stocks per Amount of Energy Produced

Source	Unit	IFPRI BAU	IFPRI FT	IPTS CG	IPTS GM
Annualized total GHG emissions from land use change (spread over 20years)	*Mt CO_2eq*	10.1	12.4	54.6	55.7
Extra Energy produced in 2020 (Scenario - Baseline)	*MJ*	300	303	865	865
Extra Energy produced in 2020 (Scenario - Baseline)	*Mtoe*	7.2	7.3	20.6	20.6
Annual GHG emissions from land use change (spread over 20 years)	*g CO_2eq/MJ*	34	41	63	64
Annual GHG emissions from land use change (spread over 20 years)	*t CO_2eq/toe*	1.4	1.7	2.7	2.7

The values given in Table 31 refer to the extra energy produced in the biofuel scenarios (the EU-RED is fully applied) compared with the production in the reference scenario (no EU-RED). The extra energy production values differ by a factor approx. 3 (IFPRI-MIRAGE 300 Million GJ vs. IPTS-AGLINK 865 Million GJ).

As prescribed in the RED the total emission from change in soil and biomass carbon stock are distributed equally over a period of 20 years. Then the annualized emissions are compared with the increase in annual biofuel production.

From Table 31 the study found that annual emissions per amount of energy produced are in the range of

- 34 - 41 g CO_2eq MJ^{-1} for the IFPRI-MIRAGE scenarios and
- approx. 63 g CO_2eq MJ^{-1} for IPTS-AGLINK.

These differences are the result of the output generated by the agro-economic models and the various assumptions made in the definition of scenarios. The model output varies with respect to the additional area of arable land, the regions to which those areas are allocated and the expansion of crops as a function of the ratio between biodiesel and bioethanol.

4.5. TOTAL EMISSIONS FROM BIOFUEL PRODUCTION

Annex V of the RED describes the methodology to calculate life cycle GHG emissions from different biofuels pathways. It also contains a list of typical and default values for their direct GHG savings, which accounts for emissions from cultivation, processing, transport and distribution, but do not include emissions from LUC. Therefore, in order to see the effect of ILUC adjunct based on the model results on the default emissions given in the legislation of the RED, the "ILUC emissions" should be added to the default values in the Directive. Since the total annual emissions due to LUC calculated in this study refer to "biofuels" demand increase (i.e. are not disaggregated by individual crop), a "weighted" default value for direct GHG savings has been calculated by the JRC, weighting the default values for individual biofuels by their proportion in EU demand in 2020 as provided by the MIRAGE and AGLINK-COSIMO simulations.

That is satisfactory for looking at the possible effect of an ILUC adder in legislation. But the RED states that for the purpose of policy analysis a different methodology should be used. Instead of allocating a proportion of emissions to by-products according to their energy content, the by-products generate an emissions credit calculated from what they replace ('substitution' or 'systems expansion') approach. The JEC consortium's (JRC – EUCAR – CONCAWE)[36], Well-to-Wheels report v3[37] applies this approach but uses the same database as that for the RED directive

Details may be found in the Impact Assessment of the proposed revision of the biofuel Directive, which also clearly explains the logical reasons for using a different approach for the purpose of legislation and for scientific research[38].

For completeness of information, it is also important to report the total GHG emissions that would result taking GHG emissions values from the WTW study.

[36] EUCAR and CONCAWE are research bodies linked to the European motor and oil industry respectively.

[37] "Well-to-wheels analysis of future automotive fuels and power trains in the European context" by JRC, EUROCAR and CONCAWE. v2c March 2007. Available on-line at http://ies.jrc.ec.europa.eu/WTW.html.

[38] Annex to the Impact Assessment. Document accompanying the Package of Implementation measures for the EU's objectives on climate change and renewable energy for 2020. Document available on-line at http://ec.europa.eu/environment/climat/pdf/climat_action/climate_package_ia_annex.pdf.

4.5.1. TOTAL EMISSIONS FROM BIOFUEL PRODUCTION UNDER IFPRI SCENARIOS

The total emissions from the production of biofuel estimated from the IFPRI scenarios are shown in Table 32.

Table 32: Total Emissions from Cultivation, Processing, Transport and Distribution of Production from IFPRI Scenarios

Feedstock	Total EU Demand (Prod. + Imports)		Total EU Demand		RED Default Value	Contribution to RED EU-Weighted Default Values		Contribution to JEC WTW Emissions	Contribution to JECWTW EU-Weighted Emissions	
	BAU - REF	FT - REF	BAU - REF	FT - REF		BAU - REF	FT - REF		BAU - REF	FT - REF
	Mtoe	*Mtoe*	*MJ*	*MJ*	*g CO_2 MJ^{-1}*	*g CO_2 MJ^{-1}*	*g CO_2 MJ^{-1}*		*g CO_2 MJ^{-1}*	*g CO_2 MJ^{-1}*
Sunflower	0.07	0.07	$2.93\ 10^{9}$	$2.93\ 10^{9}$	41	0.40	0.40	29	0.28	0.28
Soybeans	0.41	0.43	$1.72\ 10^{10}$	$1.80\ 10^{9}$	58	3.33	3.45	76	4.36	4.53
Rapeseed	0.25	0.27	$1.05\ 10^{10}$	$1.13\ 10^{9}$	52	1.82	1.94	45	1.57	1.68
Palm fruit	0.25	0.25	$1.05\ 10^{10}$	$1.05\ 10^{9}$	37*	2.38	2.35	24	0.84	0.83
Wheat	0.56	-0.19	$2.35\ 10^{10}$	$-7.96\ 10^{9}$	44**	5.48	-1.84	49	3.84	-1.29
Sugar cane + Sugar Beet	5.48	6.42	$2.30\ 10^{11}$	$2.69\ 10^{11}$	26***	22.99	26.68	14	10.73	11.24
Maize	0.13	-0.03	$5.45\ 10^{9}$	$-1.26\ 10^{9}$	43	0.78	-0.18	43	0.78	-0.18
Total	**7.15**	**7.22**	**3.00** 10^{11}	**3.03** 10^{11}		**31**	**28**		**22**	**17**

* Default value from RED, assuming methane capture at oil mill in the production process. At the moment only a tiny proportion of palm oil production uses methane capture, but it might become more important in the future. In any case, using the default value in the annex V without methane capture (70 g CO_2 MJ^{-1}) would add only 1 g CO_2 MJ^{-1} to the "weighted default value", and therefore the lower "methane capture" values has been considered here.

** The pathway considered here is assumed to be "wheat ethanol, with natural gas as process fuel in CHP plant" " which we think will be the main type of plant operating in 2020. Annex V of the RED also includes a default value for ethanol from wheat where process fuel is not specified (70 g CO_2 MJ^{-1}). As for the previous footnote, using this value would bring a negligible difference (1 g CO_2 MJ^{-1}) to the total "weighted default value".

*** Default values weighted for aggregated crops sugar cane + sugar beet. The value has been calculated as weighted average, considering all EU imports from sugar cane and all EU production from sugar beet. Default values in Annex V of RED for sugar cane and beet are respectively 24 and 40 g CO_2 MJ^{-1}.

IFPRI considers four feedstocks for vegetable oils (palm oil, soybean oil, sunflower oil and rapeseed oil) for biodiesel production, and four for ethanol (wheat, maize, sugar beet and sugar cane), aggregating in the calculation the two sugar feedstock into a single category (sugar cane + sugar beet).

According to IFPRI data (Table S2b in IFPRI on-line supporting excel files), the amount of biofuels imports has been calculated considering that for biodiesel 70% is from palm fruit (from IndoMalay region) and 30% from soybean, and for ethanol all imports are from sugar cane (Brazil and CAMCarib regions).

The "WTW-weighted values" are calculated taking emission values from Table 9.2 in Appendix 2 of the WTW report, for the pathways that are indicated in the study as the most likely for 2020.

Adding the "weighted emissions" from cultivation, processing, transport and distribution in Table 32 to the "ILUC emissions" calculated in this study results in the following total emissions:

Table 33: Sum of "Weighted Emissions" from Cultivation, Processing, Transport and Distribution and ILUC Emissions

	"RED" scenarios		"WTW scenarios"	
	BAU-REF	FT - REF	BAU-REF	FT - REF
	$g\ CO_2\ MJ^{-1}$	$g\ CO_2\ MJ^{-1}$	$g\ CO_2\ MJ^{-1}$	$g\ CO_2\ MJ^{-1}$
Total Annual Emissions	65	69	56	58

4.5.2. TOTAL EMISSIONS FROM BIOFUEL PRODUCTION UNDER JRC-IPTS SCENARIO

Concerning the JRC-IPTS study, AGLINK-COSIMO do not distinguish between the different vegetable oils used as feedstock for biodiesel production, and the same level of "oil-feedstocks disaggregation" as in MIRAGE models is therefore not available.

To calculate the "weighted default value", in this case it was assumed that the increase in biodiesel demand (all from imported oils) is satisfied by rapeseed oils, with a RED default value for cultivation, processing, transport and distribution of 52 g CO_2eq MJ^{-1}. For the ethanol sector, it was assumed that all imports (from Table 3.5 in IPTS report) are from sugar-cane ethanol (default value of 24 g CO_2eq MJ^{-1}), and sugar-beet ethanol, only from EU production, was calculated as difference between EU ethanol production

(see Table 3.5 in IPTS report) and EU-wheat and coarse grain ethanol production (from Tables 3.7 and 3.8 in IPTS report).[39]

A summary of the calculations to derive the "weighted default value" is presented in Table 34.

Table 34: Total Emissions from Biofuel Production from IFPRI Scenarios

Feedstock	Total EU Demand (Prod. + Imports)	Total EU Demand	Default Value	Contribution to "EU-Weighted" Default	Contribution to "RED EU-Weighted" Default	"WTW" Emissions	"WTW EU-Weighted" Emissions
	kt	*PJ*	*g CO_2 MJ^{-1}*	*g CO_2 MJ^{-1}*	*g CO_2 MJ^{-1}*	*g CO_2 MJ^{-1}*	*g CO_2 MJ^{-1}*
Veg Oil	17100.80	634	52	36.02	36.02	45	31.17
Wheat	2898.30	78.0	44	3.75	3.75	49	4.18
Coarse Grains	2385.76	64.2	43	3.02	3.02	43	3.02
Sugar Beet	2816.94	75.8	40	3.32	3.32	25	2.07
Sugar Cane	2343.00	63.1	24	1.65	1.65	24	1.65
Total	**27544.80**	**915**		**48**	**48**		**42**

Calculation of "EU-weighted" default value for cultivation, processing, transport and distribution from default values in Annex V of the RED and disaggregated EU demand increase for different biofuels feedstocks in IPTS-AGLINK scenario.

The total emissions (from ILUC and from cultivation, processing, transport and distribution) thus become **111 g CO_2 MJ^{-1} and 105 g CO_2 MJ^{-1}** respectively for the RED and the WTW methodology.

4.5.3. Comparison of total Annual GHG Emissions from Models

To assess the GHG savings of biofuels, the total emissions from biofuels shall be compared with the emissions of the fossil fuel comparator. This value is calculated as 83.3 g CO_2eq MJ^{-1} given in the RED and is about 87.0 g CO_2eq MJ^{-1} in the WTW

[39] The "production yield" to calculate the amount of biofuels from different feedstocks reported in tables 3.6 to 3.8 in IPTS report are:
1 tons of wheat = 0.3 tons of ethanol
1 tons of coarse grains = 0.31 tons of ethanol
1 tons of vegetable oil = 0.973 tons of biodiesel

analysis[40]. The RED sets the minimum of GHG emissions saving to >35% from biofuel compared to the fossil fuel emissions.

A summary of the total annual emission values (including emissions from LUC) calculated by the JRC for the two scenarios in IFPRI-MIRAGE (BAU and FT) and IPTS-AGLINK models compared to the emissions of the fossil fuel comparator, and the savings are given in % compared to fossil fuel emissions is presented in Table 35.

Table 35: Annual GHG Emissions from LUC, Cultivation, Processing, Transport and Distribution of the Biofuels and Default Annual Fossil Fuel Emissions

Emission Source	Method	Crop	Annual Emissions $g\ CO_2eq\ MJ^{-1}$
Annual emissions from land use change (IFPRI BAU Scenario)		averaged over all crops	34
Annual emissions from land use change (IFPRI FT Scenario)		averaged over all crops	41
Annual emissions from land use change (IPTS)		averaged over all crops	63
"Weighted values" for annual emissions from cultivation, processing, transport and distribution of the biofuel - IFPRI MIRAGE	"Default" RED methodology	BAU scenario	34
		FT scenario	27
	JEC WTW methodology	BAU scenario	22
		FT scenario	17
Annual emissions from cultivation, processing, transport and distribution of the biofuel – JRC-IPTS AGLINK-COSIMO	"Default" RED methodology		48
	JEC WTW methodology		42
Fossil Fuel Comparator	RED methodology		**83.3**
	JEC WTW methodology		**87.0**

According to the RED methodology annual emissions from LUC have been amortized over 20 years. After this period LUC emissions need to be recalculated for the different amortization time (e.g. 25 years), while the default emissions (from cultivation, transport and distribution) are assumed to remain constant over time.

[40] The exact values in the on-line WTW study are 85.8 3 g $CO_2eq\ MJ^{-1}$ for conventional gasoline and 87.4 3 g $CO_2eq\ MJ^{-1}$ for conventional diesel

The total annual emission values (including emissions from LUC) calculated by the JRC for the two scenarios in IFPRI model (BAU and FT) and from JRC-IPTS compared to the emissions of the fossil fuel comparator, and the savings achieved after 20 to 400 years since a LUC occurred are given in Table 36 for the GHG emission calculated with the RED method and using the WTW method in Table 37.

Table 36: Annual Greenhouse Gas Emissions from Biofuels Compared to Emissions of Fossil Fuel – values calculated using the methodology and default values in the RED

Years after Land Use Change	Fossil Fuel Comp.	IFPRI BAU		IFPRI FT		JRC-IPTS	
		Emission	*Saving*	Emission	*Saving*	Emission	*Saving*
Years	*g CO_2eq MJ^{-1}*	*g CO_2eq MJ^{-1}*	*%*	*g CO_2eq MJ^{-1}*	*%*	*g CO_2eq MJ^{-1}*	*%*
20	83.3	65		69	17%	111	**-34%**
25	83.3	58	30%	61	27%	98	**-19%**
30	83.3	54	35%	55	33%	90	**-8%**
35	83.3	50	39%	51	38%	84	**-1%**
40	83.3	48	42%	49	42%	80	4%
45	83.3	46	44%	46	44%	76	8%
:		:		:	:		
300	83.3	33	60%	31	63%	52	37%
:		:	22%	:	:	:	:
400	83.3	33	61%	30	64%	51	38%

Emission savings >35% occur for the first time.
Emission saving > 60%.
Emission increase.

The investigation found that emission savings are obtained in the first 20 years after the crop conversion according to LUC and scenarios in IFPRI study. For the JRC-IPTS AGLINK-COSIMO simulations a negative GHG balance in the first 35 years is computed. The emissions saving required by the RED (>35%) however is only reached after 30 years for the BAU scenario, after about 35 years for the FT scenario and only many years later for the IPTS scenarios.

Table 37: Annual Greenhouse Gas Emissions from Biofuels Compared to Emissions of Fossil Fuel – values calculated using the methodology and default values in the WTW analysis

Years after Land Use Change	Fossil Fuel Comp.	IFPRI BAU		IFPRI FT		JRC-IPTS	
		Emission	*Saving*	Emission	*Saving*	Emission	*Saving*
Years	*g CO_2eq MJ^{-1}*	*g CO_2eq MJ^{-1}*	*%*	*g CO_2eq MJ^{-1}*	*%*	*g CO_2eq MJ^{-1}*	*%*
20	87	56	36%	58	33%	105	**-21%**
25	87	49	43%	50	43%	92	**-6%**
30	87	45	49%	44	49%	84	3%
35	87	41	52%	40	54%	78	10%
40	87	39	55%	38	57%	74	16%
45	87	37	57%	35	60%	70	20%
:	87	:		:	:	:	:
300	87	24	72%	20	77%	52	40%
:	:	:	:	:	:	:	:
400	87	24	73%	19	78%	45	48%

Emission savings >35% occur for the first time.
Emission saving > 50%.
Emission saving > 60%.
Emission increase.

When GHG emissions are calculated according to the WTW methodology, the 35% savings are obtained in the first 20 years after the crop conversion for both scenarios in IFPRI study. For the JRC-IPTS AGLINK-COSIMO simulations a negative GHG balance in the first 25 years is computed.

4.5.4. UNCERTAINTY RANGES FOR INPUT DATA

When comparing the different results it has to be kept in mind that there are variations in the assumptions the JRC had to make (e.g. share of land cover subject to conversion into cropland) to set the framework conditions, and that there are high uncertainties connected to each single step in the calculation chain starting from the economic model results, the spatial allocation, the land use/cover and other input data. On overview of uncertainties in the input data is given in Table 38.

Table 38: Uncertainty Ranges for the Input Data to Calculate Emissions from LUC

Parameter	Value	Uncertainty Range	Source
Factor for direct N_2O emissions (EF_1)	0.01	0.003 - 0.03	IPCC (2006)
Factor for indirect N_2O emissions from leaching/runoff (EF_5)	0.0075	0.0005 - 0.025	IPCC (2006)
Fraction of N losses by leaching/runoff ($Frac_{LEACH-(H)}$)	0.3	0.1 - 0.8	IPCC (2006)
ABCS	all	75- 100%	Carre *et al*. (2009)
Soil carbon default values		unknown	IPCC (2006)
Management system factors		Limited coverage	IPCC (2006), Carre *et al*. (2009)
Spatial input data (land use/cover, soil parameters, climate etc.)		unknown/difficult to assess as no verification data are available	

Thus, the results have to be interpreted with caution. The focus of this work was to test and describe the method and to show the influence of different assumptions on the results. A detailed uncertainty analysis has to be undertaken to allow more robust conclusions.

5. SUMMARY AND CONCLUSIONS

The study successfully applies the methodology previously developed for estimating GHG emissions from soil and vegetation from indirect land use changes (ILUC) to the results from two different economic models on biofuel production in 2020. Using harmonised spatial data as the basis for allocating extra land demands allows for a much more detailed analysis of the effects biofuels production on GHG emissions than is possible with the data available for broad geographic regions. The various processing modules and stages present quite different challenges to be addressed and lead to some distinct constraints which should be considered when comparing the findings of this study with the results of other studies.

5.1. BASE DATA AND PREPARATION

In the preparation of the base data, great care should be taken to produce consistent thematic layers. With the marginal changes analysed being so small at the global scale, even minor geographic irregularities between spatial layers can considerably distort the results. With a land surface area of 135,708,500 km^2 (not including Antarctica) the extra land demands are minute (<0.006% for the IFPRI BAU scenario). Geographic characteristics must be uniform and the layers must also be consistent in the representation of thematic parameters. In this respect, the base data had to be substantially adjusted to the specifications of the methodology for GHG emission calculations. In particular, the two forest classes defined in the RED do not match the classification schemes generally used for global land use and cover data, so the corresponding classes had to be estimated. Information on cropland was taken from the McGill M3 dataset to provide a better correspondence with FAO statistical data on the distribution of individual crops, which are also used by the economic models. The McGill M3 dataset used in this study is not without its shortcomings. It refers to the status of crop areas as of the year 2000 and, due to the disaggregation method used, the spatial resolution is a rather nominal value.

The demand for data consistency is particularly relevant to datasets with a hierarchical structure, such as the climate regions and ecological zone layers. These thematic layers were completely generated from climate data to avoid overlaps or gaps in the delineated areas, which could lead to artefacts being introduced into the results. Only the Harmonized World Soil Database was found to be suitable for generating a suitable soil-related base data.

5.2. SPATIAL ALLOCATION OF EXTRA LAND DEMAND

When dealing with results of agro-economic models which are used as the input data for the spatial allocation procedure, the different timeframes to which the data relate had to be dealt with.

Although aligned to FAO statistics, the McGill M3 data used the year 2000 as a baseline. Data for 2008 or projections to the year 2020 are not available in any level of detail. This introduces an inconsistency with respect to the use of the reference years reported in the output data of the economic models. As a consequence, the 2020 reference scenario data projected by the models could not be used directly by this study.

Instead, the analysis was based on the marginal changes between the *policy* and the reference scenarios projected for 2020, and the differences were applied to the base data. This approach assumes that cropland expansion until 2020 will not significantly influence the characteristics of the additional land used as a consequence of growing biofuels. Specifically, soil carbon stocks, land cover types and crop yields are assumed to remain constant across the area of cropland expansion.

This assumption is justified by the fact that the aim of this exercise is to calculate the impact of ILUC due to the biofuel policies and not to the *general* changes in cropland demand. On the other hand, it represents a bias in the allocation process, because the output of the spatial allocation procedure could be affected by the absolute amount of land being allocated.

Another constraint on cropland expansion modelling is the method applied to account properly for competition for land between the various crops. The output from the AGLINK-COSIMO model is only complete for a selected set of important crops and does not provide a complete land use estimate. As a consequence, the substitution of crops for which the demand is decreasing (non-biofuel crops) by those for which demand is increasing (biofuel crops) cannot be modelled, and thus the amount of land to be converted to cropland (and the associated GHG emissions) could be overestimated.

To avoid any misunderstandings, it is worth mentioning that the spatial allocation procedure used at the JRC does not include any form of economic modelling. The economic data are taken from the model results and are converted to spatial layers using proximity and biophysical criteria.

5.3. GHG EMISSIONS FROM ILUC

The demand for extra land modelled by IFPRI for the year 2020 using the MIRAGE model come to 8,209 km^2 (BAU scenario) and 9,759 km^2 (FT scenario). The extra demands estimated by the JRC-IPTS using the AGLINK-COSIMO model come to 52,372 km^2.

According to IFPRI data, the emissions from soil as a result of land use changes on the extra land required in the BAU scenario are 201.4 Mt CO_2eq (16.7% from soil, 83.3% from vegetation) and 248.0 Mt CO_2eq (15.4% from soil, 84.6% from vegetation) in the FT scenario. Using the JRC-IPTS data, the GHG emissions are estimated at 1,108.9 Mt CO_2eq (22.3% from soil, 77.7% from vegetation). With regard to biofuel production, savings in GHG emissions of >35% are estimated to be reached after 30 years using the IFPRI data (FT scenario) and after 300 years using the JRC-IPTS data.

The economic analysis carried out by IFPRI places most of the land demands on Brazil, where the largest increase in cropland area is driven by sugar cane (7,575.1 km^2) and soybean (602.5 km^2). This increase in crop area amounts to approx. 50% of the global area of crop expansion (16,229.9 km^2 crop area expansion vs 8,020.9 km^2 crop area contraction). The output of the AGLINK-COSIMO model managed by the JRC-IPTS shows a much lower rate of exchange between existing crops and crop area expansion. The total area of cropland is reported to be modelled as 61,045.2 km^2 while the area of cropland contraction is 8,673.1 km^2. Most of the cropland expansion is allocated to the EU27 region (24.0%), while the expansion in Brazil is modelled at 16.2%.

The study found that the absolute figure of the crop land expansion area is not the only criterion that determines GHG emissions, but that type of land converted is also of significant importance. With the largest variations in carbon stock and potential emissions assigned to forests (from almost 0 to over 400 t C ha^{-1}), the proportion of forest converted to cropland is of overriding importance to the GHG emission estimates.

The following summary indicates the amount of forest that could be converted to cropland according four different studies:

Study	**Forest Converted** *% of Total*
EPA[41]	32
ICONE[42]	5
JRC[43]	36
IFPRI[44]	16

The figure in the EPA report is taken directly from the historical trends provided by Winrock with the comparison of remote sensing images between 2001 and 2004.

ICONE results are based on the use of a specific economic land use model (BLUM-Brazilian Land Use Model) that aims to analyse and project allocated areas for each activity and land use change.

[41] Table 2.6-13 of EPA (2009)

[42] Table 6 of ICONE (2009)

[43] This study.

[44] Figure 8 of IFPRI (2010). Primary and Managed forest are combined.

IFPRI provides economic results from a Computable Global Equilibrium model (MIRAGE) and then uses historical land use changes and competition between cropland, pasture and managed forest to determine the respective shares of land use types converted into cropland.

The proportion of forest converted ranges from 5% in the ICONE study to 36% in the JRC study. These differences are considered the most important factor explaining the discrepancies in the total GHG emission calculations reported by different sources.

The rather large differences between the estimated GHG emissions from biomass (43.4 Mt CO_2 in the IFPRI report vs. 167.7 Mt CO_2 in this study) are largely attributed to this dissimilarity in the allocation of the extra land. The land conversion is determined by the competition between cropland and other managed land (pasture and managed forest), and also by the assumption made with respect to the replacement of the different types of natural vegetation.

The JRC study does not distinguish pasture from grassland or managed forest from unmanaged forest, partly because the distinction between managed and natural areas using remote sensing images is problematic. EPA MODIS trends are also based on remote sensing images and do not distinguish managed land from natural land. IFPRI and ICONE deal with statistics rather than spatial information, and they model the competition between cropland, pasture and managed forest.

Concerning the expansion of cropland as compared to natural vegetation, the assumption made by ICONE (ICONE, 2009) seems to differ from the conservative approach taken in JRC study. ICONE considers that, for each region, all the expansion occurs over the majority biome type, while the JRC study keeps the share between biomes constant at local level. EPA and IFPRI use historical trends provided by Winrock.

To some degree the assumptions made about the land allocation of other models are based on conjecture and information extracted from reports. For a more in-depth analysis of the discrepancies between the different studies and a better understanding of the effect of land allocations, additional information on the specific allocation process used by IFPRI and ICONE is needed.

5.4. OUTLOOK

This study demonstrates the viability of the methodology developed for using spatial data and processing techniques to provide more detailed estimates of GHG emissions resulting from biofuels than were hitherto available. The scope of the study does not cover all areas involved in estimating GHG emissions from biofuels which occur as a result of ILUC. The following main areas were identified as being necessary to incorporate in further improvements of the methodology and expansions of the range of subjects covered:

- ***Estimation of GHG Emission Uncertainties***

  When comparing the different results, it has to be kept in mind that there are high levels of uncertainty involved in each step of the calculation chain, starting from the economic model results, spatial allocation, land use/cover and other input data up to the above- and belowground biomass values applied. Therefore, the results have to be interpreted with caution.

  The focus of this work was to test and describe the method and to show the influence of different assumptions on the results. However, a detailed uncertainty analysis has to be undertaken in order to allow robust conclusions to be drawn.

- ***Modelling to Reference Period***

  In this study the modelled reference conditions are not simulated in the spatial data. The approach used to adjust for this shortcoming is to transfer the changes between the scenario and reference data to a baseline dataset. Developing a set of reference data for climate and land use / cover for 2020 or beyond is one of the challenges facing future developments.

  The other dataset to be adjusted to the scenario period are the factors defining the management system. This information is at times available at farm level or national level, such as fertiliser application rates, but only partially at the scale of the project. Future investigations may also want to include land conservation practices (tillage) in the mapping of management systems.

- ***Effect of Climate Change***

  The study assumed no change in climatic conditions between the year of the base data (2000) and scenario (2020). Climate change models indicate geographically variable shifts in climatic conditions over this 20-year period. These changes in climatic conditions from the base to the scenario period on soil carbon and the distribution of crops could be investigated as to their effect on GHG emissions.

- ***Feedback with Economic Models***

  For future developments, a feedback mechanism to economic models is recommended. In some regions, the spatial allocation procedure has experienced difficulties in distributing the total amount of hectares reported by the economic models because the total surface of 'naturally suitable land' is less than the area given by the economic models. The aim of this study was to use the crop allocation model to spatially distribute the different economic results in order to deduce the ecological impact of biofuel policies.

There are other areas for improvement in the data used or development of the methodology applied, such as adaptation to the data available from external sources or the increase in spatial resolution of the spatial reference. At this stage most global data sets are available at 5 arc min. grid size, although a trend can be noted towards 30 arc sec. (about 1km grid size at the Equator) or even higher. However, before increasing the spatial resolution of the data, issues of uncertainty in the data should be addressed.

A new direction of investigation could be opened by including issues of biodiversity and land degradation into the analysis. While in principal the methodology allows the related constraints and demands to be incorporated, considerable effort needs to be made to produce suitable data at the global scale.

References

Al-Riffai, P., B. Dimaranan and D. La borde (2010) Global Trade and Environmental Impact Study of the EU Biofuels Mandate – Final Report. ATLASS Consortium. Specific Contract No SI2.537.787 implementing Framework Contract No TRADE/07/A2. 125pp. http://trade.ec.europa.eu/doclib/docs/2010/march/tradoc_145954.pdf

Annoni, A., C. Luzet, E. Gubler and J. Ihnde (2001) Map Projections for Europe. European Commission Joint Research Centre, Ispra, Italy. EUR 20120 EN. 131pp.

Baruth, B., G. Genovese and L. Montanarella (2006) New Soil Information for the MARS Crop Yield Forecasting System. European Commission Joint Research Centre, Ispra, Italy. ISBN 92-79-03376-X, UER 22499 EN. 95pp + Annex.

Batjes, N.H. (2008) ISRIC-WISE Harmonized Global Soil Profile Dataset (ver. 3.1). Report 2008/02. ISRIC - World Soil Information, Wageningen, The Netherlands. 52pp.

Batjes, N.H. (2006) ISRIC-WISE derived soil properties on a 5 by 5 arc-minutes global grid (version 1.0). ISRIC World Soil Information Report 2006/02.

Batjes, N.H. (2005) Total carbon and nitrogen in the soils of the world. European Journal of Soil Science. V47(2). pp. 151 - 163.

Batjes, N.H. (1996) Total carbon and nitrogen in the soils of the World. European Journal of Soil Science, June 1996, Vol. 47. pp. 151-163.

Batjes, N.H. (1992) Organic matter and carbon dioxide. In: A Review of Soil Factors and Processes that Control Fluxes of Heat, Moisture and Greenhouse Gases. Eds. N.H. Batjes & E.M. Bridges. Technical Paper 23, International Soil Reference and Information Centre, Wageningen. pp. 97-148.

Blanco Fonseca, M., A. Burrell, H. Gay, M. Henseler,A. Kavallari, R. M'Barek, I. Pérez Domínguez and A. Tonini (2010) JRC-IPTS Technical report:: Impacts of the EU biofuel target on agricultural markets and land use: a comparative modelling assessment. EUR24449 EN, 2010.
Available at http://ftp.jrc.es/EURdoc/JRC58484.pdf

Carré, F., R. Hiederer, V. Blujdea and R. Koeble (2009) Guide for the Calculation of Land Carbon Stocks Drawing on the 2006 IPCC Guidelines for National Greenhouse Gas Inventories. Administrative Arrangement No.: TREN/D1/464-2009-SI2.539303, JRC. 109pp.

de Pauw, E., F.O. Nachtergaele, J. Antoine, G. Fisher and H.T.V. Velthuizen (1996) A provisional world climatic resource inventory based on the length-of-growing-period concept. In: National Soil Reference Collections and Databases (NASREC) (eds Batjes, N.H., J.H. Kauffman and O.C. Spaargaren). International Soil Reference and Information Centre (ISRIC), Wageningen. pp. 30-43.

di Greggio, A, and L.J.M. Jansen (2000) Land Cover Classification System (LCCS): Classification Concepts and User Manual. FAO, Rome. ISBN 92-5-104216-0. http://www.fao.org/docrep/003/x0596e/x0596e00.HTM

Official Journal of the European Union (2009) Directive 2009/28/EC of the European Parliament and the Council of 23 April 2009 on the promotion of the use of

energy from renewable sources and amending and subsequently repealing Directives 2001/77/EC and 2003/30/EC. OJ L 140 form 05.06.2009, pp. 16-62 http://eur-lex.europa.eu/LexUriServ/LexUriServ.do?uri=OJ:L:2009:140:0016:0062:en:PDF

Driessen, P. J. Deckers and F.O. Nachtergaele (eds) (2001) Lecture notes on the major soil types of the World. FAO, Publishing and Multimedia Service, Information Division, , Viale delle Terme di Caracalla, 00100 Rome, Italy. ISBN 925-104637-9. http://www.fao.org/docrep/003/y1899e/y1899e00.htm#toc

Duffie, J. A. & W.A. Beckman, (1991) Solar Engineering of Thermal Processes, 2nd edn. J. Wiley and Sons, New York. 919pp.

ENSUS (2009) Comparison between EPA/MODIS and FAO Data of Forest and Crop Area changes. Technical Note, Docket No EPA-HQ-OAR-2005-0161, 1-September 2009.

EPA (2009) Draft Regulatory Impact Analysis: Changes to Renewable Fuel Standard Program. Assessment and Standards Division Office of Transportation and Air Quality U.S. Environmental Protection Agency.

FAO (2001) Global Forest Resources Assessment 2000. FAO, Rome. 479pp.

FAO (2007) C/N Ratio Class - TOPSOIL, Edition 3.6, 2007-02-08. Available at: http://www.fao.org/geonetwork/srv/en/main.home.

FAO / IIASA (2009) Land Degradation in Drylands Project (LADA) - Progress Report Compilation of Selected Global Indicators of Land Degradation. PR. No. 39701. FAO, Rome, Italy, IIASA, Laxenburg, Austria. 13pp.

FAO (1995), (2003) The Digitized Soil Map of the World Including Derived Soil Properties (version 3.5). FAO Land and Water Digital Media Series # 1. FAO, Rome.

FAO/IIASA/ISRIC/ISS-CAS/JRC (2009) Harmonized World Soil Database (version 1.1). FAO, Rome, Italy and IIASA, Laxenburg, Austria.

Fischer G., H. Van Velthuizen, M. Shah and F. Nachtergaele (2002) Global Agro-Ecological Assessment for Agriculture in the 21st Century: Methodology and Results. Research report RR-02-02, IIASA, Laxenburg, Austria.

Fischer, G., F. Nachtergaele, S. Prieler, H.T. van Velthuizen, L. Verelst and D. Wiberg, (2008) Global Agro-ecological Zones Assessment for Agriculture (2008). IIASA, Laxenburg, Austria and FAO, Rome, Italy.

Friedl, M.A., D.K. McIver, J C F. Hodges, X.Y. Zhang, D. Muchoney, A.H. Strahler, C.E. Woodcock, S. Gopal, A. Schneider, A. Cooper, A. Baccini, F. Gao and C. Schaaf (2002) Global land cover mapping from MODIS: Algorithms and early results. Remote Sens. Environ., 83. pp. 287-302.

Global Ecosystems Database Project (2000) Global Ecosystems Database Version II: Database, User's Guide, and Dataset Documentation. US Department of Commerce, National Oceanic and Atmospheric Administration, National Geophysical Data Center, Boulder, Colorado. KGRD #35. Two CD ROMs and publication on the WWW.

Global Soil Data Task (2000) Global Soil Data Products CD-ROM (IGBP-DIS). CD-ROM. International Geosphere-Biosphere Programme, Data and Information System, Potsdam, Germany. Available from Oak Ridge National Laboratory Distributed Active Archive Center, Oak Ridge, Tennessee, U.S.A. http://www.daac.ornl.gov.

Goldberg, D. (1991) What every computer scientist should know about floating-point arithmetic. Computing Surveys, Vol. 23, March, 1991. Association for Computing Machinery, Inc., New York, USA. pp. 5-48.

Hansen, M., R. DeFries, J.R. Townshend, M. Carroll, C. Dimiceli, and R. Sohlberg (2006) Vegetation Continuous Fields MOD44B, 2001 Percent Tree Cover, Collection 4, University of Maryland, College Park, Maryland, 2001.

Hijmans, R.J., S.E. Cameron, J.L. Parra, P.G. Jones and A. Jarvis (2005) Very high resolution interpolated climate surfaces for global land areas. International Journal of Climatology 25, pp.1965-1978.

Holdridge, L.R. (1947) Determination of world plant formations from simple climatic data. Science, 105, pp.367-368.

ICONE – Institute for International Trade Negotiations (2009) Impacts on Land Use and GHG Emissions from a Shock on Brazilian Sugarcane Ethanol Exports to the United States using Brazilian Land Use Model (BLUM) A. Meloni Nassar, L. Harfuch, M. Melo Ramalho Moreira, L. Chiodi Bachion, L. Barcellos Antoniazzi - Report to the U.S. Environmental Protection Agency regarding the Proposed Changes to the Renewable Fuel Standard Program.. ICONE, São Paulo, Brazil, September 2009. 31pp.

IFA (2009): available on http://www.fertilizer.org/ifa/ifadata/search

IFPRI - International Food Policy Institute (2010) Global Trade and Environmental Impact Study of the EU Biofuels Mandate Final Draft Report, March 2010. P. Al-Riffai, B. Dimaranan, D. Laborde, ATLASS Consortium. Specific Contract No SI2.537.787 implementing Framework Contract No TRADE/07/A2.

Intergovernmental Panel on Climate Change (IPCC) (2003) Good Practice Guidance for Land Use, Land-Use Change and Forestry. Penman J., M. Gytarsky, T. Hiraishi, T. Krug, D. Kruger, R. Pipatti, L. Buendia, K. Miwa, T. Ngara, K. Tanabe and F. Wagner (Eds.). IPCC/OECD/IEA/IGES, Hayama, Japan.

Intergovernmental Panel on Climate Change (IPCC) (2006) 2006 Guidelines for National Greenhouse Gas Inventories. Eggelstone, S., L. Buemdia, K. Miwa, T. Ngara and K. Tanabe (Eds.). IPCC/OECD/IEA/IGES, Hayama, Japan.

JRC/PBL (2009) Emissions Database for Global Atmospheric Research (EDGAR v4.0) online available at http://edgar.jrc.ec.europa.eu/.

Kay, A.L. and H.N. Davis (2008) Calculating potential evapotranspiration from climate model data: A source of uncertainty for hydrological climate change impacts. Journal of Hydrology (358) pp. 221-239.

Kottek, M., J. Grieser, C. Beck, B. Rudolf and F. Rubel (2006) World Map of the Köppen-Geiger climate classification updated. Meteorol. Z., 15, 259-263. DOI: 10.1127/0941-2948/2006/0130.

Lal, R. (2005) Encyclopedia of Soil Science - 2nd Edition. CRC Press. ISBN: 9780849338304. 2,060pp.

Leemans, R. (1990) Possible Changes in Natural Vegetation Patterns Due to a Global Warming. IIASA Working Paper WP¬90-08 and Publication Number 108 of the Biosphere Dynamics Project. Laxenburg, Austria: International Institute of Applied Systems Analysis. 22pp.

Monfreda C., N. Ramankutty and J. Foley (2008) Farming the planet: 2. Geographic distribution of crop areas, yields, physiological types, and net primary production in the year 2000. Global Biochemical Cycles, Vol. 22, GB1022, doi : 10.1029/ 2007GB002952.

Nachtergaele, F. and M. Petri (2009) Mapping Land Use Systems at global and regional scales for Land Degradation Assessment Analysis - Version 1.0. http://www.fao.org/nr/lada/.

OECD-FAO (2010) Agricultural Outlook 2010 – 2019. OECD-FAO OECD Publishing, 2 rue André Pascal, 75775 Paris CEDEX 16. 247pp. http://browse.oecdbookshop.org/oecd/pdfs/browseit/5110041E.

Oudin, L., F. Hervieu, C. Michel, C. Perrin, V. Andre'assian, F. Anctil and C. Loumagne (2005) Which potential evapotranspiration input for a limped rainfall-runoff model? Part 2 - Towards a simple and efficient potential evaportranspiration model for rainfall-runoff modelling. Journal of Hydrology 303, pp. 290-306.

Peel, M. C., B.L. Finlayson, and T.A. McMahon (2007) Updated world map of the Köppen-Geiger climate classification". Hydrol. Earth Syst. Sci. 11: 1633-1644.

Ramankutty N., A. Evan, C. Monfreda and J. Foley (2008) Farming the planet: 1. Geographic distribution of global agricultural lands in the year 2000. Global Biochemical Cycles, Vol. 22, GB1003. dai:10.1029/2007GB002952.

Saxton, K.E., W.J. Rawls, J.S. Romberger, and R.I. Papendick. (1986) Estimating generalized soil-water characteristics from texture. Soil Sci. Soc. Am. J. 50(4), pp.1031-1036

Siebert, S., P. Döll, S. Feick, J. Hoogeveen and K. Frenken (2007) Global Map of Irrigation Areas version 4.0.1. Johann Wolfgang Goethe University, Frankfurt am Main, Germany / Food and Agriculture Organization of the United Nations, Rome, Italy".

Stehfest E. and A.F. Bouwman (2006) N2O and NO emissions from agricultural fields and soils under natural vegetation: summarizing available measurement data and modeling of global annual emissions. Nutr. Cycl. Agroecosyst. V74 (3): 207-228. http://dx.doi.org/10.1007/s10705-006-9000-7. N2O and NO emission data set available at http://www.pbl.nl/en/publications/2006/N2OAndNOEmissionFromAgriculturalFieldsAndSoilsUnderNaturalVegetation.html

Trabucco, A. and R.J. Zomer (2009) Global Aridity Index (Global-Aridity) and Global Potential Evapo-Transpiration (Global-PET) Geospatial Database. CGIAR

Consortium for Spatial Information. Published online, available from the CGIAR-CSI GeoPortal at: http://www.csi.cgiar.org/

Valin H., M.P. Ramos, B. Dimaranan, L. Curran and A. Bouet (2009) Biofuels: Global Trade and Environmental Impact Study. Specific Contract No S12 499.331 implementing Framework Contract No TRADE/07/A2.

Van Lynden, G.W.J. and M. Lane (2004) Soil and Water protection using conswervation tillage in northern and central Europe. 13th International Soil Conservation Organisation Conference - Brisbane, July 2004. 5pp. http://www.wocat.net/fileadmin/user_upload/documents/Articles/ISCOsowap04.pdf

Appendix I

Example of Spatial Allocation of Cropland in Brazil

This section contains results of some cropland allocation simulations performed on Brazil. The methodology and dataset used are those described in the previous sections of this document.

Even if the uncertainty takes an important place in the cropland allocation modelling, it is of interest to run simulation on cropland expansion for several reasons.

First, these simulations give an order of magnitude on the impact of the different scenario policies. Despite the fact that it is not possible to determine precisely what will be the quantity of carbon released in the atmosphere by any agricultural policy in ten years time, the simulations can give a first idea on the importance of the emissions.

Second, it is useful to assess the range of possible output values under very favourable and unfavourable conditions (sensitivity analysis). Applied to GHG emission calculations it can give an indication on the maximum emission reached in case of allocating cropland in a particularly "unfavourable" environment or on the minimum GHG emission level under which it would not be possible to go down even with ecological practices and the best use of the best land available.

Third, running the model many times with slight variations in input parameters or using a stochastic approach provides a large set of results and allows statistical analysis more relevant than the result of a single simulation.

- **Crop Demand**

Table 39 indicates the level and variation of land use by crop sector in Brazil according to /IFPRI-MIRAGE study. The values are given for three different scenarios in 2020 (Baseline, Business As Usual (BAU) and Free Trade (TL)). This table is used as economic data input for the spatial allocation process.

Table 39: Crop Demands for Baseline, Business As Usual and Free Trade Scenario in 2020

Crop	Baseline *1000 ha*	BAU *1000 ha*	FT *1000 ha*
Maize	18560.6	18517.3	18470.7
Wheat	4325.3	4321.1	4301.1
Rice	3452.9	3452.9	3452.6
Sugar_cb	8571.1	9328.6	9702.2
Oilseed	39800.9	39866.2	39868.12
VegFruits	10424.6	10401.9	10391.2
Other	3724.3	3453.0	3360.0

- **Reference Year 2000**

Figure 48 presents the spatial extension of cropland in Brazil for the year 2000. The data come from the M3 Dataset provided by Wisconsin and McGill University ([Monfreda *et al*., 2008]). This spatial distribution is the reference cropland distribution in 2000 of the allocation model.

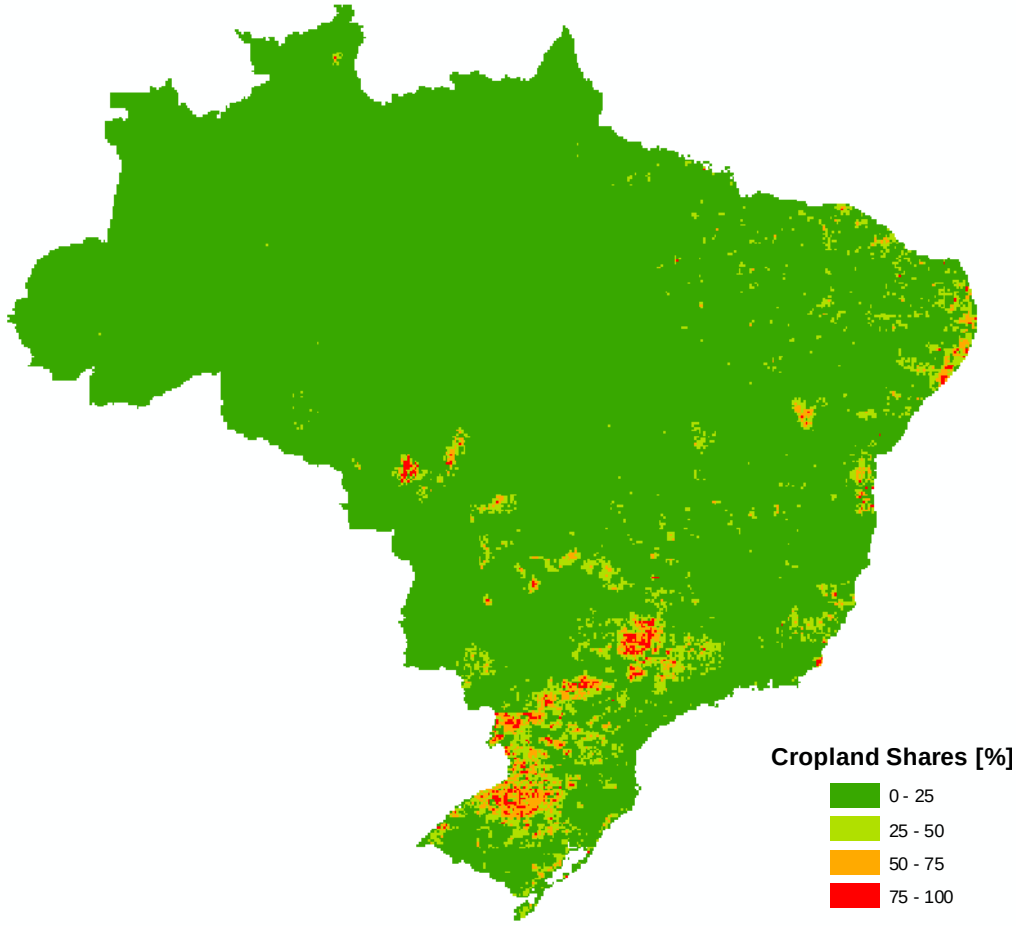

Figure 48: Distribution of Cropland in 2000 [Ramankutty *et al.* 2008]

- **Marginal Cropland Areas due to Biofuel Scenarios**

Figure 49 shows the increase in terms of cropland share due to BAU scenario compared to the baseline when the marginal cropland coming from economic model output is spatially allocated. This information is then sent to GHG emission models to estimate the increase of GHG emissions associated to different biofuel scenarios.

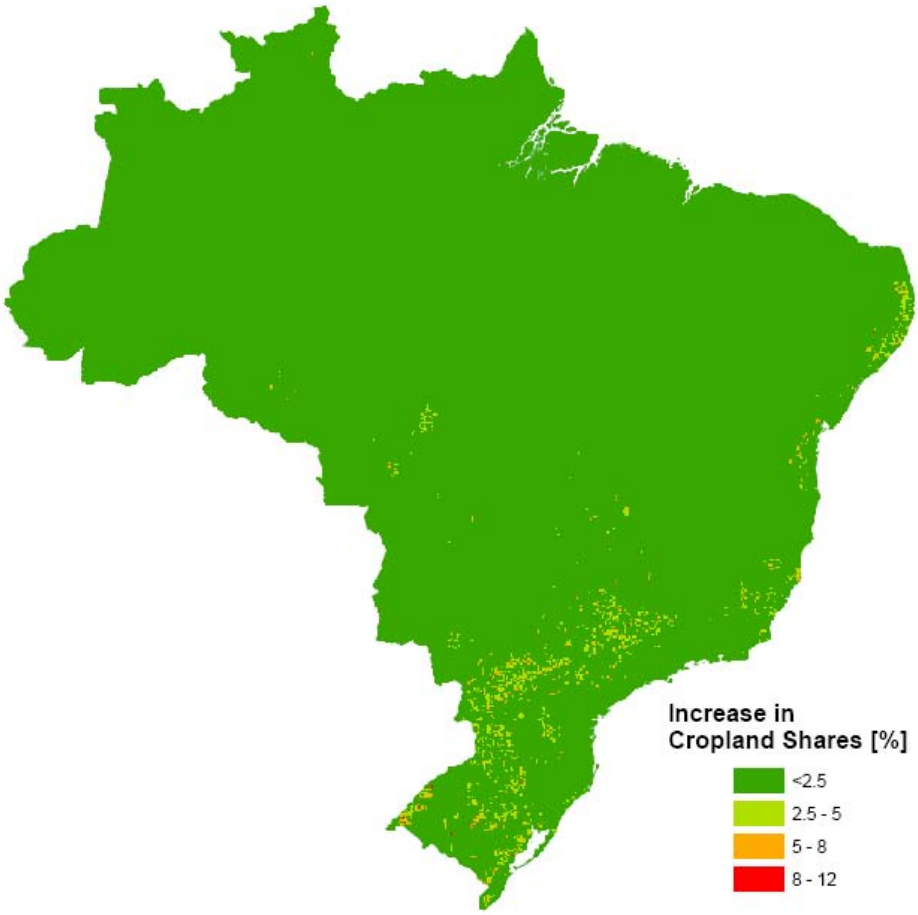

Figure 49: Spots of Marginal Increase in Cropland According to Biofuel Scenario Compare to Baseline

Appendix II

Supporting Material for Above- and Below-Ground Biomass Emissions Calculations

Table 40: World Regions Used for ABCS

Code	World Region
CA	Continental Asia
AF	Africa
EU	Europe
SA	Central and South America
AU	Australia
NA	North America
NZ	New Zealand
IA	Insular Asia

Table 41: Shares of Shrub and Tree Crops in Land Use Classes Fruits and Vegetables, Oilseeds and Sugar Crops

Country	Word region*	Fruits and Veg.	Fruit Trees	Fruit Shrubs	Oilseeds	Oilpalm	Coconut	Olive Trees	Karite	Tung	Sugar crops	Sugar cane
		10000 ha	*%*	*%*	*10000 ha*	*%*	*%*	*%*	*%*	*%*	*10000 ha*	*%*
AFGHANISTAN	CA	4.7	40	24	0.4	0	0	0	0	0	0.4	16
ANGOLA	AF	48.3	3	47	75.7	14	0	0	0	0	0.3	100
ALBANIA	EU	56.1	31	8	37.1	0	0	95	0	0	1.3	0
ANDORRA	EU	0.0	0	100	0.0	0	0	0	0	0	0.0	0
UNITED ARAB EMIR.	CA	164.0	89	0	0.0	0	0	0	0	0	0.0	0
ARGENTINA	SA	533.0	41	38	12242.7	0	0	0	0	0	267.1	100
ARMENIA	CA	53.4	38	27	0.6	0	0	6	0	0	0.0	0
AU	AU	194.5	26	60	1492.9	0	0	0	0	0	417.3	100
AUSTRIA	EU	84.2	35	56	108.5	0	0	0	0	0	45.5	0
AZERBAIJAN	CA	162.8	44	15	7.0	0	0	3	0	0	1.8	2
BURUNDI	AF	335.2	5	88	14.4	8	0	0	0	0	2.5	100
BELGIUM	EU	32.1	26	1	12.6	0	0	0	0	0	55.0	0
BENIN	AF	257.5	73	1	151.0	12	7	0	3	0	0.1	100
BURKINA FASO	AF	27.0	37	0	270.3	0	0	0	9	0	3.0	100
BANGLADESH	CA	461.9	26	12	543.5	0	6	0	0	0	188.8	91
BULGARIA	EU	302.5	20	42	558.8	0	0	0	0	0	1.8	0
BAHRAIN	CA	2.7	59	5	0.0	0	0	0	0	0	0.0	0
BOSNIA AND HERZ.	EU	148.8	19	3	4.3	0	0	3	0	0	0.3	0
BELARUS	EU	141.9	49	6	171.2	0	0	0	0	0	53.9	0
BELIZE	SA	27.3	89	9	0.7	4	31	0	0	0	25.9	100
BOLIVIA	SA	131.3	7	44	734.4	0	0	0	0	0	88.3	100
BRAZIL	SA	2643.3	65	22	14145.0	0	2	0	0	0	5003.2	100
BRUNEI DARU.	IA	10.7	6	0	0.1	64	18	0	0	0	0.0	0
BHUTAN	CA	8.8	84	0	5.5	0	0	0	0	0	0.0	100
BOTSWANA	AF	1.6	22	0	5.6	0	0	0	0	0	0.0	100
CENTRAL AFN REP.	AF	46.0	6	89	174.5	0	0	0	0	0	7.5	100
CANADA	NA	148.1	19	22	6789.5	0	0	0	0	0	11.2	0
SWITZERLAND	EU	36.7	41	41	19.2	0	0	0	0	0	17.7	0
CHILE	SA	338.3	35	44	18.3	0	0	18	0	0	42.9	0
CHINA	CA	23520.6	34	2	22878.1	0	0	0	0	0	1614.0	76
COTE D'IVOIRE	AF	608.7	17	67	334.9	42	9	0	4	0	16.3	100
CAMEROON	AF	595.9	4	42	402.4	9	0	0	0	0	136.2	100
CONGO, DEM. REP.	AF	370.6	1	86	798.4	28	0	0	0	0	31.8	100
CONGO	AF	28.8	20	65	38.6	17	1	0	0	0	11.5	100
COLOMBIA	SA	533.7	19	74	168.9	78	5	0	0	0	392.7	100
COSTA RICA	SA	144.6	44	47	37.6	90	9	0	0	0	47.5	100
CUBA	SA	414.0	31	26	35.0	0	67	0	0	0	1010.8	100
CYPRUS	EU	1.7	21	14	0.0	0	0	0	0	0	0.0	0
CZECH REPUBLIC	EU	47.0	46	19	338.2	0	0	0	0	0	70.9	0
GERMANY	EU	332.2	58	29	1077.3	0	0	0	0	0	404.3	0
DJIBOUTI	AF	1.0	0	0	0.0	0	0	0	0	0	0.0	0
DENMARK	EU	10.2	54	0	108.7	0	0	0	0	0	59.9	0
DOMINICAN REP.C	SA	155.0	37	44	53.5	18	75	0	0	0	149.8	100
ALGERIA	AF	505.6	45	10	193.6	0	0	90	0	0	0.0	0
ECUADOR	SA	402.3	18	71	168.8	68	1	0	0	0	77.7	100
EGYPT	AF	880.1	35	9	137.1	0	0	18	0	0	180.5	71
ERITREA	AF	10.9	0	0	49.8	0	0	0	0	0	0.0	100
SPAIN	EU	2059.2	29	56	3248.2	0	0	71	0	0	126.4	0
ESTONIA	EU	13.7	78	5	26.5	0	0	0	0	0	0.0	0
ETHIOPIA	AF	148.2	1	0	434.8	0	0	0	0	0	13.3	100
FINLAND	EU	9.4	16	45	66.3	0	0	0	0	0	32.8	0
FRANCE	EU	1370.2	9	62	1955.1	0	0	1	0	0	396.7	0
GABON	AF	61.3	12	80	22.1	16	0	0	0	0	3.2	100
UNITED KINGDOM	EU	136.2	7	0	528.0	0	0	0	0	0	168.5	0

Country	Word region*	Fruits and Veg.	Fruit Trees	Fruit Shrubs	Oilseeds	Oilpalm	Coconut	Olive Trees	Karite	Tung	Sugar crops	Sugar cane
		10000 ha	*%*	*%*	*10000 ha*	*%*	*%*	*%*	*%*	*%*	*10000 ha*	*%*
GEORGIA	CA	160.9	42	40	41.2	0	0	0	0	0	0.1	0
GHANA	AF	457.9	13	59	413.2	27	13	0	5	0	4.9	100
GUINEA	AF	366.5	22	36	466.2	64	1	0	0	0	4.2	100
GAMBIA	AF	2.3	32	0	102.8	3	0	0	0	0	0.0	100
GUINEA-BISSAU	AF	206.0	92	6	31.2	19	28	0	0	0	0.0	100
EQUAT. GUINEA	AF	9.5	0	100	5.5	58	42	0	0	0	0.0	0
GREECE	EU	380.5	43	29	694.5	0	0	96	0	0	40.3	0
GUATEMALA	SA	102.8	31	29	93.5	22	10	0	0	0	179.4	100
FRENCH GUIANA	SA	1.3	21	56	0.0	0	0	0	0	0	0.0	100
GUYANA	SA	5.8	8	72	15.9	0	86	0	0	0	48.9	100
HONG KONG	CA	0.2	5	29	0.0	0	0	0	0	0	0.0	0
HONDURAS	SA	75.4	28	51	37.6	95	3	0	0	0	50.4	100
CROATIA	EU	138.3	27	42	97.9	0	0	15	0	0	25.9	0
HAITI	SA	184.3	35	47	50.3	0	18	0	0	0	17.2	100
HUNGARY	EU	262.1	32	34	539.6	0	0	0	0	0	65.7	0
INDONESIA	IA	1526.4	45	20	6286.3	35	42	0	0	0	448.4	86
INDIA	CA	9359.9	38	7	25591.9	0	7	0	0	0	4241.5	100
IRELAND	EU	3.4	2	0	2.7	0	0	0	0	0	32.1	0
IRAN	CA	1546.5	49	18	195.1	0	0	2	0	0	208.3	14
IRAQ	CA	3.2	70	13	1.9	0	0	92	0	0	0.1	0
ISRAEL	CA	52.8	46	13	51.8	0	0	85	0	0	0.6	0
ITALY	EU	1618.1	26	43	1227.4	0	0	65	0	0	219.6	0
JAMAICA	SA	58.6	50	29	55.6	0	95	0	0	0	40.2	100
JORDAN	CA	42.7	30	12	43.1	0	0	100	0	0	0.0	0
JAPAN	IA	531.8	32	4	128.3	0	0	0	0	0	84.2	23
KAZAKSTAN	CA	90.7	37	6	317.8	0	0	0	0	0	11.4	0
KENYA	AF	188.6	12	46	143.1	0	6	0	0	0	52.2	100
KYRGYZSTAN	CA	62.7	52	10	59.8	0	0	0	0	0	22.2	0
CAMBODIA	CA	123.0	13	27	69.6	0	13	0	0	0	6.8	100
KOREA, REPUBLIC	CA	502.7	27	7	163.2	0	0	0	0	0	0.0	0
KUWAIT	CA	4.7	26	0	0.0	0	0	0	0	0	0.0	0
LAO P. DEM. REP.	CA	89.0	9	5	23.6	1	2	0	0	0	5.0	99
LEBANON	CA	97.1	54	18	57.0	0	0	96	0	0	3.9	0
LIBERIA	AF	43.6	4	59	28.1	54	7	0	0	0	20.5	100
LIBYAN ARAB JAM.	AF	104.6	43	7	114.6	0	0	91	0	0	0.0	0
SRI LANKA	IA	193.5	36	29	463.2	0	96	0	0	0	18.8	100
LESOTHO	AF	5.2	52	0	0.9	0	0	0	0	0	0.0	0
LITHUANIA	EU	48.9	71	0	62.4	0	0	0	0	0	29.3	0
LUXEMBOURG	EU	1.7	54	40	1.7	0	0	0	0	0	0.0	0
LATVIA	EU	13.9	56	8	10.6	0	0	0	0	0	13.9	0
MOROCCO	AF	415.7	52	11	592.3	0	0	83	0	0	72.3	21
MOLDOVA, REP.	EU	325.8	38	46	241.4	0	0	0	0	0	60.4	0
MADAGASCAR	AF	145.1	44	33	65.5	0	45	0	0	1	58.3	100
MEXICO	SA	1459.3	62	8	489.9	2	34	1	0	0	631.9	100
MACED., FYROM	EU	91.9	18	30	15.3	0	0	30	0	0	1.7	0
MALI	AF	39.9	1	1	186.3	0	0	0	14	0	2.7	100
MYANMAR	CA	564.8	46	8	2109.8	0	1	0	0	0	149.4	90
MOZAMBIQUE	AF	86.8	77	7	428.1	0	18	0	0	0	20.4	100
MAURITANIA	AF	9.4	62	0	6.5	0	0	0	0	0	0.0	100
MALAWI	AF	81.2	30	48	87.1	0	0	0	0	2	12.4	100
MALAYSIA	IA	79.7	45	35	3279.5	91	6	0	0	0	17.2	100
NAMIBIA	AF	0.1	0	15	0.1	7	0	0	0	0	0.0	0
NIGER	AF	11.9	32	0	220.2	0	0	0	0	0	1.8	100
NIGERIA	AF	2590.5	47	13	5955.3	43	1	0	3	0	2.0	100
NICARAGUA	SA	24.8	64	27	40.5	2	0	0	0	0	48.4	100
NETHERLANDS	EU	73.1	25	3	5.4	0	0	0	0	0	100.2	0
NORWAY	EU	3.1	29	27	4.6	0	0	0	0	0	0.0	0
NEPAL	CA	196.8	27	0	209.7	0	0	0	0	0	50.5	100
NZ	NZ	103.0	28	10	1.6	0	0	0	0	0	0.0	0

Country	Word region*	Fruits and Veg.	Fruit Trees	Fruit Shrubs	Oilseeds	Oilpalm	Coconut	Olive Trees	Karite	Tung	Sugar crops	Sugar cane
		10000 ha	*%*	*%*	*10000 ha*	*%*	*%*	*%*	*%*	*%*	*10000 ha*	*%*
OMAN	CA	47.0	74	6	0.0	0	0	0	0	0	0.0	0
PAKISTAN	CA	788.1	63	4	619.9	0	0	0	0	0	1026.5	100
PANAMA	SA	43.2	14	57	8.8	58	42	0	0	0	32.4	100
PERU	SA	307.8	25	41	3.6	82	0	12	0	0	58.6	100
PHILIPPINES	IA	1456.6	36	28	3438.0	0	98	0	0	0	361.3	100
PAPUA NEW GUINEA	IA	179.5	52	33	306.6	25	75	0	0	0	1.9	100
POLAND	EU	550.9	54	12	449.7	0	0	0	0	0	341.3	0
PUERTO RICO	SA	19.4	22	57	0.8	0	100	0	0	0	4.1	100
KOREA, DEM. P. REP.	CA	436.1	38	0	313.3	0	0	0	0	0	0.0	0
PORTUGAL	EU	465.8	38	48	400.1	0	0	88	0	0	5.8	0
PARAGUAY	SA	56.5	30	10	1253.8	1	0	0	0	1	54.2	100
PALEST. TERR. OCC	CA	32.3	46	11	27.4	0	0	82	0	0	0.0	0
ROMANIA	EU	651.6	28	37	1065.5	0	0	0	0	0	69.7	0
RUSSIAN FED.	CA	1143.7	46	5	4663.2	0	0	0	0	0	758.9	0
RWANDA	AF	389.7	2	89	34.5	0	1	0	0	0	1.4	100
SAUDI ARABIA	CA	275.7	62	3	1.7	0	0	0	0	0	0.0	0
SERBIA, MONTEN.	EU	409.3	50	22	271.4	0	0	0	0	0	54.5	0
SUDAN	AF	168.8	42	0	3029.7	0	0	0	0	0	57.1	100
SENEGAL	AF	31.6	77	0	641.8	1	0	0	0	0	5.7	100
SIERRA LEONE	AF	53.7	37	8	53.3	39	4	0	0	0	0.1	100
EL SALVADOR	SA	36.1	55	23	22.3	1	26	23	0	0	68.6	100
SAN MARINO	EU	0.3	25	45	0.1	0	0	6	0	0	0.1	0
SOMALIA	AF	53.7	69	0	46.1	0	0	0	0	0	0.0	100
SURINAME	SA	3.7	37	45	1.2	14	81	0	0	0	2.6	100
SLOVAKIA	EU	51.6	24	34	176.0	0	0	0	0	0	34.3	0
SLOVENIA	EU	20.2	21	74	1.2	0	0	40	0	0	6.5	0
SWEDEN	EU	11.2	4	15	63.0	0	0	0	0	0	47.6	0
SWAZILAND	AF	12.6	90	3	6.4	0	0	0	0	0	42.4	100
SYRIAN ARAB REP.	CA	275.1	40	22	486.0	0	0	94	0	0	26.2	0
CHAD	AF	8.9	78	5	298.6	0	0	0	0	0	1.3	100
TOGO	AF	30.4	14	5	76.1	16	4	0	3	0	0.0	0
THAILAND	CA	1064.9	51	21	915.9	24	36	0	0	0	968.3	100
TAJIKISTAN	CA	122.6	44	26	1.3	0	0	0	0	0	0.1	0
TURKMENISTAN	CA	84.0	24	29	0.1	0	0	0	0	0	15.6	0
TIMOR LESTE	IA	7.0	0	0	5.1	0	0	0	0	0	0.0	0
TRINIDAD AND TOB.	SA	11.5	63	22	4.0	0	100	0	0	0	21.5	100
TUNISIA	AF	224.4	48	10	623.8	0	0	98	0	0	1.7	0
TURKEY	CA	1678.9	21	31	1199.7	0	0	47	0	0	392.2	0
TAIW., PROV. CHINA	IA	247.6	47	7	33.0	0	12	0	0	0	35.3	100
TANZANIA, UN. REP.	AF	561.9	21	53	582.8	0	49	0	0	0	6.4	100
UGANDA	AF	1809.0	0	95	511.8	0	0	0	0	0	121.3	100
UKRAINE	EU	806.3	36	12	2973.1	0	0	0	0	0	830.6	0
URUGUAY	SA	40.3	62	20	124.2	0	0	0	0	0	3.1	100
UNITED STATES	NA	2301.3	35	16	31915.9	0	0	0	0	0	970.2	42
UZBEKISTAN	CA	384.6	34	25	53.3	0	0	0	0	0	8.2	0
VENEZUELA	SA	196.5	26	57	77.0	29	25	0	0	0	127.2	100
VIET NAM	CA	1156.4	43	12	541.7	0	28	0	0	0	274.5	100
YEMEN	CA	129.5	41	25	31.3	0	0	0	0	0	0.0	0
SOUTH AF	AF	275.8	37	40	751.6	0	0	0	0	0	309.4	100
ZAMBIA	AF	31.1	5	2	135.6	1	0	0	0	0	9.4	100
ZIMBABWE	AF	38.4	27	34	286.2	0	0	0	0	0	38.6	100

Table 42: Above- and Below-Ground Biomass Carbon Stocks (ABCS) in t C ha^{-1} Used in this Study

World Region	Ecozone	Grassland	Closed Forest	Open Forest	Shrubland	Sparse Veget.	Wetlands	Fruits Shrub	Fruits Tree	Oilpalm	Coconut	Olive tree	Karite	Tung	Sugar cane	Jatropha	Miscanthus	Jojoba
CA	Boreal Dry	4.3	35.0	2.0	7.4	0.6	10.0	17.5	6.2	0	0	0.0	0.0	0.0	0.0	0.0	0.0	0.0
NA	Boreal Dry	4.3	35.0	2.0	7.4	0.6	10.0	17.5	6.2	0	0	0.0	0.0	0.0	0.0	0.0	0.0	0.0
CA	Boreal Moist	4.3	53.0	12.0	7.4	0.6	15.6	17.5	43.2	0	0	0.0	0.0	0.0	0.0	0.0	0.0	0.0
EU	Boreal Moist	4.3	53.0	12.0	7.4	0.6	15.6	17.5	43.2	0	0	0.0	0.0	0.0	0.0	0.0	0.0	0.0
IA	Boreal Moist	4.3	53.0	12.0	7.4	0.6	15.6	17.5	43.2	0	0	0.0	0.0	0.0	0.0	0.0	0.0	0.0
NA	Boreal Moist	4.3	53.0	12.0	7.4	0.6	15.6	17.5	43.2	0	0	0.0	0.0	0.0	0.0	0.0	0.0	0.0
AF	Subtr. Dry	3.1	88.0	17.0	43.0	0.5	22.9	21.5	43.2	60	0	43.2	14.4	43.2	4.8	17.5	10.0	2.4
AU	Subtr. Dry	3.1	82.0	16.0	37.0	0.5	21.5	18.5	43.2	60	0	43.2	14.4	43.2	4.8	17.5	10.0	2.4
CA	Subtr. Dry	3.1	82.0	16.0	37.0	0.5	21.5	18.5	43.2	60	0	43.2	14.4	43.2	4.8	17.5	10.0	2.4
EU	Subtr. Dry	3.1	82.0	16.0	37.0	0.5	21.5	18.5	43.2	60	0	43.2	14.4	43.2	4.8	17.5	10.0	2.4
NA	Subtr. Dry	3.1	130.0	26.0	50.0	0.5	33.1	25.0	43.2	60	0	43.2	14.4	43.2	4.8	17.5	14.9	2.4
NZ	Subtr. Dry	3.1	100.0	20.0	43.0	0.5	25.9	21.5	43.2	60	0	43.2	14.4	43.2	4.8	17.5	10.0	2.4
SA	Subtr. Dry	3.1	130.0	26.0	50.0	0.5	33.1	25.0	43.2	60	0	43.2	14.4	43.2	4.8	17.5	10.0	2.4
AF	Subtr. Moist	6.8	109.0	22.0	43.0	1.0	30.3	21.5	43.2	60	75	43.2	14.4	43.2	5.0	17.5	0.0	2.4
AU	Subtr. Moist	6.8	109.0	22.0	37.0	1.0	30.3	18.5	43.2	60	75	43.2	14.4	43.2	5.0	17.5	0.0	2.4
CA	Subtr. Moist	6.8	109.0	22.0	37.0	1.0	30.3	18.5	43.2	60	75	43.2	14.4	43.2	5.0	17.5	0.0	2.4
EU	Subtr. Moist	6.8	109.0	22.0	37.0	1.0	30.3	18.5	43.2	60	75	43.2	14.4	43.2	5.0	17.5	0.0	2.4
IA	Subtr. Moist	6.8	173.0	35.0	43.0	1.0	45.7	21.5	43.2	60	75	43.2	14.4	43.2	5.0	17.5	0.0	2.4
NA	Subtr. Moist	6.8	109.0	22.0	50.0	1.0	30.3	25.0	43.2	60	75	43.2	14.4	43.2	4.8	17.5	0.0	2.4
NZ	Subtr. Moist	6.8	132.0	26.0	43.0	1.0	35.7	21.5	43.2	60	75	43.2	14.4	43.2	5.0	17.5	0.0	2.4
SA	Subtr. Moist	6.8	132.0	26.0	50.0	1.0	35.7	25.0	43.2	60	75	43.2	14.4	43.2	5.0	17.5	0.0	2.4
AF	Temp. Dry	3.3	87.0	14.0	7.4	0.5	22.2	3.7	7.0	60	0	43.2	0.0	0.0	0.0	17.5	10.0	0.0
AU	Temp. Dry	3.3	87.0	14.0	7.4	0.5	22.2	3.7	7.0	60	0	43.2	0.0	0.0	0.0	17.5	10.0	2.4
CA	Temp. Dry	3.3	87.0	14.0	7.4	0.5	22.2	3.7	7.0	60	0	43.2	0.0	0.0	0.0	17.5	10.0	2.4
EU	Temp. Dry	3.3	87.0	14.0	7.4	0.5	22.2	3.7	7.0	60	0	43.2	0.0	0.0	0.0	17.5	10.0	2.4
NA	Temp. Dry	3.3	93.0	16.0	7.4	0.5	23.8	3.7	8.0	60	0	43.2	0.0	0.0	0.0	17.5	14.9	2.4
NZ	Temp. Dry	3.3	87.0	14.0	7.4	0.5	22.2	3.7	7.0	60	0	43.2	0.0	0.0	0.0	17.5	10.0	2.4
SA	Temp. Dry	3.3	93.0	16.0	7.4	0.5	23.8	3.7	8.0	60	0	43.2	0.0	0.0	0.0	17.5	10.0	2.4
AF	Temp. Moist	6.8	84.0	21.0	7.4	1.0	25.1	3.7	10.5	60	0	43.2	0.0	0.0	4.8	17.5	10.0	2.4
AU	Temp. Moist	6.8	227.0	21.0	7.4	1.0	53.7	3.7	10.5	60	0	43.2	0.0	0.0	4.8	17.5	10.0	2.4
CA	Temp. Moist	6.8	84.0	21.0	7.4	1.0	25.1	3.7	10.5	60	0	43.2	0.0	0.0	4.8	17.5	10.0	2.4
EU	Temp. Moist	6.8	84.0	14.0	7.4	1.0	23.7	3.7	7.0	60	0	43.2	0.0	0.0	4.8	17.5	10.0	2.4
IA	Temp. Moist	6.8	227.0	21.0	7.4	1.0	53.7	3.7	10.5	60	0	43.2	0.0	0.0	4.8	17.5	10.0	2.4
NA	Temp. Moist	6.8	406.0	79.0	7.4	1.0	32.3	3.7	39.5	60	0	43.2	0.0	0.0	4.8	17.5	10.0	2.4
NZ	Temp. Moist	6.8	227.0	43.0	7.4	1.0	58.1	3.7	21.5	60	0	43.2	0.0	0.0	4.8	17.5	10.0	2.4
SA	Temp. Moist	6.8	120.0	21.0	7.4	1.0	32.3	3.7	10.5	60	0	43.2	0.0	0.0	5.0	17.5	10.0	2.4
AF	Trop. Dry	4.4	77.0	14.0	46.0	0.7	20.8	6.2	6.2	60	75	0.0	14.4	43.2	4.2	17.5	0.0	2.4
AU	Trop. Dry	4.4	83.0	16.0	46.0	0.7	22.4	6.2	6.2	60	75	0.0	14.4	43.2	4.0	17.5	0.0	2.4
CA	Trop. Dry	4.4	83.0	16.0	39.0	0.7	22.4	6.2	6.2	60	75	0.0	14.4	43.2	4.0	17.5	0.0	2.4
EU	Trop. Dry	4.4	83.0	16.0	39.0	0.7	22.4	6.2	6.2	60	75	0.0	14.4	43.2	4.0	17.5	0.0	2.4
IA	Trop. Dry	4.4	101.0	19.0	46.0	0.7	26.6	6.2	6.2	60	75	0.0	14.4	43.2	4.0	17.5	0.0	2.4
NA	Trop. Dry	4.4	131.0	25.0	53.0	0.7	33.8	6.2	6.2	60	75	0.0	14.4	43.2	4.0	17.5	0.0	2.4
SA	Trop. Dry	4.4	131.0	25.0	53.0	0.7	33.8	6.2	6.2	60	75	0.0	14.4	43.2	4.0	17.5	0.0	2.4
AF	Trop. Moist	8.1	156.0	30.0	46.0	1.2	42.1	14.4	14.4	60	75	0.0	14.4	43.2	4.2	17.5	0.0	2.4
AU	Trop. Moist	8.1	110.0	21.0	46.0	1.2	31.1	14.4	14.4	60	75	0.0	14.4	43.2	5.0	17.5	0.0	2.4
CA	Trop. Moist	8.1	110.0	21.0	39.0	1.2	31.1	14.4	14.4	60	75	0.0	14.4	43.2	5.0	17.5	0.0	2.4
IA	Trop. Moist	8.1	174.0	34.0	46.0	1.2	46.5	14.4	14.4	60	75	0.0	14.4	43.2	5.0	17.5	0.0	2.4
NA	Trop. Moist	8.1	133.0	26.0	53.0	1.2	36.7	14.4	14.4	60	75	0.0	14.4	43.2	5.0	17.5	0.0	2.4
SA	Trop. Moist	8.1	133.0	26.0	53.0	1.2	36.7	14.4	14.4	60	75	0.0	14.4	43.2	5.0	17.5	0.0	2.4
AF	Trop. Mont.	8.1	77.0	13.0	46.0	1.2	22.9	14.4	6.5	60	75	0.0	14.4	43.2	4.2	17.5	0.0	2.4
AU	Trop. Mont.	8.1	88.0	16.0	46.0	1.2	25.7	14.4	8.0	60	75	0.0	14.4	43.2	5.0	17.5	0.0	2.4
CA	Trop. Mont.	8.1	88.0	16.0	39.0	1.2	25.7	14.4	8.0	60	75	0.0	14.4	43.2	5.0	17.5	0.0	2.4
IA	Trop. Mont.	8.1	130.0	26.0	46.0	1.2	36.1	14.4	13.0	60	75	0.0	14.4	43.2	5.0	17.5	0.0	2.4
NA	Trop. Mont.	8.1	94.0	17.0	53.0	1.2	27.1	14.4	8.5	60	75	0.0	14.4	43.2	5.0	17.5	0.0	2.4
SA	Trop. Mont.	8.1	94.0	17.0	53.0	1.2	27.1	14.4	8.5	60	75	0.0	14.4	43.2	5.0	17.5	0.0	2.4
AF	Trop. Wet	8.1	204.0	40.0	46.0	1.2	53.7	23.0	34.3	60	75	0.0	14.4	43.2	4.0	17.5	0.0	2.4

World Region	Ecozone	Grassland	Closed Forest	Open Forest	Shrubland	Sparse Veget.	Wetlands	Fruits Shrub	Fruits Tree	Oilpalm	Coconut	Olive tree	Karite	Tung	Sugar cane	Jatropha	Miscanthus	Jojoba
AU	Trop. Wet	8.1	185.0	36.0	46.0	1.2	49.1	23.0	34.3	60	75	0.0	14.4	43.2	4.0	17.5	0.0	2.4
CA	Trop. Wet	8.1	185.0	36.0	39.0	1.2	49.1	19.5	34.3	60	75	0.0	14.4	43.2	4.0	17.5	0.0	2.4
IA	Trop. Wet	8.1	230.0	45.0	46.0	1.2	59.9	23.0	34.3	60	75	0.0	14.4	43.2	4.0	17.5	0.0	2.4
NA	Trop. Wet	8.1	198.0	39.0	53.0	1.2	52.3	26.5	34.3	60	75	0.0	14.4	43.2	5.0	17.5	0.0	2.4
SA	Trop. Wet	8.1	198.0	39.0	53.0	1.2	52.3	26.5	34.3	60	75	0.0	14.4	43.2	5.0	17.5	0.0	2.4

European Commission

EUR 24483 EN – Joint Research Centre – Institute for Energy

Title: Biofuels: a New Methodology to Estimate GHG Emissions from Global Land Use Change - A methodology involving spatial allocation of agricultural land demand and estimation of CO_2 and N_2O emissions

Author(s): Roland Hiederer, Fabien Ramos, Claudia Capitani, Renate Koeble, Viorel Blujdea, Oscar Gomez, Declan Mulligan and Luisa Marelli

Luxembourg: Publications Office of the European Union

2010 – 150 pp. – 21 x 29.7 cm

EUR – Scientific and Technical Research series – ISSN 1018-5593

ISBN 978-92-79-16389-0

DOI 10.2788/48910

Abstract

This study provides a new methodology developed by the JRC IES and IE for estimating changes in soil carbon stocks and GHG emissions resulting from global land use changes caused by the production of biofuels.

The methodology follows a two-step approach:

- Creation of database (e.g. land use/crop cover/soil types etc.), combining different data sources into a single harmonised database;
- Simulation based on cropland demands from the general equilibrium model MIRAGE (run by IFPRI) and on cropland demand from the partial equilibrium model AGLINK-COSIMO (run by JRC-IPTS).

For this work a dedicated set of spatial data layers was developed at 5 arc min resolution. Global cropland data for 2000 (used as the reference year) are merged with land cover data, adjusting the proportions to fully cover an area with land use and cover types whilst keeping the reference data constant.

In the simulation process data on land cover change (between 2001 and 2004) are used to identify the conversion of non-cropland into new cropland. Cropland demand for individual crops and aggregated crop classes are spatially allocated using the criteria of land suitability and distance from existing cropland.

The outcome of the simulation process is a set of land use maps describing the estimated shares of each crop or group of crops according to different biofuel scenarios. This information is then used to estimate related GHG emissions according to the Tier 1 approach as developed under the IPCC 2006 Guidelines for National Greenhouse Gas Inventories that result from a given change in biofuel demand.

How to obtain EU publications

Our priced publications are available from EU Bookshop (http://bookshop.europa.eu), where you can place an order with the sales agent of your choice.

The Publications Office has a worldwide network of sales agents. You can obtain their contact details by sending a fax to (352) 29 29-42758.

The mission of the JRC is to provide customer-driven scientific and technical support for the conception, development, implementation and monitoring of EU policies. As a service of the European Commission, the JRC functions as a reference centre of science and technology for the Union. Close to the policy-making process, it serves the common interest of the Member States, while being independent of special interests, whether private or national.

JRC
EUROPEAN COMMISSION

LB-NA-24-483-EN-C

Publications Office

ISBN 978-92-79-16389-0

9 789279 163890